U.PORTO

PHD IN PHARMACEUTICAL SCIENCES
MICROBIOLOGY SPECIALTY

Surface glycans as mediators of *Klebsiella pneumoniae* virulence and adaptation: insights from glycomics, fluid dynamics, and epidemiology

Michele Loiodice

D

2025

Surface glycans as mediators of *Klebsiella pneumoniae* virulence and adaptation: insights from glycomics, fluid dynamics, and epidemiology

Michele Loiodice

Faculdade de Farmácia

U.PORTO

PHD IN PHARMACEUTICAL SCIENCES

MICROBIOLOGY SPECIALTY

Surface glycans as mediators of *Klebsiella pneumoniae* virulence and adaptation: insights from glycomics, fluid dynamics, and epidemiology

Michele Loiodice

D

2025

Work supervised by Dr. Ângela Novais and co-supervised by Professor Dr. Luísa Peixe (Faculty of Pharmacy, University of Porto, Portugal) and Professor Dr. Angelina Palma (Department of Chemistry, NOVA University of Lisbon, Portugal).



February 2025

É AUTORIZADA A REPRODUÇÃO INTEGRAL DESTA TESE APENAS PARA EFEITOS DE INVESTIGAÇÃO, MEDIANTE DECLARAÇÃO ESCRITA DO INTERESSADO, QUE A TAL SE COMPROMETE.

Michele Loiodice



This work was performed at the Microbiology Group at the Faculty of Pharmacy, University of Porto (FFUP, Porto, Portugal). The author received financial support through an individual fellowship funded by the FCT - Fundação para a Ciência e a Tecnologia, I.P., with the reference 2020.07480.BD. This work was also supported by national funds from in the FCT, in the scope of the project UIDP/04378/2020 and UIDB/04378/2020 of the Research Unit on Applied Molecular Biosciences - UCIBIO, and the project LA/P/0140/2020 of the Associate Laboratory Institute for Health and Bioeconomy - i4HB, Faculty of Pharmacy, University of Porto, 4050-313 Porto, Portugal.













Acknowledgements

I wish to convey my appreciation to my PhD advisor, Dr. Ângela Novais, for her support throughout this project. Her advice and guidance on effective research were key in achieving a successful outcome for this work.

I am very thankful to my co-supervisors, Professor Luísa Peixe, and my Lisbon team, Professor Angelina Palma, and Dr. Benedita Pinheiro, for their valuable input and efforts in helping me address my limitations. Their patience and enthusiasm throughout our daily work have been greatly appreciated.

I would like to extend my gratitude to Prof. Paulo Costa, Prof. Maria Helena Amaral, Dr. Teresa Ribeiro, Dr. Elisabete Cappelli, and all the people who worked with me in the microbiology and technology lab, for their professional advice, personal support, and encouraging words.

I extend my heartfelt appreciation to all the PhD candidates and microbiology lab colleagues, Márcia Sousa, Ana Beatriz Gonçalves, Andreia Garcia, Liliane Ferrador and Rita Martins, with whom I have shared both joyful (few) and challenging (many) moments.

Lastly, I would like to aknowledge the Foundation for Science and Technology (FCT) of Portugal for their financial support, with reference 2020.07480.BD, which has enabled me to begin and continue this four years PhD project.

Abstract

Antimicrobial resistance (AMR) in clinically relevant pathogens is one of the most critical Public Health problems of the 20th century due to the high impact in mortality and morbility rates, and costs. *Klebsiella pneumoniae* is recognized as a critical threat due to increasing rates of infection by multidrug-resistant (MDR-*Kp*) and hypervirulent (hv*Kp*) sublineages exhibiting particular capsular (K) types. Capsular polysaccharides (CPS) not only serve as key epidemiological markers but also drive *K. pneumoniae* population diversification and influence environment-pathogen-host interactions, yet a major gap remains in understanding how CPS structural and production variations shape glycan-mediated interactions, adaptation, and virulence.

This thesis investigates the role of *K. pneumoniae* surface glycans in mediating interactions with the environment and host immunity, ultimately influencing the selection, persistence, and progression of MDR-*Kp* and hv*Kp* sublineages. By integrating knowledge in molecular epidemiology, rheology and glycomics, this work provides novel insights into how variations in capsule production and structure shape strain-specific adaptation and survival strategies. The **primary aim** is to expand knowledge on CPS properties and their impact on *K. pneumoniae* behavior, identifying key CPS-driven traits that could serve as targets for future diagnostic and therapeutic interventions.

To accomplish this goal, the prevalence and diversity of MDR-*Kp* and hv*Kp* in invasive *K. pneumoniae* isolates from a Portuguese hospital cohort was assessed, focusing on strain and capsular diversity (type and abundance). A representative set of strains of high-risk sublineages with variable capsules and production levels (hypermucoid-HM, regular mucoid-RM or non-mucoid-NM) was used to assess rheological properties and glycan-lectin recognition patterns. Hypermucoviscosity (HMV) and capsule abundance were quantified, and strains were characterized using rheological and textural assays under physiologically relevant flow conditions. Additionally, bacteria microarrays were employed to map glycan-mediated recognition patterns using a diverse set of lectins from different origins (plant, fungal, bacterial, mammalian).

The **results** of this thesis highlight a concerningly high prevalence of MDR-*Kp* (49%) in a northern Portuguese hospital, surpassing national levels (28%) and emphasizing the expansion of high-risk sublineages carrying genes encoding extended-spectrum beta-lactamases (CTX-M-15) or carbapenemases (KPC-3, OXA-48) along with specific capsular types (KL19, KL64, KL102). While hv*Kp* strains were rare (1.1%), their presence, characterized by enhanced capsule production (KL2, KL20) and hypermucoviscosity, underscores the need for improved surveillance. Integrating molecular epidemiology with rheological analysis revealed that CPS abundance and composition dictate *K. pneumoniae* physical behavior, impacting virulence and dissemination. HM strains, with

high CPS levels, exhibited low shear viscosity, which might favor rapid spread in the bloodstream, while NM strains showed greater adhesiveness, a factor that enhances tissue colonization. Notably, HM and HMV phenotypes were found to be dissociable traits, driven by genomic variability, refining hv*Kp* characterization and suggesting therapeutic strategies targeting viscosity modulation or adhesion disruption. Glycan-lectin recognition patterns analysis further demonstrated that lectin binding is dose-dependent and varies with strain-specific glycan profiles (CPS/K-types, LPS/O-types, and other unidentified glycans). We found that hypercapsule production can mask key surface ligands, reducing recognition by human lectins such as DC-SIGN, reinforcing that capsule amount is crucial for pathogen recognition and immune evasion. These findings suggest that CPS profiling can be used for risk stratification, and that interventions targeting rheological properties (e.g., viscosity modulation) or capsule production regulation may be effective. Further validation with *in vivo* and *in vitro* models is essential to advance these strategies.

This study highlights surface glycans as dynamic mediators of *K. pneumoniae* evolutionary success. By establishing a foundation for glycan-centric approaches, it proposes a paradigm shift in bacterial adaptation and infection control. Future research should integrate genomic and glycan-based surveillance of high-risk clones, explore genetic links between CPS production and biomechanical traits, and investigate how host factors influence CPS expression and virulence, paving the way for glycan-targeted vaccines and precision medicine strategies.

Keywords: *Klebsiella pneumoniae*, molecular epidemiology, capsular polysaccharides (CPS), rheology, glycomics

Resumo

A resistência aos antimicrobianos (AMR) em microrganismos patogénicos clinicamente relevantes é um dos problemas de saúde pública mais críticos do século XX devido ao seu alto impacto nas taxas de mortalidade e morbilidade, bem como nos custos associados. *Klebsiella pneumoniae* é reconhecida como uma ameaça global devido ao aumento das taxas de infeção por sublinhagens multirresistentes (MDR-*Kp*) e hipervirulentas (hv*Kp*), que exibem tipos capsulares (K) específicos. Os polissacarídeos capsulares (CPS) não só servem como marcadores epidemiológicos importantes, mas também impulsionam a diversificação da população de *K. pneumoniae* e influenciam as interações ambiente-patogénico-hospedeiro. No entanto, continua a existir uma grande lacuna no entendimento de como as variações estruturais e de produção dos CPS moldam as interações mediadas por glicanos, a adaptação e a virulência.

Esta tese investiga o papel dos glicanos de superfície de *K. pneumoniae* na mediação das interações com o ambiente e a imunidade do hospedeiro, influenciando, em última análise, a seleção, a persistência e a progressão das sublinhagens MDR-*Kp* e hv*Kp*. Ao integrar conhecimentos em epidemiologia molecular, reologia e glicómica, este trabalho fornece novas perspetivas sobre como as variações na produção e estrutura da cápsula moldam as estratégias de adaptação e sobrevivência específicas ao nível da estirpe. O **objetivo principal** é expandir o conhecimento sobre as propriedades dos CPS e o seu impacto no comportamento de *K. pneumoniae*, identificando características moduladas pelos CPS que possam servir como alvos para futuras intervenções diagnósticas e terapêuticas.Para alcançar este objetivo, foi avaliada a prevalência e diversidade de estirpes MDR-*Kp* e hv*Kp* numa coleção de isolados invasivos de *K. pneumoniae* de umhospital português, com foco na diversidade de estirpes e cápsulas (tipo e abundância). Um conjunto representativo de estirpes que representam sublinhagens de alto risco com diferentes tipos de cápsulas e variáveis níveis de produção (hipermucoides-HM, mucoides regulares-RM ou não mucoides-NM) foi utilizado para avaliar as propriedades relacionadas com a reologia e os padrões de reconhecimento glicano-lectina. A hipermucoviscosidade (HMV) e a abundância da cápsula foram quantificadas, e as estirpes foram caracterizadas usando ensaios reológicos e texturais sob condições de fluxo fisiologicamente relevantes. Além disso, *microarrays* bacterianos foram utilizados para mapear padrões de reconhecimento mediados por glicanos usando um conjunto diversificado de lectinas de diferentes origens (vegetal, fúngica, bacteriana, mamífera).

Os **resultados** desta tese destacam uma alta e preocupante prevalência de MDR-*Kp* (49%) em um hospital do norte de Portugal, superando os níveis nacionais (28%) e enfatizando a expansão de sublinhagens de alto risco que contêm genes que codificam para

beta-lactamases de espectro ampliado (CTX-M-15) ou carbapenemases (KPC-3, OXA-48) juntamente com tipos capsulares específicos (KL19, KL64, KL102). Embora as estirpes hv*Kp* sejam raras (1,1%), a sua presença, caracterizada por uma produção aumentada de cápsula (KL2, KL20) e a sua hipermucoviscosidade, sublinha a necessidade de melhorar a vigilância. A integração da epidemiologia molecular com a análise de reologia revelou que a abundância e composição dos CPS ditam o comportamento físico de *K. pneumoniae*, impactando a virulência e a disseminação. As estirpes HM, com altos níveis de CPS, exibiram baixa viscosidade, o que pode favorecer a rápida disseminação no sangue, enquanto as estirpes NM mostraram maior adesividade, um fator que melhora a colonização de tecidos. Notavelmente, os fenótipos HM e HMV foram encontrados como características dissociáveis, impulsionados pela variabilidade genómica, contribuindo para a caracterização de estirpes hv*Kp* e a identificação de estratégias terapêuticas que visam a modulação da viscosidade ou a interrupção da adesão. A análise dos padrões de reconhecimento glicano-lectina demonstrou ainda que a ligação das lectinas ocorre de forma dependente da disse e varia com perfis de glicanos específicos para cada estirpe (CPS/tipos K, LPS/tipos O e outros glicanos não identificados). Descobriu-se que a hiperprodução de cápsula pode mascarar ligandos de superfície importantes, reduzindo o reconhecimento por lectinas humanas como DC-SIGN, reforçando que a quantidade de cápsula é crucial para o reconhecimento do patógeno e evasão imunológica. Estes resultados sugerem que a caracterização de perfis dos CPS pode ser usado para estratificação de risco, e que intervenções que visam as propriedades reológicas (por exemplo, modulação da viscosidade) ou a regulação da produção da cápsula podem ser eficazes. Uma validação adicional em modelos *in vivo* e *in vitro* é essencial para avançar nessas estratégias.

Este estudo destaca os glicanos de superfície como mediadores dinâmicos do sucesso evolutivo de *K. pneumoniae*. Ao estabelecer uma base para abordagens centradas em glicanos, esta tese propõe uma mudança de paradigma na adaptação bacteriana e no controle de infeções. Estudos futuros devem integrar dados de genómica, glicómica e de biomecânica relacionados com a produção de CPS em clones de alto risco, e investigar como os fatores do hospedeiro influenciam a expressão de CPS e a virulência, abrindo caminho para novas estratégias de prevenção (vacinas) ou de tratamento (medicina de precisão).

Palavras-chave: *Klebsiella pneumoniae*, epidemiologia molecular, polissacarídeos capsulares (CPS), reologia, glicómica

Table of contents

1. Introduction **1**

1.1. *Klebsiella pneumoniae*: definition of a growing Public Health problem 3

1.2. Phylogenetic diversity and ecological distribution of *K. pneumoniae* 5

1.2.1. Taxonomy and phylogenetic relationships of *K. pneumoniae* species complex 5

1.2.2. From environmental reservoirs to opportunistic infections 7

1.3. Genomics insights into *K. pneumoniae* population structure and adaptive traits 8

1.3.1. Multidrug resistant *K. pneumoniae* subpopulations 9

1.3.2. Hypervirulent *K. pneumoniae* (hv*Kp*) 12

1.4. Diversity and roles of surface polysaccharides in *K. pneumoniae* 15

1.4.1. Structure, genetics and clinical relevance 15

1.4.2. Impact on environmental survival and adaptation 17

1.4.3. Impact on immune evasion and host interaction 18

2. Objectives **21**

3. Results **25**

3.1. Molecular epidemiology of invasive *Klebsiella pneumoniae*: unravelling the dynamics of antibiotic-susceptible and antibiotic-resistant in bloodstream infections 27

3.2 Unmasking the role of capsule rheology in *Klebsiella pneumoniae* pathogenesis 50

3.3. Strain-specific glycosignatures in representative multidrug resistant and hypervirulent *Klebsiella pneumoniae* sublineages 71

4. Discussion and conclusions **88**

5. References **93**

6. Supplementary material **108**

6.1. Emergence of NDM-1 and KPC-3 carbapenemases in *Kluyvera cryocrescens*: Investigating genetic heterogeneity and acquisition routes of $bla_{\text{NDM-1}}$ in Enterobacterales species in Portugal 110

List of Figures

Figure 1 - *Klebsiella pneumoniae*, a major Public Health problem by global health organizations 5

Figure 2 - Taxonomy and phylogeny of *Klebsiella* genus 6

Figure 3 - *K. pneumoniae* capsule structures involved in persistence and virulence 16

List of Tables

Tables S1: Fluorescence activity of lectin-bacteria microarrays 115

List of abbreviations:

AMR: anti-microbial resistance

ANI: average nucleotide identity

BSI: bloodstream infections

CDC: Centers for Disease Control and Prevention

CBM: carbohydrate-binding module

CG: clonal group

CR-hv*Kp*: carbapenem-resistant hypervirulent *K. pneumoniae*

CR*KP*: carbapenem-resistant *K. pneumoniae*

CTX-M: cefotaxime-hydrolyzing β-lactamase

EARS: European Antimicrobial Resistance Surveillance Network

ECDC: European Centre for Disease Prevention and Control

ESBL: extended spectrum β-lactamases

FT-IR: Fourier-transform infrared

GI: gastrointestinal

HGT: horizontal gene transfer

HAI: healthcare-associated infection

HMV: hypermucoviscosity

hv: hypervirulence

hv*Kp*: hypervirulent *K. pneumoniae*

ICU: intensive care units

IDSA: Infectious Diseases Society of America

IMP: imipenemase

iuc: *iuc*ABCD-*iut*A operon that encodes for aerobactin

iro: *iro*BCDEN operon involved in salmochelin synthesis

K-type: capsular type

KPC: *Klebsiella pneumoniae* carbapenemase

KL: capsular locus

LPS: lipopolysaccharide

MALDI-TOF: matrix-assisted laser desorption/ionization time-of-flight

MBL: metallo-β-lactamase

Mbp: mega base pair (x1000000 base pairs)

MDR-*Kp*: multidrug-resistant *K. pneumoniae*

MDR: multidrug resistance

MGE: mobile genetic element

mcr: mobile colistin resistance

mgrB: membrane glycoprotein regulator B

MLST: multi-locus sequence typing

NDM: New Delhi metallo-β-lactamase

OPS: O-polysaccharide

OXA: oxacillinase

PLA: pyogenic liver abscesses

peg-344: plasmid-encoded gene 344

rmpA: regulator of mucoid phenotype A

SHV: sulfhydryl variable β-lactamase

ST: sequence type

TEM: temoniera

UVC: ultra-violet C light

UTI: urinary tract infections

VIM: Verona integron-encoded metallo-β-lactamase

WGS: whole genome sequencing

WHO: World Health Organization

Introduction

1.1. *Klebsiella pneumoniae*: definition of a growing Public Health Problem

As early as in 1882, Carl Friedländer identified an encapsulated bacillus isolated from the lungs of individuals who had died from pneumonia. [1] Initially referred to as Friedlander's bacillus, the organism was officially named *Klebsiella* in honour of Edwin Klebs in 1886 for his contributions in the field of microbiology. The bacterium was classified as a rod-shaped (bacillus), encapsulated, non-motile Gram-negative organism named as *Klebsiella pneumoniae*. Since then, it evolved until today from a rare cause of pneumonia to a major global pathogen, increasingly associated with human infections.

Its incidence rose significantly throughout the 20th century, driven by antibiotic resistance and the spread of strains simultaneously resistant to different antibiotics, leaving clinicians with very few options for treatment, increased mortality and morbidity associated with these infections. In fact, resistance to first and last-line antibiotics such as β-lactams is now very common worldwide, and has significant expression in some geographic settings. [2,3] Besides the clinical concern, the economic burden is impactful, with prolonged hospital stays and increased healthcare costs due to the need for longer and more advanced treatments. [4] A report from September 2024 ranked *K. pneumoniae* as one of the six organisms with an attributable burden estimated to exceed 100,000 deaths associated with antimicrobial resistance (AMR) in 2021. [5] Of note, *K. pneumoniae* was found to be the most common pathogen causing sepsis in neonates and children under 5 years old, with special incidence and concern in low-and-middle-income countries (LMIC). [6,7] Similarly, the European Centre for Disease Prevention and Control (ECDC) recognizes *K. pneumoniae* as a major cause of healthcare-associated infections (HAIs). According to the ECDC report on surveillance data, *K. pneumoniae* ranks as the third most common pathogen in pneumonia, bloodstream infections (BSIs), and urinary tract infections (UTIs) acquired in intensive care units (ICUs). [8,9] Most of the disease burden is in hospital patients, where *K. pneumoniae* has long been a leading cause of HAI as an agent of pneumonia, BSI and UTI. [10] Vulnerable populations such as the elderly or neonate individuals, patients with high healthcare exposure, and with underlying conditions or immunocompromised states, are at a higher risk of infection. [11,12] The high incidence of infection is also affected by the heightened transmissibility of *K. pneumoniae* between patients within healthcare settings, and the difficulties in implementing infection control strategies to prevent outbreaks and subsequent dissemination. [13–15]

More recently, other syndromes responsible for a higher mortality have been increasingly described, such as pyogenic liver abscesses (PLA), endophthalmitis, and meningitis, caused by a rapid metastatic spread of the bacteria from the initial infection sites. [16–18] These infections can course towards a condition leading to multiple organ

dysfunction syndrome, septic shock, and intra-abdominal sepsis. [19] Infections are both severe and life-threatening, [20,21] and while particularly prevalent in Asian populations for reasons yet unknown, concern is raising due to their increasing incidence in Europe. [22] Thus, the high mortality and morbidity rates, the increase of AMR, the growing size of vulnerable populations and the emergence of invasive syndromes underscore the urgent necessity for a deeper understanding of this pathogen.

For these reasons, different global health institutions recognized *K. pneumoniae* as an important pathogen to tackle (Figure 1). In 2024, the World Health Organization ranked *K. pneumoniae* in the list of organisms with high priority for research and investment, including activities to promote enhanced surveillance and control of antimicrobial resistance burden (Figure 1). [9] In 2019, the US Centers for Disease Control and Prevention (CDC) defined carbapenem resistant *Enterobacteriaceae*, a family in which *K. pneumoniae* is included, as urgent antimicrobial resistance threat. [23] The Infectious Diseases Society of America (IDSA) proposed an acronym (E.S.K.A.P.E.) to encompass *Enterococcus faecium*, *Staphylococcus aureus*, *K. pneumoniae*, *Acinetobacter baumannii*, *Pseudomonas aeruginosa*, and *Enterobacter* species (sometimes extended to *Escherichia coli* too, as E.S.K.A.P.E.E.), [24] to represent the "escape" of these pathogens to the action of antibiotics. The acronym is also used to emphasize the urgent need for new antimicrobials and to enforce global research, antimicrobial stewardship, and drug development efforts.

A multisectoral and multidisciplinary approach is needed to tackle this relevant problem. While it is urgent to invest in novel antimicrobials or therapeutic strategies, this is not enough to control and sustain emergence and dissemination of bacteria of Public Health importance.

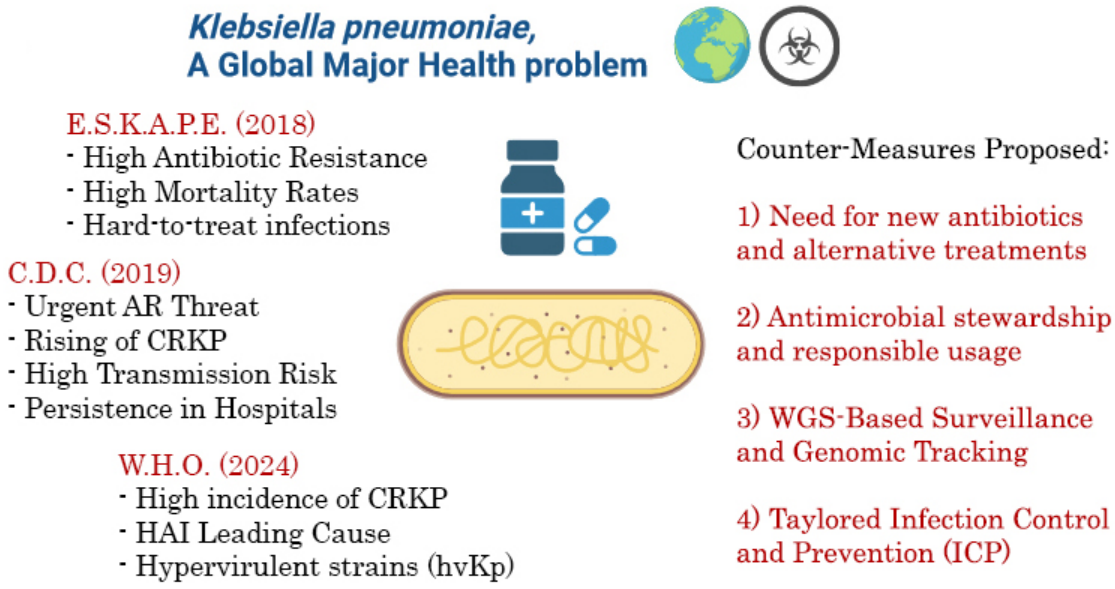


Figure 1. *K. pneumoniae*, a major Public Health problem by global health organizations.

Together with tackling research and investment in a One Health perspective, education and awareness, new diagnostics tools and improved capacity for detection and control are needed, especially in LMIC. [9] In *K. pneumoniae*, a great effort has been done by the scientific community to clarify aspects related to population genomics and evolution, virulence and pathogenicity, and to the emergence and dissemination routes of AMR and virulence traits. It is well recognized though that continuous surveillance of strains with particularly worrying AMR or virulence traits is required, as well as a deeper understanding of fundamental aspects driving persistence, invasiveness and host adaptation. [3,25]

1.2. Phylogenetic diversity and ecological distribution of *K. pneumoniae*

1.2.1. Taxonomy and phylogeny of *K. pneumoniae* species complex

K. pneumoniae is part of the genus *Klebsiella*, in the order Enterobacterales and class of Gammaproteobacteria. This species is part of the *Klebsiella pneumoniae* species complex (*Kp*SC) comprising highly related species, primarily recognized as seven phylogroups or taxa, based on *gyrA* sequences phylogeny. [26] Later, the first wide genome-based phylogenetic studies based on whole genome sequencing (WGS) allowed high-resolution phylogenetic affiliation and facilitated the identification of additional member species (Figure 2). [27,28] Accurate delineation of *K. pneumoniae* related species supported the identification of specific protein biomarkers using matrix-assisted laser desorption/ionization time-of-flight mass spectrometry (MALDI-TOF MS). [29]

Species from *Kp*SC include *K. pneumoniae sensu stricto* (phylogroup *Kp*1), [30] *Klebsiella quasipneumoniae* with its subspecies *quasipneumoniae* (*Kp*2) and *similipneumoniae* (*Kp*4), [31] *Klebsiella variicola* subsp. *variicola* (*Kp*3) [32] and *tropica* (*Kp*5), [33] *Klebsiella quasivariicola* (*Kp*6) [34] and *Klebsiella africana* (*Kp*7). [33] Prior to the identification of *K. variicola* subsp. *tropica*, *K. quasivariicola* and *K. africana,* the phylogrups of the *Kp*SC were designated as: *Kp*I for *K. pneumoniae sensu stricto*, *Kp*II for *K. quasipneumoniae* subspp. *quasipneumoniae* (*Kp*IIa) and *similipneumoniae* (*Kp*IIb), and *Kp*III for *K. variicola* subsp. *variicola*. [26,35] Other *Klebsiella* spp. have suffered great taxonomic re-structurations, namely with the reassignment of the former *Enterobacter aerogenes* to *Klebsiella aerogenes*, [36] the reassignment of *Raoutella* species to the *Klebsiella* genus, [37] and the identification of a group of species highly related to *K. oxytoca*. [38]

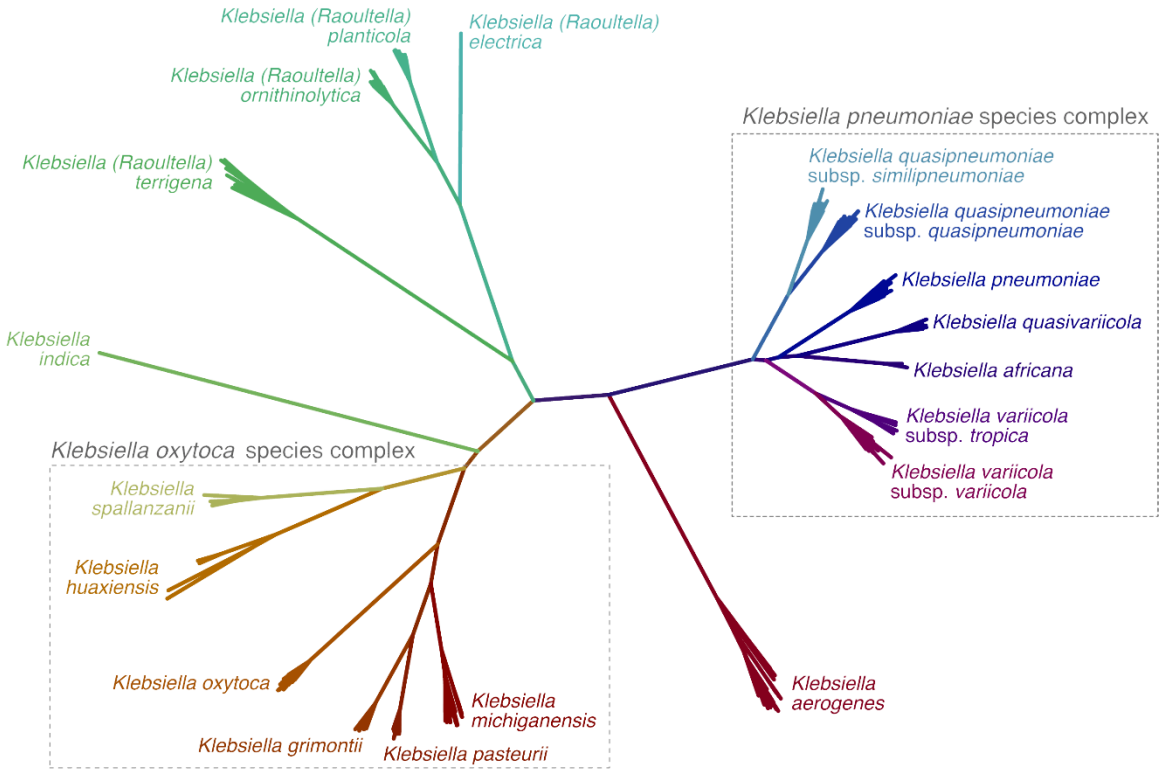


Figure 2. Taxonomy and phylogeny of *Klebsiella genus*.
Phylogenetic relationships between *Klebsiella* spp. Adapted from kleborate.readthedocs.io/en/latest/*Kp*sc_modules.html with the permission of the author.

High-resolution genomics by WGS has clarified that these *Kp*SC species and subspecies share 95-96% average nucleotide identity (ANI) with *K. pneumoniae sensu stricto*, but only 90% ANI with other *Klebsiella* species. Within the *Kp*SC, intra-species pairs show ANI values ranging from 98% to 100%, while inter-phylogroup strain comparisons have ANI

values from 92.8% to 100%. [27,39] Due to the high genetic similarity among *Kp*SC members, routine clinical microbiology identification methods often result in inaccurate recognition at species level. [29,39] This is explained with the limited resolution of automated systems (e.g. VITEK 2), which rely on biochemical profiles, and the insufficient coverage of available databases used in commercial MALDI-TOF MS-based systems. Difficulties in accurate differentiation of these highly related species are on the basis of the recommendation to identify them as members of the *Kp*SC group.

1.2.2. From environmental reservoirs to opportunistic infections

The genomic diversity of *Kp*SC species favours the ability of the members of this group to occupy diverse ecological settings. In fact, these species can be found and adapt to different environments including soil, water, plants, and hosts (humans and animals). [10,40] The successful distribution of the *Kp*SC is facilitated by high phenotypic heterogeneity and metabolic diversity. [41,42] The wide ecological range, together with the high genome plasticity, make *Kp*SC ideal reservoirs and traffickers of AMR genes, from environmental sources to specific pathogenic strains as well as to other species. [40]

K. pneumoniae is found as a commensal in the normal microbiota in the gastrointestinal (GI) tracts of healthy humans and animals (including food animals), specifically in the colon, intestinal and biliary tract, with carriage rates that vary significantly among different populations and dietary habits. It may also colonize the skin, pharynx, wounds and urine, whereas oropharyngeal carriage has been associated with endotracheal intubation, impaired host defence, and antimicrobial use. [43]

As a natural inhabitant in humans, *K. pneumoniae* can exploit host vulnerabilities to cause opportunistic infections, taking profit of comorbidities, weakened or immunocompromised immune systems, hence why most of the disease burden is associated with hospitalized patients or patients with relevant health conditions. [16,17] These infections often result from strains that are present in the patient's own microbiota, or otherwise acquired within hospital settings from other patients, through contaminated items or environments, such as sinks or drains. [44,45] As such, GI colonization is recognized as a heightened risk factor for subsequent infections, with increased risk if *K. pneumoniae* acquisition occurs during hospitalization, reinforcing the necessity to monitor high-risk strain colonization. [44,46]

Other species from the *Kp*SC complex are also well-known opportunistic pathogens, though they are, in comparison, less frequently associated with HAIs and have less pathogenic potential. While *K. pneumoniae* causes about 10% of HAIs globally, *K. variicola* and *K. quasipneumoniae* collectively account for <2% of reported cases. [17,47] In one study,

K. variicola represented around 14% of HAI infections, [47] but it has also been identified as an endophyte in plants, [48] contributing to nitrogen fixation in certain natural environments, [49] and is particularly frequent in bovines. [50] *K. quasipneumoniae* has been mainly associated with environmental reservoirs, humans and colonization over infection. [51] Only recently it has been recognized that these species represent about 20% of nosocomial infections since knowledge on ecology, pathogenicity and molecular epidemiology has been limited by difficulties in species differentiation. [17,27]

1.3. Genomics insights into *K. pneumoniae* population structure and pathogenic traits

The *K. pneumoniae* genome typically ranges in size from 5.3 to 5.6 megabase pairs (Mbp), including a core and accessory genome, with an average of >5000 genes. [3] Around 1700 genes are classified as core genes since they are present in >95% of all sequenced genomes, exhibiting a high degree of conservation across the species. [27] Additionally, *K. pneumoniae* possess a vast accessory genome, characterized by genes that vary across different strains, and that are present in <10% of genomes, making them rare in the population. [27,52] Overall, the pan-genome, which include core and accessory genome, comprises >100,000 coding genes. [27] *K. pneumoniae* accessory genome is characterized by adaptability traits, including virulence and resistance-associated functions that can be shared between different strains. [3,27] Thus, the accessory genome influences the behaviour of the strain, i.e., if it acts as an asymptomatic colonizer or as a pathogen. [17,27] Moreover, this genetic repertoire can also be shared between members of *Klebsiella* genus other than *Kp*SC, as well as other species within the Enterobacterales order, promoting the intra- and inter-species acquisition of traits through horizontal gene transfer (HGT). [53]

Genomic surveillance studies [54,55] have been key not only to define the composition of the *K. pneumoniae* genome but also to identify hundreds of deep-branching phylogenetic lineages, defined by core-genome multilocus sequence typing (cgMLST) and designated as clonal groups (CGs), or based on core genome phylogenetic analyses within *K. pneumoniae*. [3,27] These high-resolution approaches allowed a more precise definition of genetically related strains that evolved from a common ancestor and belong to the same clonal sublineage. [58] Despite the high diversity, the *K. pneumoniae* population is highly structured in two subpopulations, defined essentially as two primary pathotypes: multidrug-resistant (MDR-*Kp*) strains, responsible for HAIs in hospitalized patients, and hypervirulent (hv*Kp*) strains, associated with hypervirulence phenotypes and life-threatening infections, frequently acquired in the community. From these, a set of sublineages are responsible for

the majority of human infections, and are usually referred to as “global problem” clones, [3] or “high-risk” clones, [54,55] for being recognized as globally distributed subpopulations with enhanced ability to colonize, spread and persist in different niches, through the acquisition of particular adaptive traits that include antimicrobial resistance and virulence factors.

Comparative genomics studies have elucidated the evolutionary dynamics, genetic variation, and pathogenicity of the two pathotypes, with the aim of clarifying mechanisms of antimicrobial resistance, invasiveness and virulence in *K. pneumoniae*. These aspects will be further explored in the following subchapters.

1.3.1. Multidrug resistant *K. pneumoniae* subpopulations

Multidrug resistance (MDR) refers to the ability of a microorganism to exhibit resistance to at least one antimicrobial drug from three or more different classes. [58] *K. pneumoniae* is intrinsically resistant to ampicillin due to the production of a chromosomally-encoded Amber class A β-lactamase named SHV, reason why ampicillin is not recommended for phenotypic testing in this species. [59] MDR arises from the acquisition of AMR genes by HGT or, less commonly, by acquisition of mutations in chromosomal genes. [25] In *K. pneumoniae*, acquired genes are usually co-located in mobile genetic elements (MGE), most frequently plasmids (e.g. $bla_{\text{CTX-M-15}}$-IncF), transposons (e.g. bla_{KPC-3}-Tn*4401*) or integrons (e.g. *aadA1*) to mention just a few examples. [25] These elements have a mosaic structure and evolve through genetic events that promote shuffling and acquisition of additional resistance traits, conferring a high plasticity to this part of the accessory genome. The presence of different genes in the same genetic platforms results, frequently, in combined resistance to first- and last-line β-lactams (e.g. *bla* genes), fluoroquinolones (e.g. *qnrA*, *qnrB*) or aminoglycosides (*aph*, *aad*, *aac*) in *K. pneumoniae*. [8] Other common mechanisms of resistance are the acquisition of mutations in topoisomerase genes (*gyrA*, *parC*), resulting in fluoroquinolone resistance, [60] and mutations or disruption in main porins (OmpK35, OmpK36) [61] or genes associated with efflux pumps regulation, affecting permeability and enhancing extrusion of β-lactams and other antibiotics.

The spread of MDR pathogens can have severe consequences. In some cases, the bacteria become resistant to most (if not all) available antibiotics, further complicating treatment and infection control efforts. [62] This situation leads to increased morbidity, mortality, and healthcare costs, further exacerbated by the risk of transmission within healthcare settings and the community. [63] In fact, pandrug-resistant infections have been

reported, leading to fatal outcomes among patients infected with MDR-*Kp*. [64–66] This results in few therapeutic options, often combinations of different antibiotics, new therapeutic approaches such as new inhibitor combinations, and/or phage therapies as last resort. [67]

The incidence and diversity of MDR-*Kp* bacteria have greatly increased throughout time, strongly impacting therapeutic options and clinical outcomes. Since the early 1990s, resistance to third generation cephalosporins increased significantly, due to the acquisition and expansion of genes encoding extended-spectrum β-lactamases (ESBLs). Though the molecular epidemiology varies considerably within countries, the steady rates of ESBL-producing *K. pneumoniae* have increased in Europe (from 1.7% to 64.9% in 2023), [8] and there are regions with high endemicity, such as Eastern European, Mediterranean, and South Asian countries. [8,9] The main ESBL families include CTX-M (cefotaxime-hydrolyzing β-lactamase), TEM (temoniera β-lactamase), and SHV (sulphydryl variable enzyme), with CTX-M variants (particularly CTX-M-15) being the most prevalent globally.

In the 1990s, the emergence of carbapenem resistant *K. pneumoniae* (CRKP) marked a critical shift, as these strains were resistant to last-line β-lactams and posed significant Public Health threats in terms of infection treatment and control. The European Antimicrobial Resistance Surveillance Network (EARS-Net, 2023 data) estimated the incidence of CRKP bloodstream infections in the EU at 3.97 cases per 100,000 population, representing a +57.5% increase compared to 2019, with a statistically significant upward trend between 2019 and 2023. [68] In fact, CRKP strains are associated with high mortality rates (42%) in HAI, and demonstrate high transmissibility within healthcare settings, contributing to intra- and inter-hospital outbreaks. [69,70] CRKP have been rising globally and notably in Europe, [8] including in specific countries like Portugal. [71,72] The European population-weighted mean percentage of carbapenem resistance in invasive *K. pneumoniae* increased from 10.4% in 2019 to 13.3% in 2023, reflecting a 28% relative rise over four years. [73]

The first gene encoding a carbapenemase ($bla_{\text{KPC-1}}$, currently $bla_{\text{KPC-2}}$), an enzyme capable of hydrolysing carbapenems, was described in 2000 in the US. [74] Soon after its emergence, *K. pneumoniae* strains with bla_{KPC} caused outbreaks in US hospitals and in the middle 2000's they spread in several EU countries, the first cases associated with travelling patients. KPC-producing *K. pneumoniae* are currently endemic in certain parts of the world. North America has reported around 14% of KPC-producing isolate, whereas much higher rates have been reported for South Asia (66%), Greece or India (~70%). Apart from bla_{KPC} (class A carbepenemase), other families encoding class B (NDM, VIM, IMP) and class D (OXA-48) carbapenemases contribute for a high diversity of phenotypes and epidemiological landscapes. [75] OXA-48 and OXA-181 have been involved in several

outbreaks and are currently endemic in certain regions (Middle East, North Africa, Spain, France, and Belgium for OXA-48, Sub-Saharan Africa and the Indian Subcontinent for OXA-181), [76] VIM and IMP metallo-β-lactamases have emerged sporadically but recent reports suggest they are increasing. [77,78] NDM (New Delhi metallo-β-lactamase) has been firstly reported in 2008, and it is currently endemic in the Indian subcontinent, Middle East, and the Balkans. [79] Other mechanisms of resistance to carbapenems can also occur, such as reduced outer membrane permeability caused by porin loss or higher efflux pump activity, though they are much less relevant. [69,80]

The rise in carbapenems resistance forced the reintroduction of older antibiotics like colistin, which carry significant toxicity risks. [81] Colistin has been often used as a last-resource antibiotic but the emergence and rapid spread of plasmid-mediated colistin resistance through *mcr* (mobile colistin resistance) genes has further limited treatment options. [82,83] Colistin resistance has emerged as a global health threat, with first reports from China, [84] and then diffused to the Indian subcontinent. [85–87] Clonal outbreaks driven by *mgrB* gene disruptions have also been reported in Europe and Asia (15% increase in 2014-2022). [88–90]

Clonal expansion has also greatly contributed to the increasing rates of MDR-*Kp* at local, national and global levels, and specific sublineages are recognized as high-risk due to their enhanced ability to colonize, spread and persist. Many of these are globally disseminated and contribute to both intra- and inter-hospital spread of carbapenemase-producing strains. [70] The 2013/2014 European Survey of Carbapenemase-producing *Enterobacteriaceae* (EuSCAPE) identified ST11, ST15, ST101, and ST258/512 as the most CRKP sequence types (STs) in Europe. [70] These STs remained prevalent across European hospitals in 2019, [91] while other high-risk clones, such as ST147, ST307, and ST39, have since emerged and became dominant in multiple geographies. [92] Other globally distributed clones, including ST147, [93,94] ST307 (frequently linked to $bla_{\text{CTX-M-15}}$), [95] ST340, [96,97] and ST437, [98] show regional variability but continue to spread internationally through travel networks and healthcare-associated transmission.

High resolution genomic studies have also revealed that many of these successful CGs are composed by distinct sublineages, each of them carrying a specific capsular locus, which has been used as an epidemiological marker for detection and infection control. [99,100] For example, CG258 (including ST258) comprises two main sublineages linked to KL107 or KL106. [80,101] Similarly, CG14 and CG15 strains show geographical differences in KL-types, with CG15 exhibiting most frequently KL24, or KL112 variants in European outbreaks, while CG14 being associated with KL2 or KL16. [102] Other widespread sublineages are ST147-KL64 or ST307-KL102. [94,103] Although the capsular locus is a recombination hotspot that

drives high variability in *K. pneumoniae* populations, only a few KL types are linked to a higher disease burden. While this may result from selection pressures on the strain's genetic background or niche-specific advantages, it is crucial to investigate the role these capsules play in the selection and expansion of specific sublineages, a topic that remains largely unexplored. The next section will explore how structural diversity in surface polysaccharides impacts *K. pneumoniae* pathogenesis, environmental adaptation, and inform alternative therapeutic strategies.

1.3.2. Hypervirulent *K. pneumoniae* (hv*Kp*)

Hypervirulent *K. pneumoniae* (hv*Kp*) is an increasingly recognized pathotype defined by enhanced virulence and the ability to cause severe and invasive infections in healthy individuals, while being usually antibiotic susceptible. [16,104] It was firstly described in Taiwan in 1986, [105] although genomic analyses suggest it may have existed as early as the 1920s. [106] Since its emergence, hv*Kp* strains have increasingly been reported from the Asian Pacific Rim, especially in South Korea, Japan, and China, and are now expanding in different geographical areas, being increasingly recognized in Europe. [22] Often, hv*Kp* involve multiple sites of infection due to the metastatic spread to distant organs, such as the eye and the central nervous system. [20, 88] Usually from primary hepatic abscess (in absence of biliary pathology), common clinical presentations include pneumonia, and, less frequently, necrotizing fasciitis, endophthalmitis, and meningitis. [104,108,109]

Hv*Kp* strains share with MDR-*Kp* a set of core chromosomal genes that constitute the asset required to cause opportunistic infections, such as *ent* (encoding for enterobactin), *fim* and *mrk* (encoding for type 1 and type 3 fimbriae respectively), and the biosynthesis loci for capsular polysaccharide (K antigen) and lipopolysaccharide (O antigen) production, respectively encoded by *cps* and *rfb*. [141] Besides, the hypervirulent phenotype seems to be encoded by a set of genes located on a large virulence plasmid of about 200 Kb (pK2044 or pLVPK) and/or integrative and conjugative elements (ICEs), facilitating the horizontal transfer of virulence determinants to other strains. These include several genes encoding for siderophores. The siderophores aerobactin (gene cluster *iuc*), salmochelin (gene cluster *iro*), and yersinabactin (gene cluster *ybt*), are crucial molecules serving as iron chelators, enhancing hv*Kp* ability to thrive in host tissues by efficiently scavenging iron and competing to host iron-chelating proteins, thereby contributing to hv*Kp* survival and proliferation at the expenses of the host during infection. [104,107,110] All of them have been shown to increase virulence in the *in vivo* models. [111,112] Furthermore, genes encoding regulators of the mucoid phenotype (*rmpA* and *rmpA2*) contribute to enhance hv*Kp*

virulence by increasing capsule production, potentially by impeding phagocytosis and facilitating intracellular survival within macrophages. [104] The putative metabolite transporter *peg-344* is another plasmid-located gene which may play a role in nutrient uptake, contributing to virulence in pulmonary infection models. [104,113]

Additionally, some hv*Kp* strains contain colibactin (*clb*) within an ICE (ICE*Kp10*), a genotoxin that promotes tissue colonization and has been implicated in the invasion of the central nervous system. [107] Supported by genetic surveillance studies and experimental models, these virulence markers are incorporated into algorithms for rapid and accurate detection of hv*Kp* strains. Russo *et al.* [110] proposed the screening of *iucA*, *iroB*, *peg-344*, $_{p}$*rmpA*, and $_{p}$*rmpA2*, whose presence is highly predictive of hv*Kp* status (>95% of accuracy). Lam *et al.* [114] designed a virulence score (from 0 to 5, calculated on a risk stratification), based on the presence of *ybtS*, *iuc*, *iro*, *clb*, and *rmpA* gene markers, weighting *ybt* < *col* < *iuc*. This score has been incorporated in KLEBORATE, a genomic surveillance tool specifically designed for *K. pneumoniae* characterization. [114]

Hv*Kp* strains typically show a hypermucoviscous (HMV) phenotype. [104,108] It is identified by the "string test", during which a viscous filament exceeding 5 mm in length is observed after stretching a *Klebsiella* spp. colony with a loop on an agar plate. [110] Traditionally, hypervirulence and HMV have been used indistinctly to represent strains with the ability to cause invasive infections in apparently healthy individuals. However, there is an increasing evidence that the hypermucoviscous phenotype alone does not confer hypervirulence, and that not all the hypervirulent *K. pneumoniae* variants causing invasive infections are HMV. [115,116] This indicates that hypermucoviscosity and hypervirulence should be considered as distinct traits. [117] Consequently, the string test lacks the sensitivity and specificity for a definitive hv*Kp* identification, necessitating consideration of invasion-related clinical characteristics, and recognition requiring clinical data and molecular detection of other virulence-associated determinants. Besides, the exact biophysical properties of HMV (e.g. textural or rheological) that enhance survival or immune evasion remain underexplored. [118]

The strong association of hv*Kp* strains with K1 or K2 capsular (K) types (~70%) [119] has historically led to the assumption that capsule production is the primary virulence factor in hv*Kp*. However, studies have revealed that HMV does not necessarily correlate with hypermucoidy (capsule overproduction) or virulence, highlighting important distinctions among these traits. Further supporting this notion, the discovery of *rmpD* (part of the *rmpA* operon) demonstrated that the HMV phenotype can be disrupted without affecting capsule biosynthesis. As such, *rmpD* mutants lose the HMV phenotype while retaining wild-type capsule levels. [118,120]

The geographic prevalence of hv*Kp* is highly variable. Endemic regions in Asia report hv*Kp* rates between 12% and 45%, with K1-ST23 being the dominant lineage. [121] North America shows greater genetic diversity among hv*Kp* strains, where K2 lineages are associated with ST66 and ST375. In Europe, CG23 (including ST23, ST25, ST57, and ST1633) is the most frequently identified lineage, [106] followed by CG65 (ST65, ST375) [122] and CG86. [123] Cases involving K2-ST380 and K2-ST86 have also been documented. [119] While hv*Kp* was previously rare in the EU/EEA, sustained healthcare-associated transmission of hv*Kp* ST23 carrying carbapenemase genes has now been documented in Ireland, and the ECDC raised awareness on increasing sporadic reports and possible unnoticed dissemination in Europe [22]

Of particular concern is the emergence of carbapenem-resistant hypervirulent *K. pneumoniae* (CR-hv*Kp*), which poses a significant threat due to clinical impact and the potential for cross-border dissemination. [124] According to the ECDC, the risk of further spread and establishment of CR-hv*Kp* in healthcare settings across EU/EEA countries is considered high, with potentially severe consequences for morbidity and mortality. [22] Such phenomenon results from the mobile nature of both virulence and AMR traits, which can be acquired, respectively, by MDR-*Kp* or hv*Kp* strains via HGT. For reasons not fully understood, possibly related to capsule-imposed restrictions, [125] the majority of the convergent strains result from acquisition of hypervirulent plasmids or by the formation of AMR-HV hybrid plasmids in widespread MDR sublineages, such as ST11, ST15, ST147 or ST307. [126]

While genomic studies have been key to elucidate diversity, evolutionary trends, and the genetic support for pathogenicity, there are several aspects that require further clarifications. First, *in vivo* studies have confirmed the role of specific genetic traits in virulence, but there are also conflicting results, such as HMV inconsistent correlation with virulence, [127,128] and lethality in rare strains (e.g. ST661) lacking traditional virulence genes. [129] Second, it is well known that certain capsular types are epidemiological markers of critical, high-risk *K. pneumoniae* sublineages. However, key knowledge gaps include understanding the role of specific K-types and particular phenotypes in persistence and pathogenesis. Addressing these gaps is essential for developing targeted strategies to combat hv*Kp* infections. Following, we will delve into surface polysaccharides variation among *K. pneumoniae* strains and how this impacts their pathogenicity and immune system evasion.

1.4. Diversity and roles of surface polysaccharides in *K. pneumoniae*

1.4.1. Structure, genetics, and clinical relevance

The main surface polysaccharides of bacteria are capsular polysaccharides (CPS) and lipopolysaccharides (LPS), being the most diverse structures on the bacterial cell surface. [130] Other polysaccharides found on bacterial surfaces include peptidoglycan, exopolysaccharides, and surface glycoconjugates. [131] These surface glycans have important roles in bacterial adaptation, survival and immune escape. Their polysaccharide nature offers a high potential for structural diversity that influences several aspects of disease establishment and progression, bacterial evolution and diagnostics (through serotyping), as well as strategies for prevention and control of diseases through the development of glycoconjugate vaccines.

The CPS of *K. pneumoniae* constitutes the outermost layer of the cell and consists in a loose arrangement of a mucoid layer that plays critical roles in adaptation, protection and communication. CPS structural integrity and composition are essential for its protective capabilities, as it aids in evading phagocytosis and resisting the actions of antimicrobial peptides and complement proteins, thereby enhancing the survival of the pathogen in hostile environments. [131] The CPS consists of repeating units of three to six monosaccharides (mannose, glucose, galactose, fucose, and rhamnose) linked by glycosidic bonds. Their variable composition, chain length, and the presence of glucuronic and galacturonic acids confer an anionic character, while modifications by pyruvate or O-acetyl further enhance polysaccharide diversity, influencing immunogenicity and virulence. For example, it has been shown that acetylated CPS in K57 enhances intestinal epithelial adhesion via increased fimbriae production, but reduces serum resistance by exposing antigenic epitopes. [132] In K1/K2 isolates, CPS modifications on pyruvate groups balance immune evasion and pro-inflammatory cytokine induction, promoting systemic spread. [131]

As to date, 186 distinct capsular locus (KL) have been recognized by wide genomic surveillance studies. [133] Part of these (>77) have been serologically defined and named K antigens (K1 to K81, excluding K75–K78). [134] Their structures have been elucidated through various chemical and enzymatic techniques, including methylation analysis, bacteriophage-borne endo-glycanases, Smith degradation analysis, ^{1}H- and ^{13}C-NMR (nuclear magnetic resonance) spectroscopy, optical rotatory dispersion (ORD) and circular dichroism (CD) spectroscopy. [135,136] For all of the remaining KL-types, inferred by genomics, the sugar composition remains unknown.

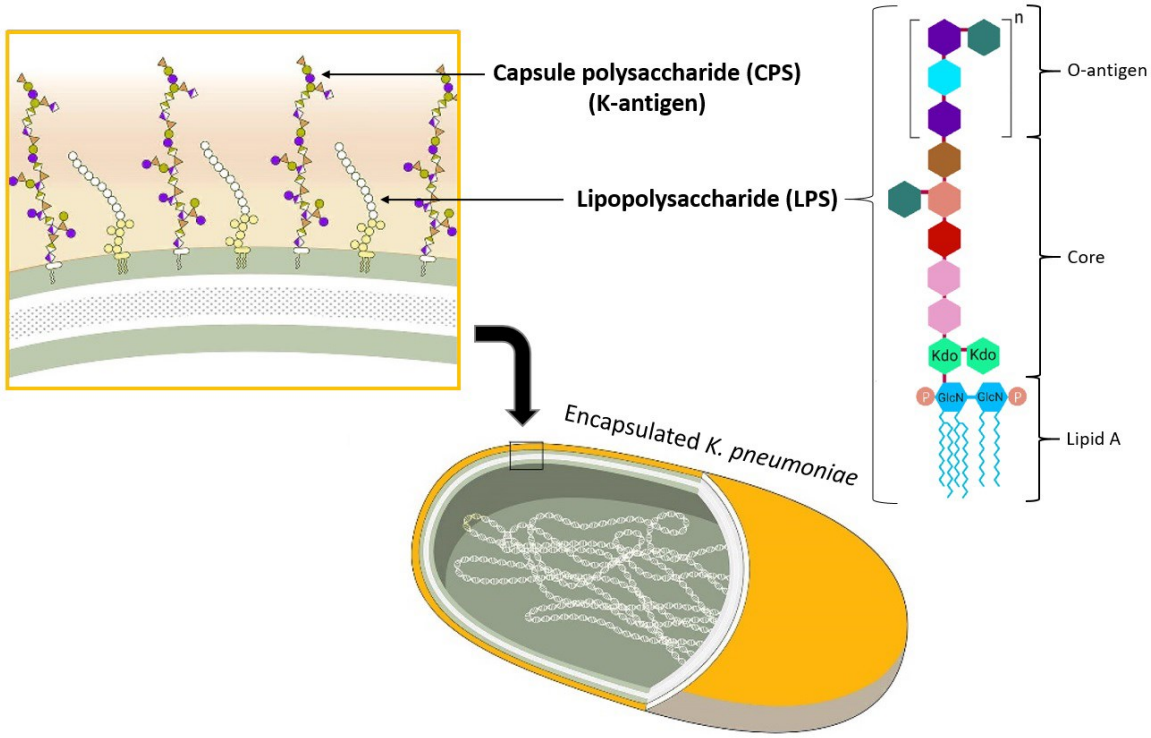


Figure 3. *Klebsiella pneumoniae* capsule structures involved in persistence and virulence.

Genes controlling the CPS biosynthesis are located within the capsular polysaccharide synthesis (*cps*) cluster, which spans approximately 21-30 Kb and contains about 10-30 genes, including the conserved cluster *galF*, *orf2* (*cpsACP*), *wzi*, *wza*, *wzb*, and *wzc,* and a highly variable middle region changing according to different K-types, due to the variation in the sugar composition, steroisomoeric form, substituent and linkage. [131] This highly heterogeneous region encodes for proteins for capsule assembly and polymerization, influencing the variable capsular glyco-composition, based on serotype-specific sequences. [131,135] Among regulatory genes, *wcaJ/wbaP* code for the first glycosyltransferase initiating the capsular biosynthesis, therefore acting as a direct regulator. [131,137] Other essential genes within the *cps* include *wzx* and *wzy*, which are involved in biosynthesis and export mechanisms. [131] The *wzi* gene, encoding for an outer membrane protein, serves as a molecular marker for capsular typing, preferred over the *wzy* gene due to its hypervariable region, enabling a superior discriminatory power (98.3% vs. 94.4% for *wzy*). [138] Software tools as KLEBORATE and PathogenWatch integrate *wzi* alleles with AMR and virulence profiling, facilitating rapid serotype prediction. [114] Outside the *cps* cluster, the genes *rmpA* and *rmpA2* (regulator of mucoid phenotype A), often located on a large plasmid or in the chromosome, are key trans-regulators, acting on three different *cps* cluster promoters to upregulate capsule synthesis. [137,139]

LPS, comprising lipid A, a core oligosaccharide, and the O-polysaccharide (OPS), is an essential component of the outer membrane of *K. pneumoniae*. The OPS, also known as O-antigen or somatic antigen, is the outermost component of the LPS and consists of repeating glycan polymers that enhance antigenic diversity among strains, promote bacterial adhesion to host tissues and facilitates colonization. [140] The toxicity of LPS is primarily associated with Lipid A, which triggers strong inflammatory responses in the host. Additionally, LPS contributes to serum resistance and immune evasion, particularly through interactions between the core oligosaccharide and the complement system. O-type structures show much lower diversity when compared to K-types (12 O-types are currently recognized). [141,142] Serotypes O1 and O2 are the most prevalent, accounting for approximately 80% of all the infections. [141] Analysing the diversity of capsular and somatic antigens in *K. pneumonae* is crucial for understanding virulence, immune evasion, epidemiology, and vaccine development. Different capsular serotypes are linked to varying levels of virulence and specific clinical manifestations, [143] and may contribute to the observed differences in pathogenicity and persistence. Studying these markers facilitates tracking the spread of hv*Kp* and MDR-*Kp*, and contributes to the development of targeted interventions and vaccines. [144]

1.4.2. Impact on environmental survival and adaptation

K. pneumoniae, as most of bacteria, is highly susceptible to external stressors such as desiccation, starvation, heat or ultraviolet (UVC) light exposure. Variations in capsular composition and therefore CPS structure may correlate with differing levels of resistance to these stressors, potentially affecting survival rates. [133] *K. pneumoniae* have adapted to stress through mechanisms like biofilm production or regulation of CPS production. The increased resilience and ability to adapt to new niches through *cps* locus regulation suggest that environmental adaptive processes influence capsule evolution. Consequently, the role of capsule in virulence and infection may be considered a by-product of this environmental adaptation. [145] Building and maintaining capsule implies a consistent metabolic burden in a nutrient-rich environment, while in nutrient-poor environment this cost is balanced by the protective role against biotic threats (e.g. immune attacks) and abiotic stressors (e.g. desiccation), therefore gaining a fitness advantage. [146] Capsule biosynthesis consumes up to 30% of the cell carbon flux in nutrient-poor conditions, depleting resources from important process like replication or stress response; [118] plus, capsule retention does not serve as carbon resource or other survival benefits during starvation or desiccation. [146,147] A study showed that capsule-deficient (Cap^-) mutants outcompete wild-type strains by 15-

40% in rich media, confirming the burden, and that the cost is variable across strains (e.g. KL24), showing fitness disadvantage in certain culture media over others. [146] Though, signal pathways linking nutrient sensing to capsule regulation, and ecological factors driving capsule modulation in the environment are still unknown. [118,146,147]

The adaptation potential of *K. pneumoniae* is influenced by both biochemical and biophysical aspects of its surface glycans, including the CPS. However, research has historically prioritized genetic approach and *cps* locus characterization over mechanical characterization. For example, there are still critical knowledge gaps regarding how phenotypic aspects, including rheological (shear flow, deformation) and textural (mechanical conduct) properties, modulate virulence. To characterize how capsule thickness variations affect bacterial architecture and motility under shear flow conditions can aid our understanding variations in colonization efficiency and systemic dissemination. [148–150] Moreover, textural assessments of properties such as adhesivity (attachment strength), firmness (structural rigidity), and stretchability (deformation capacity) may explain strain-specific differences in host tissue adherence, bacterial aggregation patterns, and resistance to phagocytic clearance. Integrating these biomechanical analyses with traditional K-type profiling offers a multidimensional framework to investigate virulence and mechanisms of dissemination in the host. Mechanobiological insights could help bridge the existing knowledge gap between capsule genetics, sugar polymer chemistry, and clinical manifestations, paving the way for novel therapeutic strategies to combat pathogen persistence in severe infections.

1.4.3. Impact on immune evasion and host interaction

Bacterial surface glycosignatures represent a dynamic molecular interface with the role, among others, of mediating cross-kingdom interactions, where protein recognition of pathogen-specific glycans directly influences microbial ecology, phage predation dynamics, and host immune responses. In pathogens like *K. pneumoniae*, variations in the structure of surface carbohydrates, which define strain-specific K-type configurations and altered mucoidity or capsule production patterns, create distinct immunological footprints that impact microbial survival strategies.

Host interactions are based on recognition of bacterial glycans by lectins from the innate immune system, which are carbohydrate-binding proteins that recognize pathogen-associated glycans, playing a key role in microbial recognition, immune signalling, and host defense. Key lectin classes include: i) C-type lectins (e.g. LOX-1, DC-SIGN), which bind

pathogen-specific glycans; ii) galectins, targeting β-galactosides to modulate inflammation; and iii) siglecs, sialic acid-binding receptors regulating immune tolerance. [151,152] *K. pneumoniae* utilizes glycan mimicry, such as sialylated CPS resembling host structures, to evade detection and suppress immune activation. [141,153] On the other hand, anomalous glycan motifs alert lectins, enabling complement activation or neutrophil recruitment. [151] Surface glycans also mediate adhesion via biofilm-forming adhesins or enzymatic carbohydrate-binding modules (CBMs). [141]

K. pneumoniae surface polysaccharides, particularly the capsule, are central to survival strategies, serving as its primary defence against host immunity. The capsule masks bacterial surface receptors, such as LOX-1, [154,155] reducing phagocytosis by macrophages (5-10 times less) compared to capsule-deficient mutants. [156] Highly encapsulated strains (e.g. K1 or K2) evade Kupffer cell surveillance in the liver, enabling bloodstream persistence. [156] Complementing this, LPS in the outer membrane release vesicles that sequester complement proteins, further shielding bacteria from immune clearance. [142,151]

Adaptation to host niches involves a process of dynamic regulation of surface glycans. Capsule switching plays a crucial role in modulating *K. pneumoniae* interactions with the host. While capsule hyperproduction seems to favour pathogen diffusion through the bloodstream and various tissues evading immune responses, reduced or no CPS expression may enhance attachment and adhesion to epithelial surfaces, promoting colonization in the gut or lungs. [157–159] However, CPS abundance alone does not predict virulence, as strains with similar capsule levels can exhibit contrasting infection outcomes. [155,160,161] For example, low CPS promotes lung epithelial attachment, but increases complement deposition and phagocytosis risk, whereas systemic infections require robust encapsulation to resist immune clearance. [157,158,162] This plasticity highlights *K. pneumoniae* ability to balance immune evasion with tissue-specific colonization needs.

In vivo assays assessed the impact of the capsule on complement deposition, phagocytosis by immune cells (e.g. macrophages, neutrophils), and resistance to antimicrobial peptides. [151] Real-time *in vivo* imaging have been used to visualize the interaction of encapsulated and non-capsulated strains with immune cells in the bloodstream and organs like the liver, allowing the direct observation of bacterial capture and killing by Kupffer cells. [156] Another approach consisted in obtaining capsule-switched strains, by genetically replacing the *cps* genes of low-virulence strains with those of high-virulence strains, and then assessing the resulting impact on bacterial clearance from the bloodstream and organ colonization. [163] Moreover, flow cytometry has been employed to quantify the binding of antibodies or complement components to the bacterial surface, providing insights into capsule-mediated immune evasion. [164]

Bacterial microarrays provide a high-throughput profiling of strain-specific glycosignatures, mapping interactions between lectins and surface glycans to identify immunomodulatory epitopes and adaptive remodelling during infection. [165] Advances in microarray technology allow a systematic mapping of these glycan landscapes across bacterial populations, capturing real-time structural modifications with a lineage-level resolution. This high-throughput approach can elucidate: i) the immunomodulatory role of capsules in evading host defenses, ii) the accessibility patterns of surface glycans to immune recognition molecules, and iii) the adaptive re-modelling of carbohydrate architectures during infection processes. By correlating specific glycan profiles with microbial behaviour, it is possible to identify diagnostic biomarkers, predict pathogen vulnerabilities, and develop targeted therapies that prevent important glycan-mediated interactions in host-microbe ecosystems.

Among the objective of this work are to systematically characterize surface polysaccharides (CPS, LPS) across strains, define how their structural diversity impacts niche adaptation, and identify lectin-glycan interactions critical for immune evasion. By linking glycan profiling with genomic and clinical datasets, we aim to disclose glyco-determinants of virulence and colonization.

Objectives

The global dissemination of *Klebsiella pneumoniae* has been driven by the emergence of high-risk sublineages that represent a Public Health concern due to multidrug resistance (MDR-*Kp*) and/or hypervirulence (hv*Kp*) phenotypes. While genomic advances have been key to clarify the genetic basis of antibiotic resistance, virulence mechanisms and population structure through molecular epidemiology, the field remains disproportionately focused on DNA-centric analyses. This narrow focus has limited the exploration of critical phenotypic and structural adaptations that directly influence pathogen behaviour, transmission dynamics, and clinical outcomes. Surface glycans, and particularly capsular polysaccharides (CPS), are epidemiological markers of certain high-risk *K. pneumoniae* sublineages and have an important role in bacterial pathogenicity and protection against environmental stresses and host defences. A major gap lies in understanding how variations in CPS structure and production influence glycan-mediated interactions with the environmental and host, shaping adaptation and virulence.

This thesis introduces a *novel perspective* which includes **phenotypic** and **structural profiling** of *K. pneumoniae* surface glycans, integrated with **genomic** and **epidemiological** data. Providing insights into how variations in capsule production and structure modulate strain behaviour will improve our understanding on strain-specific survival and adaptation strategies to different environments.

This thesis explores the **hypothesis** that the composition and amount of surface glycans mediate *K. pneumoniae's* interactions with physical environments and host innate immunity defenses, ultimately driving the selection, persistence, and disease progression of multidrug-resistant (MDR) and hypervirulent (hv*Kp*) sublineages in clinical settings.

The **primary aim** of this thesis is to expand knowledge on *K. pneumoniae* surface polysaccharides properties and elucidate the role of CPS in modulating strain adaptation and behaviour, by integrating phenotypic insights with genomic and epidemiological data to identify key CPS-driven traits as targets for future interventions.

The **specific goals** of this work are:

I- To characterize the diversity and prevalence of invasive MDR-*Kp* and hv*Kp* sublineages from a northern Portuguese hospital, focusing on CPS composition (KL-types) and production levels.

II- To integrate knowledge on molecular epidemiology (strain genetic background, CPS profile) and rheology (rheological and textural properties), to understand bacterial survival and dissemination strategies in the environment or inside the host.

III- To identify lectin-binding signatures of MDR-*Kp* and hv*Kp* strains with varying surface glycans composition and CPS abundance, elucidating their role in bacterial interactions with the environment and the human host.

IV- To correlate clinical, molecular epidemiology, genomic and glycan-mediated phenotypic data to define CPS-driven traits of interest and propose putative diagnostic markers or therapeutic targets.

Results

OXFORD UNIVERSITY PRESS | Journal of Antimicrobial Chemotherapy

Molecular Epidemiology of invasive Klebsiella pneumoniae: unravelling the dynamics of antibiotic-susceptible and antibiotic-resistant in bloodstream infections

Journal:	*Journal of Antimicrobial Chemotherapy*
Manuscript ID	JAC-2024-1632
Manuscript Type:	Original Article
Date Submitted by the Author:	19-Dec-2024
Complete List of Authors:	Loiodice, Michele; UCIBIO, i4HB, Faculdade de Farmácia da Universidade do Porto Ribeiro, Tatiana; UCIBIO, i4HB, Faculdade de Farmácia da Universidade do Porto Silva, Luis; Centro Hospitalar Universitário do Porto EPE Castro, Ana Paula; Centro Hospitalar Universitário do Porto EPE Peixe, Luísa; UCIBIO, i4HB, Faculdade de Farmácia da Universidade do Porto Novais, Ângela; REQUIMTE. Faculdade Farmacia Universidade Porto, Laboratorio Microbiologia
Keywords:	Bloodstream Infection, Molecular epidemiology, Multidrug resistance, Hypervirulent Klebsiella pneumoniae

SCHOLARONE™
Manuscripts

Molecular Epidemiology of invasive *Klebsiella pneumoniae*: unravelling the dynamics of antibiotic-susceptible and antibiotic-resistant in bloodstream infections

Michele Loiodice[1], Tatiana Ribeiro [1], Luís Marques Silva[2], Ana Paula Castro[2], Luísa Peixe[1], Ângela Novais[1, *]

[1]UCIBIO, i4HB, Faculdade de Farmácia da Universidade do Porto,
Rua Jorge Viterbo Ferreira 228, 4050-313 Porto, Portugal
[2]Serviço de Microbiologia. Centro Hospitalar Universitário de Santo António, Largo Prof. Abel Salazar 10, 4099-001 Porto, Portugal.

*Corresponding author: Ângela Novais (aamorim@ff.up.pt)

Manuscript submitted

SYNOPSIS

Background: *Klebsiella pneumoniae* (*Kp*) is a major cause of bloodstream infections (BSI) globally, yet comprehensive knowledge about its impact is fragmented.

Objectives: This study investigates the molecular epidemiology and population dynamics of antibiotic-susceptible and antibiotic-resistant *Kp* causing invasive infections in a northern Portuguese hospital, to elucidate resistance emergence and dissemination.

Patients and Methods: *Klebsiella* sp. strains (n=175 in blood culture; n=3 in cerebrospinal fluid), isolated from hospitalized patients between 2017 and 2018, were identified by VITEK2/MALDI-TOF MS and *rpoB* sequencing. Antibiotic resistance phenotypes were defined by reference methods, ß-lactamases screened by PCR and sequencing, and clonal lineages characterized by FT-IR spectroscopy, MLST and/or WGS, including for hypervirulent strains (hv*Kp*).

Results: Isolates (177 *K. pneumoniae*, 1 *Klebsiella variicola*) were grouped as multidrug-resistant (MDR-*Kp*; 49%) or non-multidrug-resistant (non-MDR-*Kp*; 51%). Most MDR-*Kp* produced ESBL (67%; all CTX-M-15); the remaining, carbapenemases (25%; KPC-3, OXA-48 together or not with CTX-M -15) or no acquired β-lactamase (8%). Half of these (51%) belonged to three high-risk lineages (17% each: ST15-KL19, ST307-KL102, and ST147-KL64). A greater diversity emerged in the non-MDR cohort, with frequent ST14-KL2, consistently resistant to amoxicillin-clavulanate (13%). Some lineages had specific β-lactamase content (ST307-CTX-M-15, ST147-KPC-3), others circulated with variable (or without) β-lactamases, suggesting multiple acquisition and dissemination patterns. Two hv*Kp* were identified (1.1%; ST380-KL2, ST268-KL20).

Conclusions: MDR-*Kp* rates were much higher than reported at national level (26.7-28.4%), driven by the expansion of common high-risk lineages/ß-lactamases, and infection progression likely shaped by host factors and/or pathogen opportunities. Detection of hv*Kp* strains (1.1%) underscores the need for enhanced surveillance and improved detection methods.

Keywords: Molecular Epidemiology, Bloodstream Infection (BSI), Multidrug Resistance (MDR), Hypervirulent *Klebsiella pneumoniae* (hv*Kp*)

Introduction

Klebsiella pneumoniae represents a leading cause of healthcare-associated infections worldwide, most frequently causing pneumonia, urinary tract and bloodstream infections (BSI). *K. pneumoniae* ranks as the third most prevalent species responsible for hospital or community-onset bacteremia, [1] linked to high mortality rates. [2]

Most *K. pneumoniae* infections are caused by classical strains (c*Kp*), often associated with multidrug resistant (MDR) patterns, including first and last-line antibiotics, leading to difficult-to-treat infections. [3] Patients with compromised immune function, relevant comorbidities, frequent hospitalizations, and/or prior antibiotherapy are at increased risk of infection. [1,2] MDR-*Kp* patterns are frequently associated with the acquisition of plasmids carrying genes encoding extended-spectrum β-lactamases (ESBLs) and/or carbapenemases, [4] intra and intercountry disseminated by a few clonal groups widely adapted to the hospital setting. [3,5] Portugal is one of the countries where the increase of MDR-*Kp* causing invasive infections is alarming (+19.3%, 2010 to 2020) [6], as well as is carbapenemase-producing *K. pneumoniae* (CP-*Kp*) (3.4% in 2015 to 10.9% in 2019). [6] However, detailed molecular epidemiology of MDR-*Kp* strains causing invasive infections in Portugal is unknown, and knowledge is still fragmented in the rest of Europe. [7,8] It is important to have a broader view on the population diversity to understand the dynamics of emergence and dissemination of antibiotic resistance.

Additionally, there is a growing concern for the emergence and dissemination of hypervirulent *K. pneumoniae* (hv*Kp*) strains. The hv*Kp* pathotype typically belongs to distinct genetic backgrounds compared to c*Kp*. [3] While antibiotic susceptible, it is responsible for aggressive and severe infections in healthy individuals, [9] and the virulence potential is granted by the acquisition of certain virulence factors favoring persistence, invasion and immune escape. [3,10] The hv*Kp* pathotype is more frequent in Asian countries, [11,12] though its circulation in Europe is acknowledged [13] and it might be underestimated. [11,12]

This study aims at understanding the dynamics of susceptible and antibiotic-resistant *K. pneumoniae* populations, causing invasive infections in a representative hospital from northern Portugal.

Material and Methods

Bacterial sample and identification

A total of 178 putative *Klebsiella* strains were acquired from blood (n=175/178) or cerebrospinal fluid (n=3/178) samples from patients of a district hospital in northern Portugal, between December 2016 and September 2018. Isolates were preliminarily identified as *K. pneumoniae* by automated VITEK® 2 (bioMérieux) and/or MALDI-TOF mass spectrometry. Molecular validation was obtained by sequencing the housekeeping *rpoB*, and comparing it with the BIGSdb database (bigsdb.pasteur.fr).

Antimicrobial susceptibility testing and β-lactamases identification

Antibiotic resistance profiles of MDR-*Kp* were assessed for twenty antibiotics by disk diffusion, following the EUCAST (eucast.org) and CLSI reference methods and guidelines. [14] Susceptibility to fosfomycin and colistin were confirmed in β-lactamase-producing MDR-*Kp* strains following reference methods (agar dilution and broth microdilution, respectively). Double-disk synergy and Blue-Carba tests [15] were performed to phenotypically detect acquired mechanisms of resistance to β-lactams. Genes encoding ESBL (CTX-M) or carbapenemases (OXA-48, IMP, NDM, KPC and VIM) were identified by PCR and sequencing, as reported. [16,17] The Fisher's exact test [18] was applied to determine the statistical significance of the resistance profiles distribution among patients. Isolates were considered MDR when meeting the criteria defined by Magiorakos *et al.* [19]

Strain typing

Capsular (KL)-types and strain relationship were inferred by attenuated total reflectance Fourier-transform infrared spectroscopy (ATR-FTIR), a phenotypic-based approach with high potential for routine strain typing. A simple and quick protocol, similar to the MALDI-TOF MS-based microbial identification, generated strain-specific spectra, identified using a machine-learning model for KL-type identification and strain typing. [20] Additionally, *wzi* gene sequencing was used to validate KL-type predictions, or when no reliable identification could be obtained by FT-IR. *In silico* correlation of *wzi* alleles and KL-types was established using the BIGSdb database. [21] Clonal assignment was performed based on total or partial multi-locus sequence typing (MLST) on representative isolates showing variable *wzi* and/or KL-types. [22]

Screening of hypervirulent strains

Hypermucoviscous (hmv) phenotype was preliminarily identified by string test, considered positive when a string of >5 mm in length was formed upon stretching agar-plated colonies with a loop. [9] Additionally, all non-MDR *K. pneumoniae* were searched for gene markers predictive for hypervirulence: *peg344* (metabolite transporter), *iucA* (aerobactin synthetase, a siderophore), *iroB* (virulence-associated C-glycosyltransferase), plasmid-borne *rmpA* (positive regulator of capsular polysaccharide biosynthesis) and *ybtS* (yersiniabactin salicylate synthase, siderophore), as described by Russo *et al.* [9] Isolates predicted as hv*Kp* were further characterized by whole genome sequencing (WGS) using Illumina NovaSeq short reads sequencing technology (Illumina, USA). Short reads were quality checked with FASTQC (v. 0.11.9, github.com/s-andrews/FastQC), *de novo* assembled with SPAdes (v. 3.15.5, github.com/ablab/spades) and annotated with RAST (v. 2.0, rast.nmpdr.org). WGSs were deposited on NCBI (ncbi.nlm.nih.gov) under accession numbers SAMN45655588 and SAMN45660187. Resistome and virulome of hv*Kp* were characterized with KLEBORATE (v. 2.3.2). [23]

Results and Discussion

Bacterial collection and patient data

All isolates, with the exception of one *Klebsiella variicola*, were confirmed as *K. pneumoniae*. These strains represented 7% (n=178/2667) of all bacteria identified in blood or cerebrospinal fluid from patients of the same hospital during the period of study, more frequent than *E. faecalis* (n=64; 2.4%) and *E. faecium* (n=54; 2%), but much less common than *E. coli* (n=521; 19.5%) and *S. aureus* (n=271; 10.2%).

Patients' demographic and epidemiological data are represented in Table 1. Of note, most infections were hospital-acquired (66%), with a prevalence of male patients (62%) aged over 65 years (59%). Patients were predominantly outpatients (34%) or located in medical wards (32%), with the remainder in surgical wards (18%) or intensive care unit (16%).

A subset of patients (19%) qualified for rectal screening, and a significant proportion of these resulted positive to CP-*Kp* (71%, n=24/34). Among this group, 58% (14/24) subsequently developed a BSI caused by CP-*Kp*, with eleven patients becoming presumptively colonized by CP-*Kp* within 30 days of the initial isolation, according to immunochromatographic tests.

Although these rectal colonization strains were not characterized, they could potentially represent the same strains that later re-appeared in the bloodstream. In fact, previous studies suggested a probable gastrointestinal reservoir for some CP-*Kp* infections, emphasizing an increased risk factor when colonization occurs during hospitalization. [24,25]

Antibiotic resistance phenotypes and genotypes

Isolates were grouped in two main cohorts, according to antibiotic resistance profiles: multidrug-resistant (MDR-*Kp*; 49%, n=88/178) and non-multidrug-resistant (non-MDR-*Kp*; 51%, n=90/178). MDR-*Kp* and non-MDR-*Kp* were observed in both inpatients (50% each) and outpatients (44-56%, respectively). The rates of MDR-*Kp* appeared significantly higher than those reported for the country by ECDC in 2017 (28.4%) and 2018 (26.7%), and higher than the average of EU countries. [26] These data suggest heterogeneity in rates between different healthcare institutions in Portugal, and reflect variability influenced by local epidemiology, population susceptibility, infection control and antimicrobial stewardship policies.

Most MDR-*Kp* were ESBL-producers (67%, n=59/88), all CTX-M-15. The remaining strains produced carbapenemases (17%, n=15/88), in all cases KPC-3, or co-produced both ESBL (CTX-M-15) and carbapenemases (KPC-3 or OXA-48) (8%, n=7/88). Of note, a small number of MDR-*Kp* isolates (8%, n=7/88) were neither ESBL nor carbapenemases producers (MDR-*Kp*-nonβL). ESBL-producing MDR-*Kp*, or ESBL concomitantly with carbapenemases, revealed high resistance rates to all the tested β-lactams (96-100%), ciprofloxacin (86-97%), gentamycin (81-100%) and trimethoprim-sulphametoxazole (92-100%) (Figure 1). Conversely, carbapenemase-producing MDR-*Kp* showed high resistance to the tested carbapenems (87-100%) and ciprofloxacin (82%), but lower to gentamycin (50%) and trimethoprim/sulfamethoxazole (36%) (Figure 1). Differences between the two cohorts suggest variable genetic platforms and/or plasmids carrying $bla_{\text{CTX-M-15}}$, $bla_{\text{KPC-3}}$ and $bla_{\text{OXA-48}}$. Notably, MDR-*Kp*-nonβL were frequently resistant to amoxicillin-clavulanate, ciprofloxacin and trimethoprim-sulphametoxazole (86% each), suggesting the prevalence of mechanisms of resistance to these antibiotics independently on the acquisition of β-lactamases (Figure 1). Importantly, ESBL and/or carbapenemase producing MDR-*Kp* were occasionally resistant to fosfomycin (17%) and colistin (6%, in two isolates carrying *mcr-1*).

Non-MDR-*Kp* were, occasionally, resistant to amoxicillin-clavulanate (26%), fosfomycin (24%, tested by disk diffusion), ciprofloxacin (11%, n=10/90) and/or trimethoprim-sulphametoxazole (9%, n=8/90) (data not shown). These patterns appear common among drug-susceptible *K. pneumoniae* causing BSIs. [7]

Clonal diversity amongst invasive *Kp*

Overall, a total of 87 distinct *Kp* lineages were identified, with a statistically significant higher variation within the non-MDR (n=65/90) compared to the MDR (n=21/88) cohorts ($p < 0.05$). Data show that a high diversity of genetic backgrounds can cause invasive infections, in line with previous observations. [7,27–29] Moreover, the composition and the relative frequency of particular lineages varied across cohorts, with distinct associations between certain lineages and the production of ESBL and/or carbapenemases, suggesting clonal transfer. Half (51%; n=45/88) of the MDR-*Kp* cohort was dominated by three main lineages (17% each of ST15-KL19, ST307-KL102 and ST147-KL64), followed by other less frequent clones (Table 2). The prevalence of these clones here and in other infection types suggests clonal spread, [30–32] and that BSIs result from infections in other primary sites and/or factors associated with host immune status.

While clones ST307-KL102, ST15-KL19 and ST348-KL62 produced CTX-M-15 exclusively, others (e.g. ST147-KL64, ST45-KL24) had variable β-lactamase content, suggesting multiple and independent acquisition events (Table 2). ST307-KL102 resulted to be more frequently acquired in the community, whereas others appeared to be particularly associated with hospital exposure, including previous hospitalization or surgery (Table 3). Two different ST15 lineages were detected, none of those corresponding to the most common worldwide. [33] ST15-KL19 is being more frequently detected in hospitals from northern Portugal, [32] while a new lineage, putatively responsible for an outbreak, carried a KL23 capsular locus with a different polysaccharide composition (KL23-like), as determined by FT-IR (data not shown) (Table 2, Table 3).

The non-MDR cohort was linked to a high number of clones (n=58) and capsular types (n=42), in different associations (Supplementary Table 1). These data indicate community gastrointestinal colonization by a diverse and extensive pool of *K. pneumoniae*, which can subsequently lead to hospital infections, [34] representing a potential source for diversification and resistance acquisition that warrants further investigation. Among those, ST14-KL2 was the most frequently identified lineage (13%; n=12/90), consistently showing amoxicillin-clavulanate resistance (Supplementary Table 1). While infrequent in the MDR cohort in analysis, this lineage has been detected for decades in Portugal [30] and in other regions, either as a colonizer or causing bloodstream infections, [34,35] suggesting a worldwide expansion. [33] Occasionally, some lineages appeared in common with the MDR cohort, but without acquired

β-lactamases (ST307-KL102, ST45-KL24, ST348-KL62, ST147-KL64), including some previously described in Portugal and elsewhere (ST13-KL3, ST15-KL24, ST405-KL151). [30,33] Overall, these results showed that the same *Kp* lineages circulated with or without multidrug resistance plasmids, and that their acquisition preceded clonal expansion and persistence.

Hypervirulent strains

Two non-MDR-*Kp* (1.1%) were classified as hypervirulent according to both KLEBORATE (virulence score = 5) and the classification proposed by Russo *et al.* [9] Both isolates exhibited hypermucoviscosity and showed susceptibility to antibiotics. The first strain belonged to the well-characterized ST380-KL2, isolated in a patient with a severe clinical course and an unfavorable outcome. The second strain was recognized as ST268-KL20, having acquired a hypervirulence plasmid. However, due to the patient's transfer to an alternative hospital, data regarding the infection severity and progression were unavailable. In both cases, a history of international travel was excluded.

This study firstly reports a ST380-KL2 lineage in the country, while carbapenemase-producing ST268-KL20 had been previously detected. [32] Although the incidence of hv*Kp* in this BSI collection is low (1.1%), it is of note that hypervirulent strains have been sporadically detected. [13,36] Such result highlights the circulation of hv*Kp* within community settings, and the necessity for enhanced monitoring of hv*Kp* and possible convergent strains. Moreover, considering the difficulties in hv*Kp* recognition with both phenotypic and genotypic methods, [9] there is the possibility that these high-risk isolates are being undiagnosed and underestimated.

Conclusions

Data suggest a much higher rate of MDR-*Kp* than that reported at a national level. This result is associated with a remarkable clonal diversity, with some lineages shared between antibiotic resistant and susceptible populations. A great diversity of colonizing strains may precede the acquisition of antibiotic resistance, a critical factor in the selection and amplification of specific lineages, with the infection progression likely shaped by a combination of host factors and pathogen opportunities. Although detected at a low frequency, the identification of hv*Kp* strains is noteworthy, and highlights the necessity for enhanced surveillance and the refinement of detection methodologies.

Funding

This work was supported by national funds from FCT - Fundação para a Ciência e a Tecnologia, I.P., in the scope of the project UIDP/04378/2020 and UIDB/04378/2020 of the Research Unit on Applied Molecular Biosciences - UCIBIO, and the project LA/P/0140/2020 of the Associate Laboratory Institute for Health and Bioeconomy - i4HB, Faculty of Pharmacy, University of Porto, 4050-313 Porto, Portugal. This research received also support by HEALTH-UNORTE I&D&I project (NORTE-01–0145-FEDER-0 00039) co-financed by European Regional Development Fund (ERDF), through the NORTE 2020 (Programa Operacional Regional do Norte 2014/2020). M. Loiodice is supported by FCT - Fundação para a Ciência e a Tecnologia, I.P. (grant number 2020.07480.BD). Â. Novais is supported by national funds through FCT - Fundação para a Ciência e a Tecnologia, I.P., through Scientific Employment Stimulus Program (2021.02252.CEECIND/CP1662/CT0009).

Transparency declaration

All the authors involved in the writing of this document have nothing to declare.

References

1. Holmes CL, Anderson MT, Mobley HLT, Bachman MA. Pathogenesis of Gram-Negative Bacteremia. *Clin Microbiol Rev* 2021; **34**: e00234-20.

2. Li D, Huang X, Rao H, *et al*. *Klebsiella pneumoniae* bacteremia mortality: a systematic review and meta-analysis. *Front Cell Infect Microbiol* 2023; **13**: 1157010.

3. Wyres KL, Lam MMC, Holt KE. Population genomics of *Klebsiella pneumoniae*. *Nat Rev Microbiol* 2020; **18**: 344–59.

4. .Wyres KL, Holt KE. *Klebsiella pneumoniae* as a key trafficker of drug resistance genes from environmental to clinically important bacteria. *Current Opinion in Microbiology* 2018; **45**: 131–9.

5. David S, Reuter S, Harris SR, *et al*. Epidemic of carbapenem-resistant *Klebsiella pneumoniae* in Europe is driven by nosocomial spread. *Nat Microbiol* 2019; **4**: 1919–29.

6. European Centre for Disease Prevention and Control, WHO Regional Office for Europe. Surveillance of antimicrobial resistance in Europe, 2023 data: executive summary. *Stockholm: European Centre for Disease Prevention and Control*; 2024.

7. Lipworth S, Vihta K-D, Chau K, *et al.* Ten-year longitudinal molecular epidemiology study of *Escherichia coli* and *Klebsiella* species bloodstream infections in Oxfordshire, UK. *Genome Med* 2021; **13**: 144.

8. Gürntke S, Kohler C, Steinmetz I, *et al.* Molecular epidemiology of extended-spectrum beta-lactamase (ESBL)-positive *Klebsiella pneumoniae* from bloodstream infections and risk factors for mortality. *Journal of Infection and Chemotherapy* 2014; **20**: 817–9.

9. Russo TA, Marr CM. Hypervirulent *Klebsiella pneumoniae*. *Clin Microbiol Rev* 2019; **32**: e00001-19.

10. Chen J, Zhang H, Liao X. Hypervirulent *Klebsiella pneumoniae*. *IDR* 2023; **Volume 16**: 5243–9.

11. Sanikhani R, Moeinirad M, Shahcheraghi F, *et al.* Molecular epidemiology of hypervirulent *Klebsiella pneumoniae*: a systematic review and meta-analysis. *IJM* 2021.

12. Wang W, Ye C, Zhao B, *et al.* Epidemiological and Molecular Characteristics of Hypermucoviscous and Hypervirulent *Klebsiella pneumoniae* Isolates in Community Patients in Shanghai, China. *IDR* 2024; **Volume 17**: 2685–99.

13. European Centre for Disease Prevention and Control. Emergence of hypervirulent *Klebsiella pneumoniae* ST23 carrying carbapenemase genes in EU/EEA countries, first update. *LU: Publications Office*; 2024.

14. Lewis JS. CLSI. Performance Standards for Antimicrobial Susceptibility Testing. 32nd ed. CLSI supplement M100. *Clinical and Laboratory Standards Institute; 2022*.

15. Pires J, Novais Â, Peixe L. Blue-Carba, an Easy Biochemical Test for Detection of Diverse Carbapenemase Producers Directly from Bacterial Cultures. *J Clin Microbiol* 2013; **51**: 4281–3.

16. Bogaerts P, Rezende De Castro R, De Mendonca R, Huang T-D, Denis O, Glupczynski Y. Validation of carbapenemase and extended-spectrum -lactamase multiplex endpoint PCR assays according to ISO 15189. *Journal of Antimicrobial Chemotherapy* 2013; **68**: 1576–82.

17. Machado E, Cantón R, Baquero F, *et al.* Integron Content of Extended-Spectrum-β-Lactamase-Producing *Escherichia coli* Strains over 12 Years in a Single Hospital in Madrid, Spain. *Antimicrob Agents Chemother* 2005; **49**: 1823–9.

18. Sprent P. Fisher Exact Test. In: Lovric M, ed. *International Encyclopedia of Statistical Science*. Berlin, Heidelberg: Springer Berlin Heidelberg, 2011; 524–5.

19. Magiorakos A-P, Srinivasan A, Carey RB, *et al.* Multidrug-resistant, extensively drug-resistant and pandrug-resistant bacteria: an international expert proposal for interim standard definitions for acquired resistance. *Clinical Microbiology and Infection* 2012; **18**: 268–81.

20. Novais Â, Gonçalves AB, Ribeiro TG, *et al.* Development and validation of a quick, automated, and reproducible ATR FT-IR spectroscopy machine-learning model for *Klebsiella pneumoniae* typing Simner PJ, ed. *J Clin Microbiol* 2024; **62**: e01211-23.

21. Brisse S, Passet V, Haugaard AB, *et al. wzi* Gene Sequencing, a Rapid Method for Determination of Capsular Type for *Klebsiella* Strains. *J Clin Microbiol* 2013; **51**: 4073–8.

22. Diancourt L, Passet V, Verhoef J, Grimont PAD, Brisse S. Multilocus Sequence Typing of *Klebsiella pneumoniae* Nosocomial Isolates. *J Clin Microbiol* 2005; **43**: 4178–82.

23. Lam MMC, Wick RR, Watts SC, Cerdeira LT, Wyres KL, Holt KE. A genomic surveillance framework and genotyping tool for Klebsiella pneumoniae and its related species complex. *Nat Commun* 2021; **12**: 4188.

24. Cano Á, Gutiérrez-Gutiérrez B, Machuca I, *et al.* Association between Timing of Colonization and Risk of Developing *Klebsiella pneumoniae* Carbapenemase-Producing *K. pneumoniae* Infection in Hospitalized Patients. Wesley Long S, ed. *Microbiol Spectr* 2022; **10**: e01970-21.

25. Gorrie CL, Mirčeta M, Wick RR, *et al.* Gastrointestinal Carriage Is a Major Reservoir of *Klebsiella pneumoniae* Infection in Intensive Care Patients. *Clinical Infectious Diseases* 2017; **65**: 208–15.

26. European Centre for Disease Prevention and Control., World Health Organization. Antimicrobial resistance surveillance in Europe 2022: 2020 data. *LU: Publications Office*; 2022.

27. Gomez-Simmonds A, Greenman M, Sullivan SB, *et al.* Population Structure of *Klebsiella pneumoniae* Causing Bloodstream Infections at a New York City Tertiary Care Hospital: Diversification of Multidrug-Resistant Isolates Carroll KC, ed. *J Clin Microbiol* 2015; **53**: 2060–7.

28. Liao C-H, Huang Y-T, Hsueh P-R. Multicenter Surveillance of Capsular Serotypes, Virulence Genes, and Antimicrobial Susceptibilities of *Klebsiella pneumoniae* Causing Bacteremia in Taiwan, 2017–2019. *Front Microbiol* 2022; **13**: 783523.

29. Kochan TJ, Nozick SH, Medernach RL, *et al.* Genomic surveillance for multidrug-resistant or hypervirulent *Klebsiella pneumoniae* among United States bloodstream isolates. *BMC Infect Dis* 2022; **22**: 603.

30. Spadar A, Phelan J, Elias R, *et al.* Genomic epidemiological analysis of *Klebsiella pneumoniae* from Portuguese hospitals reveals insights into circulating antimicrobial resistance. *Sci Rep* 2022; **12**: 13791.

31. Guerra AM, Lira A, Lameirão A, *et al.* Multiplicity of Carbapenemase-Producers Three Years after a KPC-3-Producing *K. pneumoniae* ST147-K64 Hospital Outbreak. *Antibiotics* 2020; **9**: 806.

32. Gonçalves AB, Alves V, Neves I, *et al.* Real-time identification of carbapenemase-producing *Klebsiella pneumoniae* lineages and outbreak detection using FT-IR ATR. 2024.

33. Rodrigues C, Lanza VF, Peixe L, Coque TM, Novais Â. Phylogenomics of Globally Spread Clonal Groups 14 and 15 of *Klebsiella pneumoniae* Hall RM, ed. *Microbiol Spectr* 2023; **11**: e03395-22.

34. Lewis JM, Mphasa M, Banda R, *et al.* Genomic and antigenic diversity of carried *Klebsiella pneumoniae* isolates mirrors that of invasive isolates in Blantyre, Malawi. 2021.

35. Choi M, Hegerle N, Nkeze J, *et al.* The Diversity of Lipopolysaccharide (O) and Capsular Polysaccharide (K) Antigens of Invasive *Klebsiella pneumoniae* in a Multi-Country Collection. *Front Microbiol* 2020; **11**: 1249.

36. Pereira A, Petrucci T, Simões MJ. *Klebsiella pneumoniae* do Serotipo K1 e do Clone Hipervirulento ST23: Primeiro Caso Documentado em Portugal. *Acta Med Port* 2017; **30**: 496–9.

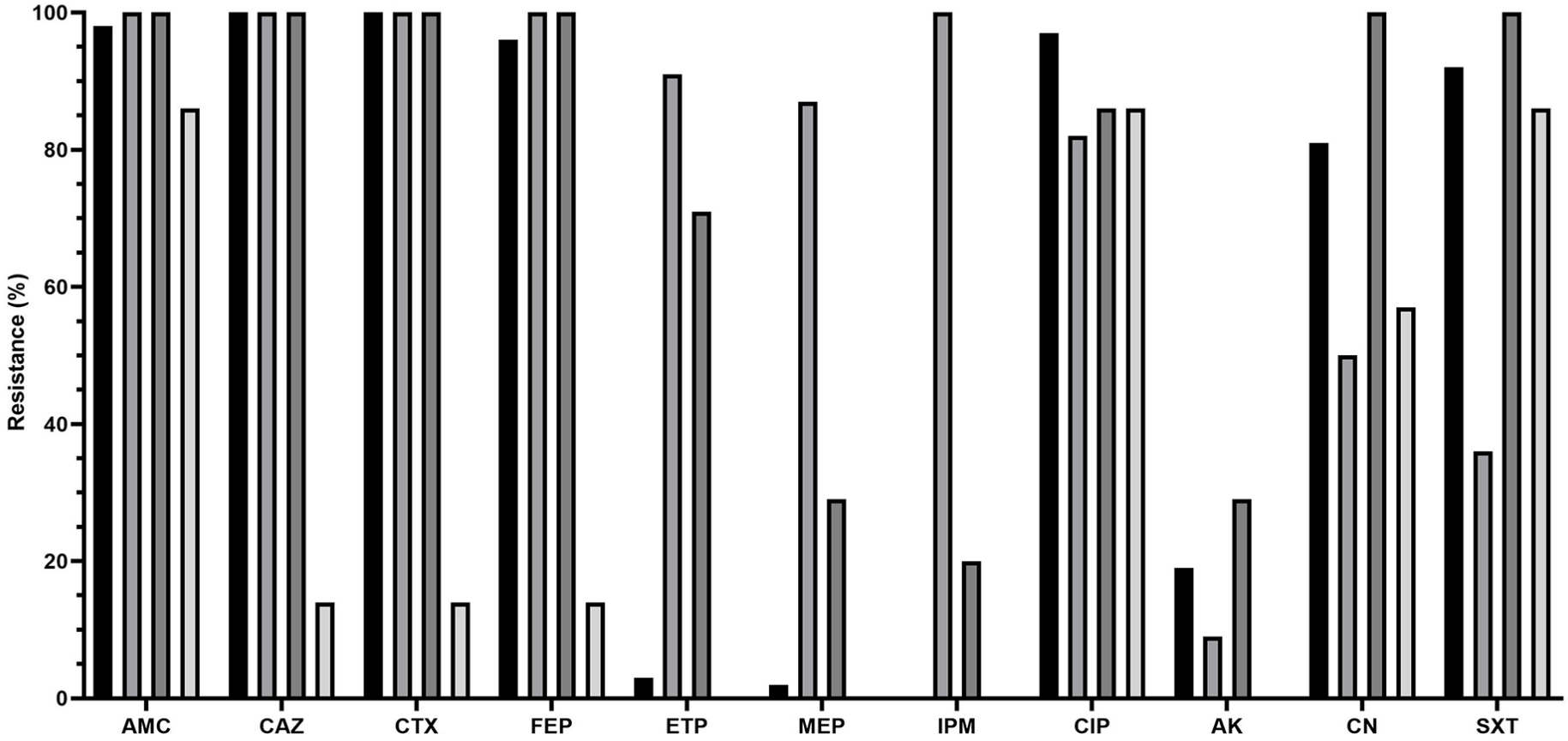


Figure 1: Antimicrobial resistance profile for MDR-*Kp* groups. Tested antibiotics: AMC = amoxicillin/clavulanate, CAZ = ceftazidime, CTX = cefotaxime, FEP = cefepime, ETP = ertapenem, MEP = meropenem, IPM = imipenem, CIP = ciprofloxacin, AK = amikacin, CN = gentamicin, SXT = trimethoprim/sulfamethoxazole.

Table 1. Patients' demographic and epidemiological data.

Characteristic	Proportion
Sex	
Male	62%
Female	38%
Age range	
> 65	59%
20-64	39%
5-19	2%
Origin	
Outpatients	34%
Medical Wards	32%
Surgical Wards	18%
ICU	16%
Type of Infection	
Healthcare-Associated (HAI)	66%
Community-Acquired (CAI)	34%

Table 2. Clonal diversity and antibiotic resistance profiles of MDR-*Kp* isolates.

Capsular Type (*wzi*)[a]	Sequence Type[a]	Acquired β-lactamase	N. Isolates	Resistance Profiles to β-lactams	Resistance Profiles to non-β-lactams
K. pneumoniae					
KL102 (173)	**ST307**	CTX-M-15	15	AMC, CAZ, CTX, FEP	CIP, CN, (SXT), (COL*)
KL19 (19)	**ST15**	CTX-M-15	15	AMC, CAZ, CTX, FEP	CIP, (AK), CN, SXT, (COL*), (FOS*)
KL64 (64)	**ST147**	KPC-3	11	AMC, CAZ, CTX, FEP, ETP, MEP	(CIP), (CN), (SXT*), (FOS)
		CTX-M-15	2	AMC, CAZ, CTX, FEP	CIP, SXT, (FOS*)
		CTX-M-15 + KPC-3	1	AMC, CAZ, CTX, FEP, ETP, MEP	CIP, CN, SXT
KL64 (33)		-	1	AMC, CAZ	CIP, SXT
KL24 (101)	**ST45**	CTX-M-15	7	AMC, CAZ, CTX, FEP, (ETP*)	(CIP), (AK*) (CN**), SXT, (COL*), (FOS)
		KPC-3	1	AMC, CAZ, CTX, FEP, ETP, MEP	CIP, CN
		CTX-M-15 + KPC-3	2	AMC, CAZ, CTX, FEP, (ETP*), MEP	(CIP*), (AK*), CN, SXT, (COL*)
KL23-like (732)[b]	**ST15**	CTX-M-15	5	AMC, CAZ, CTX, FEP, (ETP*)	CIP, (CN**), SXT
		CTX-M-15 + OXA-48	3	AMC, CAZ, CTX, FEP, (ETP**)	CIP, CN, SXT
		CTX-M-15 + KPC-3	1	AMC, CAZ, CTX, FEP, ETP	CIP, AK, CN, SXT
KL62 (94)	**ST348**	CTX-M-15	5	AMC, CAZ, CTX, (FEP)	(CIP), (CN), (SXT)
KL62 (149)	ST45	CTX-M-15	1	AMC, CAZ, CTX, FEP	CIP, AK, CN, SXT
KL112 (93)	ST15	CTX-M-15	2	AMC, CAZ, CTX, FEP	CIP, SXT, (FOS*)
KL27 (187)	ST392	KPC-3	2	AMC, CAZ, CTX, FEP, ETP, (MEP*)	CIP, (COL*), (FOS*)
KL2 (2)	ST14	CTX-M-15	1	AMC, CAZ, CTX, FEP	CIP, SXT
KL10 (236)	ST34	CTX-M-15	1	AMC, CAZ, CTX	CIP, AK, CN, SXT, FOS
KL10 (100)	ST525	-	1	AMC	CIP, CN
KL16 (247)	ST215-like	CTX-M-15	1	AMC, CAZ, CTX, FEP	CIP
KL23 (82)	ST280	CTX-M-15	1	AMC, CAZ, CTX, FEP	CIP, CN, SXT
		-	1	CTX, FEP	CIP, CN, SXT, FOS
KL28 (84)	ST661	CTX-M-15	1	CAZ, CTX	CIP, SXT, FOS
KL30 (276)	N/A	-	1	AMC	CN, SXT
KL54 (115)	ST465	CTX-M-15	1	AMC, CAZ, CTX	CIP, SXT

Capsular Type (*wzi*)	Sequence Type	Acquired β-lactamase	N. Isolates	Resistance Profiles to β-lactams	Resistance Profiles to non-β-lactams
K. pneumoniae					
KL110 (89)	ST15	-	1	AMC	CIP, SXT, FOS
N/A (633)	N/A	CTX-M-15	1	CTX	CIP, SXT, FOS
N/A (681)	N/A	-	1	AMC	CIP, SXT
N/A (754)	N/A	-	1	AMC, CAZ, CTX, FEP	CIP, CN, SXT
K. variicola					
KL123 (586)	ST1563	KPC-3	1	AMC, CAZ, CTX, FEP, ETP	-

[a] = Most frequent clones are depicted in bold. [b] = KL23 predicted by Kleborate but different from KL23 by FT-IR. Brackets = partial resistance in the same lineage group. * = Resistance in one isolate only. ** = Susceptibility in one isolate only.

Tested antibiotics: AMC = amoxicillin/clavulanic acid, CAZ = ceftazidime, CTX = cefotaxime, FEP = cefepime, ETP = ertapenem, MEP = meropenem, CIP = ciprofloxacin, AK = amikacin, CN = gentamicin, SXT = trimethoprim/sulfamethoxazole, COL = colistin, FOS = fosfomycin.

Table 3. Epidemiological data and putative risk factors associated with most representative MDR-*Kp* lineages.

Lineage	Acquired β-lactamase	HAI	CAI	Isolation date range	Patients' age range	Patient's sex distribution	Previous CP-*Kp* colonization	Previous hospitalization	Previous surgery
ST307-KL102	CTX-M-15	64%	36%	06/2017 - 08/2018	36-90	53% M, 47% F	N/A	36%	57%
ST15-KL19	CTX-M-15	77%	23%	02/2017 - 07/2018	52-86	54% M, 46% F	67%	62%	69%
ST147-KL64	CTX-M-15, KPC-3	80%	20%	02/2017 - 08/2018	41-89	80% M, 20% F	100%	57%	64%
ST45-KL24	CTX-M-15, KPC-3	90%	10%	12/2016 - 07/2018	31-84	70% M, 30% F	67%	50%	50%
ST15-KL23-l	CTX-M-15, KPC-3, OXA-48	78%	22%	04/2018 - 08/2018	40-86	78% M, 22% F	50%	34%	67%

HAI = Healthcare-associated infections. CAI = Community-acquired infections. N/A = Data not available for these patients.

***Kp* Lineage**	**Capsular Type**	***wzi* allele**	**Sequence Type**	**N. of Isolates**	**Resistance Profile**
*Kp*_01	KL2*	2	ST14	12	(CAZ), (AMC)
*Kp*_02			ST380*	1	FOS
***Kp*_03**	**KL24**	**101**	**ST45**	**2**	AMC, SXT
*Kp*_04		24	ST15	2	AMC, (SXT)
*Kp*_05	KL64	33	ST20	2	(AMC), (CIP), (FOS)
*Kp*_06			ST_UN01	2	FOS
*Kp*_07			ST35	1	AMC, FOS
*Kp*_08			ST147	1	CIP, FOS
*Kp*_09			ST_UN02	1	AMC
*Kp*_10			ST_UN03	1	FOS
*Kp*_11	KL30	85	ST754	3	(FOS)
*Kp*_12			ST198	1	-
*Kp*_13	KL20*	95	ST268*	1	-
*Kp*_14	KL1	128	ST310	1	-
*Kp*_15	KL10	236	ST_UN04	1	-
*Kp*_16		100	N/A	1	-
*Kp*_17	KL27	27	ST528	2	(FOS)
*Kp*_18			ST_UN05	2	(SXT), (FOS)
*Kp*_19			ST36	1	FOS
*Kp*_20			ST_UN06	1	-
*Kp*_21	KL25	141	ST17	1	-
*Kp*_22			N/A	1	AMC
*Kp*_23	KL22KL37	37	ST35	1	AMC
*Kp*_24			N/A	1	AMC
***Kp*_25**	**KL62**	**94**	**ST348**	2	(FOS)

Kp Lineage	Capsular Type	*wzi* allele	Sequence Type	N. of Isolates	Resistance Profile
*Kp*_26	KL23	83	ST39	1	-
*Kp*_27			N/A	1	-
*Kp*_28	KL23KL18KL38	82	ST280	1	AMC, SXT
*Kp*_29	KL102	173	ST307	1	-
*Kp*_30		173	ST_UN07	1	-
*Kp*_31		383	ST_UN08	1	CIP, SXT
*Kp*_32	KL116	180	ST133	1	CIP
*Kp*_33			N/A	1	FOS
*Kp*_34	KL17	137	ST870	1	-
*Kp*_35			N/A	1	-
*Kp*_36	KL21	262	ST_UN09	1	-
*Kp*_37	KL108	105	ST_UN10	1	-
*Kp*_38	KL103	210	ST936	1	-
*Kp*_39		337	N/A	1	-
*Kp*_40	KL113	351	ST_UN11	1	-
*Kp*_41	KL114	354	ST_UN12	1	AMC
*Kp*_42	KL3	40	ST13	1	FOS
*Kp*_43			N/A	1	FOS
*Kp*_44	KL14	244	ST_UN13	1	-
*Kp*_45	KL151	143	ST405	1	-
*Kp*_46	KL15KL17KL51KL52	50	ST309	1	-
*Kp*_47			ST678	1	-
*Kp*_48			N/A	1	-
*Kp*_49	KL28	84	ST1189	1	-
*Kp*_50			ST_UN14	1	-
*Kp*_51	KL38	96	ST_UN15	1	-

Kp Lineage	Capsular Type	*wzi* allele	Sequence Type	N. of Isolates	Resistance Profile
*Kp*_52	KL46	97	ST_UN16	1	CIP, FOS
*Kp*_53	KL54	117	ST_UN17	1	-
*Kp*_54	KL58	130	ST_UN18	1	FOS
*Kp*_55	KL61	413	ST_UN19	1	-
*Kp*_56	KL63	63	ST111	1	SXT
*Kp*_57			N/A	1	AMC
*Kp*_58	KL7	7	ST_UN20	1	-
*Kp*_59	N/A	633	ST1562	1	FOS
*Kp*_60			ST_UN21	1	AMC, FOS
*Kp*_61		458	ST_UN22	1	FOS
*Kp*_62		535	ST_UN23	1	-
*Kp*_63		576	ST_UN24	1	-
*Kp*_64		586	ST_UN25	1	TE
*Kp*_65		739	ST_UN26	1	AMC, FOS
*Kp*_66		740	ST_UN27	1	AMC, FOS
*Kp*_67		753	ST_UN28	1	-
*Kp*_68		164	ST1602	1	CIP, SXT
*Kp*_69			N/A	1	CIP, SXT
*Kp*_70			N/A	1	-

Supplementary Table 1. Non-MDR-*Kp* cohorts, clonal diversity and resistance profiles.

In bold are the lineages in common with MDR-*Kp* cohort. * = hypervirulent strains (hv*Kp*). Tested antibiotics: AMC = amoxicillin/clavulanic acid, CAZ = ceftazidime, CTX = cefotaxime, FEP = cefepime, ETP = ertapenem, MEM = meropenem, CIP = ciprofloxacin, AK = amikacin, CN = gentamicin, TE = tetracycline, SXT = trimethoprim/sulfamethoxazole, COL = colistin, FOS = fosfomycin, CZA = ceftazidime-avibactam.

Unmasking the Role of Capsule Rheology in *Klebsiella pneumoniae* Pathogenesis

Michele Loiodice[1,3], Liliane Ferrador[1,3], Paulo Costa[2,3], Maria Helena Amaral[2,3], Ângela Novais[1,3], Luísa Peixe[1,3].

[1] UCIBIO - Applied Molecular Biosciences Unit, Laboratory of Microbiology, Department of Biological Sciences, Faculty of Pharmacy, University of Porto, 4050-313 Porto, Portugal
[2]UCIBIO - Applied Molecular Biosciences Unit, MedTech - Laboratory of Pharmaceutical Technology, Department of Drug Sciences, Faculty of Pharmacy, University of Porto, 4050-313 Porto, Portugal
[3]Associate Laboratory i4HB Institute for Health and Bioeconomy, Faculty of Pharmacy, University of Porto, 4050-313 Porto, Portugal

Manuscript under preparation for submission

Abstract

Klebsiella pneumoniae (*Kp*), fuels a rising tide of multidrug-resistant (MDR) and hypervirulent (hv*Kp*) infections, with capsular polysaccharide (CPS) as a cornerstone of its virulence. This study probes how CPS shapes flow behavior and stickiness in *Kp*, driving its invasive potential. Fourteen clinical isolates, spanning MDR-c*Kp* and hv*Kp* strains plus their non-capsulated mutants, were assessed via CPS quantification, rheology, texturometry, and whole-genome sequencing. Hypermucoid (HM) strains (CPS: 10.5 ± 2.3 ng/μL) showed low viscosity (35.1-202.1 Pa·s), easing bloodstream spread, while non-mucoid (NM) strains (1.7 ± 0.4 ng/μL) displayed high adhesiveness (0.52-1.24 N·mm), aiding tissue attachment. Hypermucoviscosity (HMV) tracked CPS levels non-linearly ($r^2 = 0.35$), with A12 CPS fluidity tied to *cps* mutations (e.g., *wcaJ* p.Thr89Ile). In contrast, mutant A12M exhibited extreme viscosity (5x) and adhesiveness (12x) stemmed from fimbrial exposure, despite a *wzc* frameshift suggesting export disruption over typical *wcaJ*/*wbaP* loss. These CPS-driven traits enable *Kp* to evade immune clearance and colonize host niches, with genomic variability amplifying sublineage success. Targeting CPS fluidity with viscosity enhancers or degrading it to expose adhesins offers new avenues to curb *Kp* clinical toll.

Keywords: *Klebsiella pneumoniae*, capsule, hypermucoviscosity (HMV), rheology, texture properties

1. Introduction

Klebsiella pneumoniae (*Kp*) poses a significant global health challenge due to the complex interplay of antimicrobial resistance and virulence. The epidemiology of *Kp* infections is increasingly complicated by two major trends: the spread of multidrug-resistant strains (MDR-*Kp*) [1] and the emergence and global dissemination of hypervirulent strains (hv*Kp*). [2]

MDR-*Kp* strains primarily cause localized infections such as pneumonia, urinary tract and wound infections and affect typically vulnerable populations like the elderly, immunocompromised patients, and individuals with prolonged healthcare exposure. [3] The difficulty in treating MDR-*Kp* infections contributes to high morbidity and mortality rates worldwide. [4] In contrast, hv*Kp* strains, which were initially recognized in Asia and the Pacific region but are now emerging globally including Europe, can cause severe, life-threatening infections even in healthy individuals, with mortality rates reaching 12–56%. [2,5,6] Hv*Kp* infections are characterized by a distinctive metastatic, invasive syndrome, including pyogenic liver abscess, meningitis, and endophthalmitis. [2]

The capsule of *K. pneumoniae*, a complex exopolysaccharide structure, is a well-established virulence determinant that contributes to immune evasion, biofilm formation, and resistance to phagocytosis. [7] Global genomic studies have demonstrated that specific lineages possessing distinct capsular types are responsible for the global disease burden, with certain serotypes strongly associated with each pathotype (MDR-*Kp*: KL24, KL64, KL106, KL112; hv*Kp*: KL1, KL2, KL20). [8–10] These studies have also revealed that hypermucoidity (HM), consisting of capsule overproduction, and hypermucoviscosity (HMV), a highly specific phenotype, are interrelated traits linked to hypervirulence through genomic, [2] immunologic, and *in vivo* studies in animal models, [11,12] with varying expression levels among strains. [11] However, the specific mechanisms by which the capsule influences bacterial behavior, particularly in relation to infection dynamics within the host, remain incompletely understood. Recent studies highlight the importance of bacterial biophysics and rheology in infectious disease, suggesting that the physical properties of bacteria can significantly influence their ability to colonize, disseminate, and cause disease. [13,14]

We hypothesize that the capsular polysaccharide significantly influences bacterial fluid dynamics, with implications for *K. pneumoniae* invasiveness and dissemination. We propose that the capsule composition, quantity, and resulting rheological properties impact bacterial adhesion, cohesion, and flow resistance in physiologically relevant fluid environments. [15]

In this study, we bridge existing knowledge gaps by investigating the relationship between distinct capsular phenotypes and bacterial rheology. We employ a combined approach, integrating capsule quantification, rheological and textural analyses, and genomic

characterization of *K. pneumoniae* strains representing both MDR-*Kp* and hv*Kp* pathotypes. By characterizing the rheological properties of strains with varying capsular phenotypes, we aim to elucidate the contribution of capsule-mediated rheology to *K. pneumoniae* virulence and invasiveness, defined here as the capacity to spread systemically (e.g., bloodstream dissemination) and establish persistent infections (e.g., tissue colonization). This knowledge is critical for developing novel, biology-driven countermeasures against this increasingly problematic pathogen.

2. Materials and Methods

2.1. Selection of representative *K. pneumoniae* strains

The study encompasses a diverse collection of *K. pneumoniae* isolates representing clinically significant sublineages from both MDR-*Kp* and hv*Kp* pathotypes. We analyzed fourteen genotypically distinct strains with varying surface antigen compositions and capsule production capabilities (Table 1).

The collection includes six hv*Kp* strains expressing capsule types KL1, KL2, and KL20, selected to represent phylogenetically distinct hypervirulent sublineages. Additionally, we examined seven MDR-*Kp* strains expressing capsule types KL2, KL20, KL24, and KL64, representative of endemic sublineages circulating in Portugal and internationally. Notably, one *Kp* strain (A12, Table 1) displayed hypermucoid (HM) and hypermucoviscous variant (HMV) phenotypes. Additionally, five non-capsulated mutants (marked as -M, Table 1) were generated from hypermucoid strains, as described in the following section.

2.2. Experimental inactivation of the capsule

Hypermucoid isolates (Table 1) were subjected to a short-term evolution experiment in rich media to induce the emergence of non-capsulated (C_{sp}-) mutants, as previously described. Each HM strain was independently grown at 37 ºC for 24h in 1 mL of LB broth, then diluted (1:100) in 1 mL of fresh LB broth, and re-incubated overnight. Subsequently, each culture was again diluted (1:100) in LB broth and plated on cystine-lactose-electrolyte-deficient (CLED) agar until reaching more than 100 colonies per plate. This process was repeated during consecutive days until the detection of non-capsulated (C_{sp}-) mutants, visualized by naked eye as smaller, rough and translucent colonies. Three non-capsulated isolates from each population were randomly selected and re-striked twice, to distinguish capsule inactivation by phase variation (transient) or genetic mutations (stable). Colonies that maintained the non-capsulated phenotype were confirmed by capsule quantification and whole-genome sequencing (WGS), as further described.

2.3. Hypermucoviscosity assessment

2.3.1. String test

HMV was preliminarily assessed with the string test, as previously described.[16] Briefly, strains were inoculated in rich LB broth media and incubated at 37°C overnight, and colonies were stretched with a bacteriologic loop to form a string. A strain was considered positive for the string test if the viscous string extended beyond 5mm in length. In order to obtain precise and consistent measurements, the string length was quantified using a TA-XT2i Texture Analyser (Stable Micro System, Godalming, UK) with a cylindrical probe (1/2" Delrin, p/n P/05). Bacteria grown overnight on CLED agar were tested in triplicate, then allowing the culture plates to stabilize at room temperature for 3h. Colonies were directly applied to the sample target, and a probe stretched them upwards at a constant speed of 10 mm/s. The maximum string length *r* was recorded using a ruler (mm).

2.3.2. Sedimentation assay

HMV was further quantified using a sedimentation assay, as previously described. [17] Over day (10-12h) cultures of *K. pneumoniae* grown in LB broth at 37°C were diluted 1:100 into fresh LB broth and incubated for 24h at 37°C. After vigorous vortexing, the optical density at 600 nm (OD_{600}) of the top layer of the culture was measured using a spectrophotometer and the OD_{600} adjusted to 0.85 with LB broth. Adjusted suspensions were centrifuged at 2500 x g for 5 minutes at room temperature, and the optical density OD_{600} of the supernatant (200 µL) was measured. To normalize the results, the HMV level was expressed as the ratio of the OD_{600} of the supernatant to the OD_{600} before centrifugation.

2.4. Capsular extraction and quantification

Capsular polysaccharide content was quantified using uronic acid measurement, following the protocols described by Domenico *et al.* [18] and Blumenkrantz *et al.*, [19] and it was performed for all the wild-type strains (hv*Kp*, MDR-*Kp*) and non-capsulated mutants obtained in this study.

2.4.1. Capsule extraction

Briefly, overnight cultures in LB broth were adjusted to OD_{600}=1.2 (500 µL) based on the first OD_{600} read, treated with 100 µL of 1% Zwittergent 3-14 in 100 mM citric acid of pH 2.0 at 56°C for 20 minutes and centrifuged at 13000 rpm for 5 minutes. The supernatant (300 µL) was washed with absolute ethanol (1.2 mL, 80%) and refrigerated on ice for 20 minutes. The mixture was centrifuged at 13000 rpm for 5 minutes, and the polysaccharides contained in the pellet were washed with 70% ethanol, dried and re-suspended in 250 µL of double-distilled water.

2.4.2. Uronic acid quantification

A 200 µL fraction of capsular extracts was dissolved in 1200 µL of 0.0125 M tetraborate (borex) in concentrated H_2SO_4, the solution vigorously vortexed, placed in a 100°C water bath for 5 minutes, and cooled on ice; as such, concentrated H_2SO_4 hydrolyzed polysaccharides into uronic acid monomers under high-temperature boiling, while borax reacted with H_2SO_4 to generate boric acid, which stabilized the uronic acids by forming borate-uronic acid complexes, enhancing the specificity of the assay. The solution was then incubated with 20 µL of 0.15% 3-phenylphenol in NaOH 0.5%; the alcohol reacted specifically with uronic acids in the presence of borate complexes, to form a readable pink chromophore, while NaOH neutralized the acidic reaction mixture, creating the alkaline conditions required for the color formation. The optical density of 200 µL of the solution was then measured at 520nm, and the uronic acid concentration inferred based on a glucuronic acid standard curve, expressed in micrograms per OD_{600}. The uronic acid concentration was used as a proxy for capsule abundance, assuming uronic acids were a significant component of the capsular polysaccharides.

2.5. Texture analysis

A TA-XT2i Texture Analyser (Stable Micro System, Godalming, UK) was used to assess the mechanical properties of *K. pneumoniae* cultures, specifically deformability and adhesiveness, as surrogates for capsule viscosity, aggregation behavior, and biofilm-related mechanical properties. Strains were grown on CLED agar at 37°C for 24 hours, followed by equilibration at 22±1°C for 3 hours to ensure thermal and rheological stability. Bacterial samples were carefully transferred to the testing platform using a sterile spatula to maintain structural integrity. Xanthan gum (1% w/v), a polysaccharide with well-characterized rheological properties, was used as a reference material for inter-experimental calibration and

comparative analysis. Mechanical properties were assessed using a precision cylindrical probe (1/2" Delrin, p/n P/05) with uniform surface characteristics (roughness Ra<0.8 μm) to ensure reproducibility. Testing was conducted under controlled environmental conditions (22±1°C, 45±5% relative humidity). The Texture Exponent 32 software (version 6.1.12.0, Stable Micro Systems; Godalming, UK) was used to determine the deformability and adhesiveness.

2.5.1. Deformability assessment

Uniaxial compression tests were performed with the following specifications: test speed: 60 mm/min; post-test speed: 180 mm/min; compression gap: 0.3 mm; trigger force: 1 N. Stiffness was calculated as the slope of the force-distance curve in the linear region (0.2-0.8 mm displacement), expressed as N·mm, representing bacterial culture consistency and resistance to deformation.

2.5.2. Adhesiveness measurement

Adhesion tests were conducted using: test speed: 60 mm/min; post-test speed: 180 mm/min; compression gap: 0.3 mm; trigger force: 1 N. Adhesiveness was quantified as the maximum negative force during probe withdrawal normalized to displacement (N·mm), representing the cohesive strength and surface adhesion properties of the bacterial culture. Each strain was analyzed in quintuplicate with independent biological replicates, and measurements were performed on three separate occasions to ensure reproducibility. Statistical analysis was performed using GraphPad Prism v8.0.2, with significance determined at $p < 0.05$.

2.6. Rheological Analysis

Rheological properties of *K. pneumoniae* cultures were characterized using a rotational rheometer (Kinexus lab+, Malvern Instruments; Worcestershire, UK) equipped with a parallel plate measuring system (geometry PU20 SR4367) with a 1 mm gap at 25 °C (Peltier plate cartridge). This methodology quantified shear viscosity and viscoelastic behavior, providing critical insights into capsular material properties that can influence the dissemination, immune evasion, and persistence in the host. Bacterial cultures were grown on CLED agar for 24 hours at 37°C, followed by equilibration at 22±1°C for 3 hours to ensure rheological stability. Samples were carefully transferred using a sterile 10 μL inoculating loop onto the

lower stationary plate of the rheometer. A xanthan gum solution (1% w/v) was analyzed in parallel as a reference material with established non-Newtonian behaviour. The upper plate, of a specific radius (R), rotated at programmed angular velocities (ω) creating sheer in the sample, while the lower plate remained stationary. The torque measurement at the upper plate enabled to calculate the shear stress (τ) experienced by each sample. During the experiment, the shear rate ($\dot{\gamma} = \omega \cdot R/h$) swept from 0.1 to 100 s^{-1}. The values of shear viscosity ($\eta = \tau/\dot{\gamma}$, Pa·s) expressed a quantitative measurement of the internal resistance of the samples to the applied flow, characterizing bacterial rheology under physiologically relevant flow conditions.

2.6.1. **Steady Shear Rheology**

Viscosity measurements were conducted under controlled shear rate conditions. Following a 180-second pre-shear equilibration ($\dot{\gamma} = 0.1\ s^{-1}$), samples underwent logarithmic shear rate sweeps from 0.1 to 100 s^{-1}, with 10 points per decade and 15-second equilibration per measurement point. Shear stress (τ) was continuously recorded, with viscosity (η) calculated as the ratio of shear stress to shear rate ($\eta = \tau/\dot{\gamma}$). Flow curves were fitted to the Herschel-Bulkley model ($\tau = \tau_0 + K \cdot \gamma^n$) to determine yield stress (τ_0), consistency index (K), and flow behavior index (n), providing quantitative parameters for comparative analysis between strains.

2.6.2. **Oscillatory Rheology**

Initial strain sweep tests (γ = 0.01-100%, ω = 1 rad/s) established the linear viscoelastic region (LVER). Subsequent frequency sweep measurements within this identified LVER (γ = 0.5%) spanned angular frequencies from 0.1 to 100 rad/s, recording storage modulus (G'), loss modulus (G''), and complex viscosity (η*). Three key parameters were analyzed: the crossover point where G' equals G'' identified gel-sol transition frequency, the loss tangent ($\tan \delta = G''/G'$) quantified elastic versus viscous contributions, and mechanical strength evaluated through relative proportions of elastic/viscous components. The oscillatory deformation approach was specifically chosen over continuous shear to preserve sample integrity in viscous biological systems.

All measurements were conducted in triplicate with biological replicates. Data processing used rSpace software (v. 1.75, Malvern Panalytical) for rheological analysis, while statistical significance was determined through one-way ANOVA with Tukey's post-hoc test in GraphPad

Prism 8.0.2, considering *p*-values below 0.05 as significant. This methodology enabled precise characterization of bacterial viscoelastic behavior while maintaining structural stability through controlled deformation within the linear response range of the sample.

2.7. Genomic analyses

WGS was obtained with Illumina NovaSeq technology (Illumina, USA). Short reads were *de novo*-assembled with SPAdes (v. 3.13.0, github.com/ablab/spades) and annotated by RAST (v. 2.0, rast.nmpdr.org). Single nucleotide polymorphisms (SNPs) within the *cps* region and genome-to-genome alignments were performed using Genious software v. 2025.0.2.

3. Results

3.1. Capsular abundance defines bacterial categories

To investigate the role of CPS in *Kp* physical properties, a set of clinical isolates (Table 1) and their non-capsulated (C_{sp}-) mutants were categorized based on CPS levels, quantified via the uronic acid assay (Figure 1). Tested hypermucoid (HM) strains (n=4), including hv*Kp*, (e.g., A26/KL1- ST23, H2351/KL20-ST268), exhibited the highest CPS abundance (mean 10.5 ± 2.3 ng/µL) , followed by regular-mucoid (RM) strains (n=5; 5.8 ± 1.2 ng/µL) and non-mucoid (NM) strains (n=5; 1.7 ± 0.4 ng/µL), with significant differences between groups (ANOVA, $p < 0.001$, n=6 replicates per strain) (Figure 1).

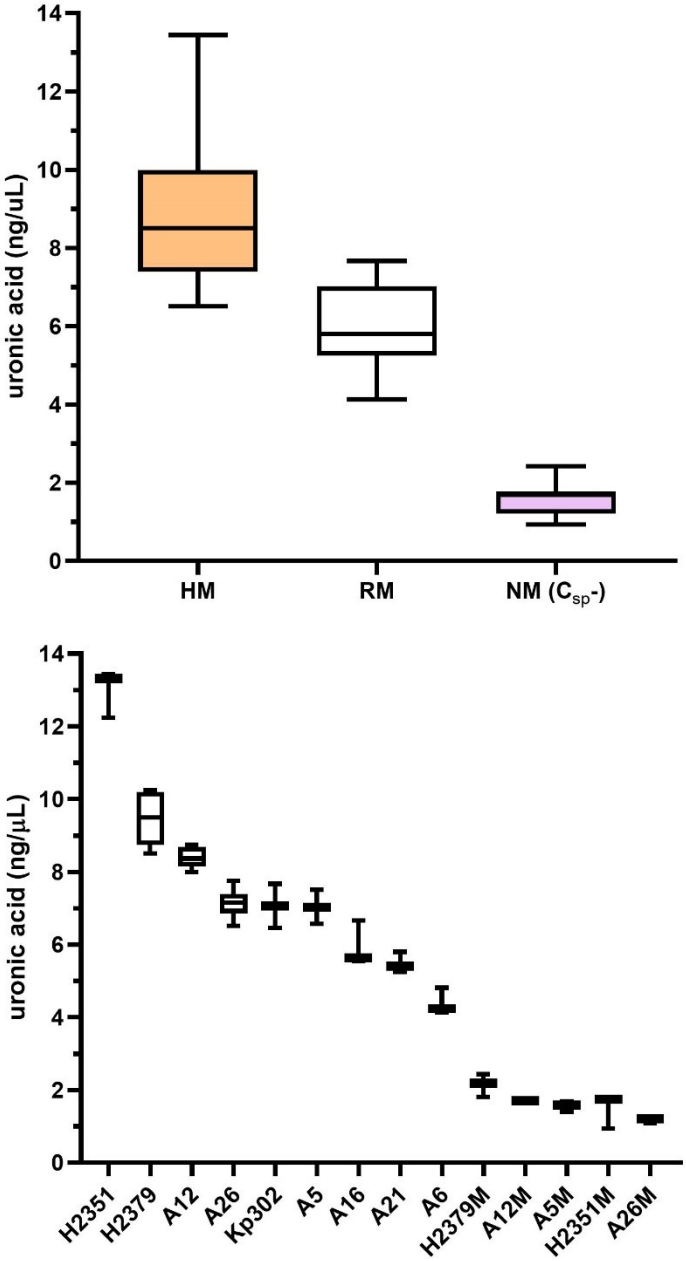


Figure 1. *Kp* uronic acid quantification.
Strains were grouped in three categories: HM = hypermucoid, RM = regular-mucoid, and NM = non-mucoid without capsule (C_{sp}-).

C_{sp}- mutants, generated via serial passaging, showed negligible CPS amounts (<2.14 ng/µL, $p < 0.001$ vs. wild-type), validating their non-capsulated status. The number of serial passages needed for C_{sp}- was strain-dependent and varied between 4 to 7 days (Table 1). Notably, H2351 (KL20-ST268) produced the highest CPS levels (12.8 ± 1.9 ng/µL) exceeding

other HM strains, suggesting strain-specific overproduction. All the other MDR-*Kp* were grouped as RM strains.

3.2. Hypermucoviscosity correlates non-linearly with CPS levels

Hypermucoviscosity (HMV) was assessed using sedimentation assays (Figure 2) and string tests. HM strains displayed higher bacterial concentration in the supernatant after centrifugation (OD600 ratio: 0.65 ± 0.12) when compared to RM (0.42 ± 0.09) and NM (0.18 ± 0.05) ($p < 0.01$), reflecting increased viscosity and lower sedimentation rates (Figure 2). Stretchability followed a similar trend, with HM averaging 23 ± 8 mm, RM 12 ± 4 mm, and NM <5 mm (string test negative, $p < 0.001$). However, CPS quantity and HMV showed a non-linear correlation ($r^2 = 0.35$, $p < 0.05$, $n=14$), indicating that additional factors influence HMV.

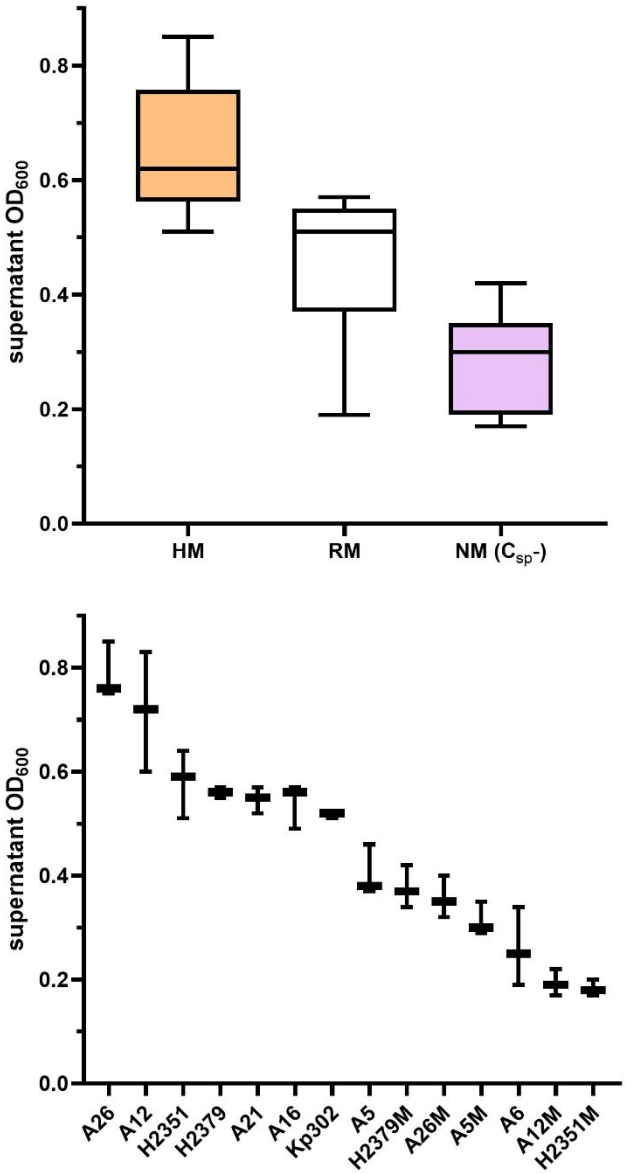


Figure 2. *Kp* HMV quantification by sedimentation test.
HMV values were correlated but not directly proportional with capsule amount.
Legend: HM = hypermucoid, RM = regular-mucoid, and NM = non-mucoid without capsule (C_{sp}-).

The same was observed when comparing the HMV quantification and the stretchability of the string. When bacteria were subjected to a mechanical and controlled stretch of the string, most of the HM strains stretched at an average distance of 23 mm (ranging 8-48mm), while the most stretchable strain A12 (KL64-ST147), a HM MDR-*Kp*, reached 168 mm, which is over 7 times the average of all the other strains. Of note, values were variable within strains exhibiting KL1 (range 11-28 mm) and KL2 (18-47 mm). The least stretchable strain was H2351 (KL20-ST268).

3.3. Mechanical properties reflect CPS-mediated adhesion

Texture analysis revealed distinct mechanical profiles (Figure 3). NM strains exhibited higher stiffness (0.32-0.84 N·mm, mean 0.58 ± 0.19 N·mm) and adhesiveness (0.52-1.24 N·mm, mean 0.88 ± 0.27 N·mm) compared to HM (stiffness: 0.13-0.21 N·mm, mean 0.17 ± 0.03 N·mm; adhesiveness: 0.24-0.32 N·mm, mean 0.28 ± 0.04 N·mm) ($p < 0.001$, n=5). RM strains were intermediate (stiffness: 0.22-0.35 N·mm; adhesiveness: 0.34-0.48 N·mm). A12M stood out with extreme values (stiffness: 3.6 ± 0.5 N·mm, 21x higher than A12; adhesiveness: 3.0 ± 0.4 N·mm, 12x higher, $p < 0.001$ vs. all groups), suggesting CPS loss unmasked adhesive structures. Genomic analysis identified intact *fim* and *mrk* loci in A12M, encoding Type 1 and 3 fimbriae. These and other unidentified traits may potentially drive this phenotype.

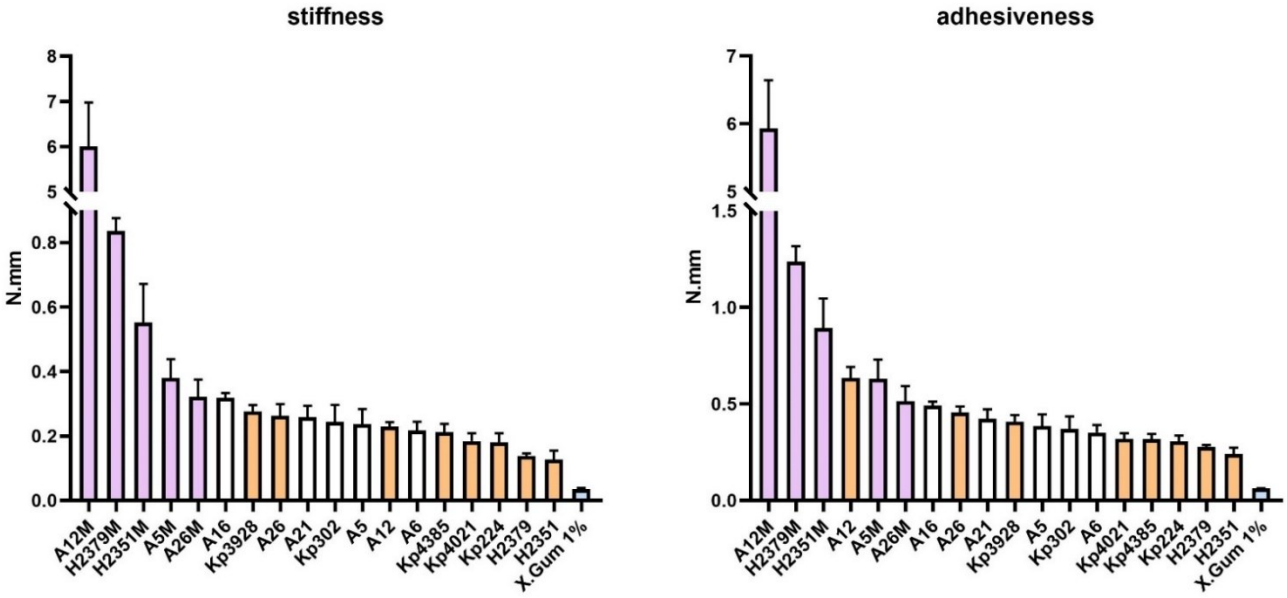


Figure 3. *Kp* textural properties.
On the left, the deformability test quantified the stiffness of each strain. On the right, the adhesiveness test.
Color code: purple = NM (non-mucoid w/o capsule), white = RM (regular-mucoid), yellow = HM (hypermucoid).

3.4. Flow resistance varies with CPS abundance

Rheological assays at a physiological shear rate (0.1 s^{-1}) showed HM strains had lower shear viscosity (SV: 35.1–202.1 Pa·s, mean 118 ± 62 Pa·s) than NM strains (618–1340 Pa·s, mean 978 ± 312 Pa·s, $p < 0.001$, n=5) (Figure 4). RM strains ranged from 245–512 Pa·s (mean 378 ± 108 Pa·s), distinct from both ($p < 0.01$). The shear viscosity of A12M (SV: 601 ± 85 Pa·s, 5x higher than A12) deviated markedly, reinforcing its outlier status (Figure 4). All strains exhibited non-Newtonian behaviour (Herschel-Bulkley model, $R^2 > 0.95$), with HM showing

greater shear-thinning (n = 0.4-0.6) than NM (n = 0.7-0.9), indicating CPS reduces flow resistance. WGS linked C_{sp}- phenotypes to *wcaJ*/*wbaP* mutations (e.g., p.Lys327Glu in H2379M), while A12 harbored multiple *cps* SNPs, potentially enhancing CPS fluidity.

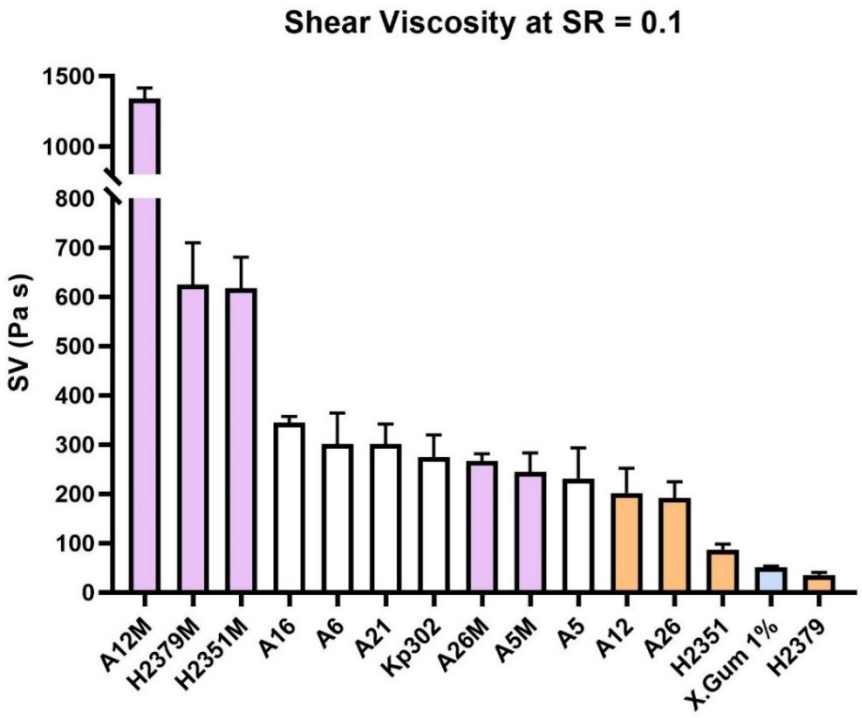


Figure 4. *Kp* Shear Viscosity (SV) at shear rate = 0.1 s^{-1}.
NM strains (purple) showed higher SV than RM (white) and HM (yellow).

3.4.1. CPS loss and flow resistance reveal genomic/phenotypic variability

WGS analyses linked CPS loss in most C_{sp}- mutants to point mutations in CPS biosynthesis genes *wcaJ* or *wbaP* (H2351M: p.His39Arg and p.Glu50Gln in *wbaP*; H2379M: p.Lys327Glu in *wcaJ*, A5M: p.Ser142Pro in *wbaP*), disrupting colanic acid or galactose incorporation. [20] However, A12M and A26M lacked *wcaJ*/*wbaP* mutations, retaining intact *cps* loci, except for a frameshift in *wzc* (A12M: c.1285delA) and a promoter SNP in *rmpA* (A26M: g.-53C>T), suggesting alternative inactivation pathways such as export disruption or transcriptional downregulation. Conversely, wild-type A12 harbored multiple *cps* SNPs (e.g., *wcaJ* p.Thr89Ile, *wzp* p.Gln154Arg), potentially enhancing CPS fluidity and stretchability.

4. Discussion

The capsular polysaccharide of *K. pneumoniae* is a well-established virulence factor, conferring resistance to phagocytosis and complement-mediated killing. [11] This study demonstrates that CPS also governs *Kp* rheological and textural properties, revealing a previously underexplored dimension of its pathogenesis. By categorizing strains into hypermucoid (HM), regular-mucoid (RM), and non-mucoid (NM) based on CPS abundance, we uncovered distinct physical phenotypes that align with *Kp* invasive capabilities.

Our findings highlight a nuanced distinction between CPS quantity and hypermucoviscosity (HMV). While HM strains exhibited the highest CPS levels (mean 10.5 ± 2.3 ng/µL, $p < 0.001$ vs. RM/NM), the HMV values, assessed via sedimentation and stretchability, did not scale linearly with the CPS amount ($r^2 = 0.35$, $p < 0.05$). This aligns with recent genomic insights implicating RmpA/D and metabolic regulators in HMV, [21,22] suggesting that CPS composition and structural assembly, beyond quantity, contribute to this phenotype. Notably, strain A12 (HM, KL64-ST147) harboured multiple *cps* locus mutations, potentially enhancing CPS cross-linking and stretchability, a trait connected with HMV and metastatic spread. [16] In contrast, its non-capsulated mutant A12M lacked *cps* mutations typically associated with CPS loss (e.g., *wzc),* hinting at alternative regulatory mechanisms, possibly metabolic or transcriptional, that warrant further investigation.

Rheologically, HM strains displayed significantly lower shear viscosity (SV: 35.1-202.1 Pa·s) compared to NM strains (618-1340 Pa·s, $p < 0.001$), reflecting a fluid-like behavior conducive to dissemination in low-shear environments like the bloodstream (0.1-10 s^{-1}). [14] This may explain hv*Kp* ability to evade shear-induced immune clearance, such as neutrophil entrapment under flow, a mechanism observed in other pathogens. [23] Conversely, NM strains exhibited higher stiffness (0.32-0.84 N·mm) and adhesiveness (0.52-1.24 N·mm), traits that could enhance tissue colonization by promoting adherence to epithelial surfaces. [24] The outlier A12M, with its outstanding SV (5x higher), stiffness (21x), and adhesiveness (12x) compared to the corresponding wild-type strain, suggests CPS loss exposes underlying adhesins, potentially fimbriae or afimbrial proteins, as supported by prior lectin-binding data, showing heightened recognition of non-capsulated mutants by mannose-specific receptors like Dectin-2 (Loiodice *et al.*, unpublished data). Genomic analysis of A12M revealed intact *fim* and *mrk* loci (Type 1 and 3 fimbriae), supporting this hypothesis, though direct protein profiling is needed for confirmation.

These physical properties have profound implications for host-pathogen interactions. Low SV in HM strains likely facilitates rapid dissemination during bacteremia, a hallmark of hv*Kp* infections, [12] while shielding CPS from innate immune lectins like DC-SIGN, as we previously observed (Loiodice *et al.*, unpublished data). This dual mechanism, fluid evasion of mechanical clearance and molecular evasion of immune recognition, underscores the CPS role as a multifaceted virulence determinant. NM strains adhesiveness, conversely, may enhance persistence in mucosal niches (e.g., lungs), where stickiness could thwart ciliary clearance and promote biofilm formation. [25] The absence of CPS in NM mutants, however, renders them vulnerable to phagocytosis, aligning with reduced virulence in *wcaJ* mutants. [26]

Therapeutically, these findings suggest that targeting CPS rheology could disrupt *Kp* pathogenesis. Agents that increase SV (e.g., viscosity-enhancing polymers) might impede HM dissemination, while CPS-degrading enzymes could expose NM adhesins to immune attack, enhancing clearance. [24] Such strategies could complement existing antimicrobials, particularly against MDR-hv*Kp*, or clones like ST147-KL64, prevalent in Portugal (Loiodice *et al.*, unpublished data). However, limitations remain: our rheological assays used saline suspensions instead of physiological fluids (e.g., blood, mucus), and lack *in vivo* validation. Future studies should test these phenotypes in flow chambers or infection models to confirm their clinical relevance.

In conclusion, CPS rheology offer a new lens on *K. pneumoniae* virulence, linking physical traits to ecological fitness and immune evasion. This interdisciplinary approach bridges mechanobiology and microbiology, paving the way for innovative interventions against this urgent pathogen.

5. Conclusions and future perspectives

The low correlation between capsule amount and HMV assays emphasizes the need to consider these as distinct but complementary phenotypes in *K. pneumoniae*. HM (copious CPS production) and HMV (high viscosity/elasticity of the CPS) are dissociable traits, with variable correlations between capsule quantity and rheological properties. This understanding is crucial for accurately characterizing hv*Kp* strains and developing phenotype-targeted strategies to combat their infections. [27,28]

Non-Newtonian fluid properties of bacteria reveal HM-HMV *K. pneumoniae* with lower shear viscosity propagate faster in flow conditions, potentially enhancing dissemination in fluids (e.g., bloodstream). Conversely, the heightened adhesive capacity observed in NM strains may result from surface fimbrial or afimbrial adhesins, promoting host tissue

colonization and persistence at infection sites, due to reduced CPS-mediated masking of outer membrane proteins.

Therapeutic strategies targeting structural/rheological properties (e.g., biofilm disruption) may complement metabolic inhibitors, given the multifactorial nature of HMV. This multilayered regulation underscores HMV as an adaptive virulence strategy involving transcriptional control, metabolic integration, and physical properties distinct from CPS-mediated protection. Further research into strain-specific rheological profiles and their environmental modulation could improve anti-virulence approaches.

ACKNOWLEDGEMENTS

We are thankful to Olaya Rendueles-Garcia for sharing optimized protocols for capsule quantification and hypermucoviscosity assay, and Sylvain Brisse for providing some of the hypervirulent strains used in this study.

Bibliography

1. Navon-Venezia S, Kondratyeva K, Carattoli A. *Klebsiella pneumoniae*: a major worldwide source and shuttle for antibiotic resistance. *FEMS Microbiology Reviews* 2017; **41**: 252–75.

2. Russo TA, Marr CM. Hypervirulent *Klebsiella pneumoniae*. *Clin Microbiol Rev* 2019; **32**: e00001-19.

3. Li D, Huang X, Rao H, *et al. Klebsiella pneumoniae* bacteremia mortality: a systematic review and meta-analysis. *Front Cell Infect Microbiol* 2023; **13**: 1157010.

4. Russo A, Fusco P, Morrone HL, Trecarichi EM, Torti C. New advances in management and treatment of multidrug-resistant *Klebsiella pneumoniae*. *Expert Review of Anti-infective Therapy* 2023; **21**: 41–55.

5. Tang Y, Liu H, Zhao J, Yi M, Yuan Y, Xia Y. Clinical and Microbiological Prognostic Factors of in-Hospital Mortality Caused by Hypervirulent *Klebsiella pneumoniae* Infections: A Retrospective Study in a Tertiary Hospital in Southwestern China. *IDR* 2020; **Volume 13**: 3739–49.

6. Bhardwaj V, Annapandian V, Sinazer A, Alva A, Prasad S. Incidence, risk factors and clinical outcomes of patients with hypermucoviscoid *Klebsiella* in a tertiary intensive care unit. *J Global Infect Dis* 2020; **12**: 202.

7. Paczosa MK, Mecsas J. *Klebsiella pneumoniae*: Going on the Offense with a Strong Defense. *Microbiol Mol Biol Rev* 2016; **80**: 629–61.

8. Wyres KL, Lam MMC, Holt KE. Population genomics of *Klebsiella pneumoniae*. *Nat Rev Microbiol* 2020; **18**: 344–59.

9. Gorrie CL, Mirčeta M, Wick RR, *et al.* Genomic dissection of *Klebsiella pneumoniae* infections in hospital patients reveals insights into an opportunistic pathogen. *Nat Commun* 2022; **13**: 3017.

10. Martin RM, Cao J, Brisse S, *et al.* Molecular Epidemiology of Colonizing and Infecting Isolates of *Klebsiella pneumoniae* Castanheira M, ed. *mSphere* 2016; **1**: e00261-16.

11. Mike LA, Stark AJ, Forsyth VS, *et al.* A systematic analysis of hypermucoviscosity and capsule reveals distinct and overlapping genes that impact *Klebsiella pneumoniae* fitness Mecsas J, ed. *PLoS Pathog* 2021; **17**: e1009376.

12. Walker KA, Miller VL. The intersection of capsule gene expression, hypermucoviscosity and hypervirulence in *Klebsiella pneumoniae*. *Current Opinion in Microbiology* 2020; **54**: 95–102.

13. Weber A, Tyrakowski D, Toca-Herrera JL. Power Laws Describe Bacterial Viscoelasticity. *Langmuir* 2022; **38**: 15552–8.

14. Dufrêne YF, Persat A. Mechanomicrobiology: how bacteria sense and respond to forces. *Nat Rev Microbiol* 2020; **18**: 227–40.

15. Echols R, Ariyasu M, Nagata TD. Pathogen-focused Clinical Development to Address Unmet Medical Need: Cefiderocol Targeting Carbapenem Resistance. *Clinical Infectious Diseases* 2019; **69**: S559–64.

16. Fang C-T, Chuang Y-P, Shun C-T, Chang S-C, Wang J-T. A Novel Virulence Gene in *Klebsiella pneumoniae* Strains Causing Primary Liver Abscess and Septic Metastatic Complications. *The Journal of Experimental Medicine* 2004; **199**: 697–705.

17. Khadka S, Ring BE, Pariseau DA, Mike LA. Characterization of *Klebsiella pneumoniae* Extracellular Polysaccharides. *Current Protocols* 2023; **3**: e937.

18. Domenico P, Schwartz S, Cunha BA. Reduction of capsular polysaccharide production in *Klebsiella pneumoniae* by sodium salicylate. *Infect Immun* 1989; **57**: 3778–82.

19. Blumenkrantz N, Asboe-Hansen G. New method for quantitative determination of uronic acids. *Analytical Biochemistry* 1973; **54**: 484–9.

20. He J, Shi Q, Chen Z, *et al.* Opposite evolution of pathogenicity driven by *in vivo* wzc and wcaJ mutations in ST11-KL64 carbapenem-resistant *Klebsiella pneumoniae*. *Drug Resistance Updates* 2023; **66**: 100891.

21. Xu Q, Yang X, Chan EWC, Chen S. The hypermucoviscosity of hypervirulent *K. pneumoniae* confers the ability to evade neutrophil-mediated phagocytosis. *Virulence* 2021; **12**: 2050–9.

22. Catalán-Nájera JC, Garza-Ramos U, Barrios-Camacho H. Hypervirulence and hypermucoviscosity: Two different but complementary *Klebsiella* spp. phenotypes? *Virulence* 2017; **8**: 1111–23.

23. Xu L, Li J, Wu W, Wu X, Ren J. *Klebsiella pneumoniae* capsular polysaccharide: Mechanism in regulation of synthesis, virulence, and pathogenicity. *Virulence* 2024; **15**: 2439509.

24. De Astorza B, Cortés G, Crespí C, Saus C, Rojo JM, Albertí S. C3 Promotes Clearance of *Klebsiella pneumoniae* by A549 Epithelial Cells. *Infect Immun* 2004; **72**: 1767–74.

25. Roe JM, Seely K, Bussard CJ, *et al.* Hacking the Immune Response to Solid Tumors: Harnessing the Anti-Cancer Capacities of Oncolytic Bacteria. *Pharmaceutics* 2023; **15**: 2004.

26. Mike LA, Stark AJ, Forsyth VS, *et al.* A systematic analysis of hypermucoviscosity and capsule reveals distinct and overlapping genes that impact *Klebsiella pneumoniae* fitness Mecsas J, ed. *PLoS Pathog* 2021; **17**: e1009376.

27. Chen J, Zhang H, Liao X. Hypervirulent *Klebsiella pneumoniae*. *IDR* 2023; **Volume 16**: 5243–9.

28. Arena F, Menchinelli G, Di Pilato V, *et al.* Resistance and virulence features of hypermucoviscous *Klebsiella pneumoniae* from bloodstream infections: Results of a nationwide Italian surveillance study. *Front Microbiol* 2022; **13**: 983294.

Table 1. Representative hv*Kp* and MDR-*Kp* used in this study.

Name	Pathotype	Mucoidy	ST	KL-Type	O-Type	Acquired β-lactamase	C_{sp}- occurrence (nº serial passages)	Reference (DOI)
A12 (K473)	MDR-*Kp*	HM	ST147	KL64	O2a	KPC-3	-	10.3390/antibiotics9110806
A26 (SB53)	hv*Kp*	HM	ST23	KL1	O1	-	-	10.3201/eid2011.140206
Kp4385	hv*Kp*	HM	ST23	KL1	O1	-	-	10.3201/eid2011.140206
Kp3928	hv*Kp*	HM	ST23	KL1	UN	-	-	10.3201/eid2011.140206
H2379	hv*Kp*	HM	ST380	KL2	O1	-	-	Loiodice *et al.*, unpublished
Kp4021	hv*Kp*	HM	ST86	KL2	O1	-	-	10.3201/eid2011.140206
H2351	hv*Kp*	HM	ST268	KL20	O2a	-	-	Loiodice *et al.*, unpublished
A16 (H49)	MDR-*Kp*	RM	ST14	KL2	O1	TEM-24	-	10.1128/mSystems.00386-19
Kp224	MDR-*Kp*	RM	ST25	KL2	O1	KPC-3	-	This study
Kp302	MDR-*Kp*	RM	ST268	KL20	O2a	KPC-3	-	This study
A21 (H1098)	MDR-*Kp*	RM	ST15	KL24	O1	SHV-28	-	10.1128/mSystems.00386-19
A5 (M11)	MDR-*Kp*	RM	ST45	KL24	O2a	KPC-3	-	10.1128/aac.00890-21
A6 (K506)	MDR-*Kp*	RM	ST147	KL64	O2a	KPC-3	-	10.3390/antibiotics9110806
A26M	hv*Kp*	NM	ST23	KL1	O1	-	7	This study
H2379M	hv*Kp*	NM	ST380	KL2	O1	-	4	This study
H2351M	hv*Kp*	NM	ST268	KL20	O2a	-	4	This study
A5M (M1A)	MDR-*Kp*	NM	ST45	KL24	O2a	KPC-3	*in vivo*	10.1128/aac.00890-21
A12M	MDR-*Kp*	NM	ST147	KL64	O2a	KPC-3	7	This study

Legend: HM = hypermucoid; RM = regular-mucoid; NM = non-mucoid. ST = Sequence Type, obtained by MLST; KL-Type = Capsular type (CPS); O-Type = O-antigen type (LPS). UN= Unknown.

Strain-specific glycosignatures in representative multidrug resistant and hypervirulent *Klebsiella pneumoniae* sublineages

Michele Loiodice[1], Benedita Pinheiro[2], Angelina Palma[2], Luísa Peixe[1], Ângela Novais[1]

[1]UCIBIO, i4HB, Faculdade de Farmácia da Universidade do Porto, Rua Jorge Viterbo Ferreira 228, 4050-313 Porto, Portugal.

[2] UCIBIO, i4HB, Department of Chemistry/Department of Life Sciences, School of Science and Technology, NOVA University of Lisbon, 2829-516 Caparica, Portugal.

Manuscript under preparation for submission

Abstract

Klebsiella pneumoniae poses a global health threat due to antimicrobial resistance and virulence linked to its polysaccharide capsule, which enables immune evasion. Hypervirulent (hv*Kp*) and multidrug-resistant (MDR-*Kp*) strains exhibit distinct capsular serotypes and phenotypes, yet glycan-mediated host-pathogen interactions remain underexplored. This study aims at investigating strain-specific glycosignatures and their differential recognition by lectins to elucidate mechanisms of immune evasion.

Bacterial microarrays comprising 12 clinically relevant *K. pneumoniae* strains (hv*Kp*, MDR-*Kp*, hypermucoid/non-capsulated mutants) were prepared. Strains were fluorescently labeled, printed on nitrocellulose slides, and probed with nine lectins targeting glycans of diverse origin (plant, fungal, bacterial, mammalian). Binding patterns were analysed using fluorescence microscopy, with non-capsulated mutants generated to assess CPS masking effects.

Non-capsulated strains exhibited broader lectin recognition (7/7 lectins) compared to hypermucoid variants (4/7), highlighting CPS quantity, not composition, as the primary determinant of immune evasion. Specific patterns were identified: DC-SIGN binding exclusively to non-capsulated/regular-mucoid strains, and LecA strong affinity for O1 LPS galactose residues. Hypermucoid phenotypes masked fucose/mannose epitopes targeted by AAL and Dectin-2.

Capsule production levels critically modulate immune lectin engagement, enabling hv*Kp* strains to evade detection. These findings underscore CPS as a dynamic shield, with implications for developing anti-adhesion therapies and glycan-based diagnostics.

1. Introduction

Klebsiella pneumoniae, a Gram-negative bacterium commonly found in the human nasopharynx and gastrointestinal tract, [1] poses significant health risks due to its association with multidrug resistance (MDR) phenotypes. Its virulence is largely attributed to its polysaccharide capsule, which protects against immune responses and enhances pathogenicity. [2] *K. pneumoniae* has over 186 capsular serotypes (K antigens), [3] with hypervirulent strains (hv*Kp*) linked to increased invasiveness and severe infections, even in healthy individuals. These strains often show hypermucoviscous (HMV) phenotype, carrying genes like as *rmpA* that boost capsule production. [4,5] Recently, the convergence of the two phenotypes, hv*Kp* strains carrying carbapenemase genes (MDR-hv*Kp*), have emerged as a significant concern. [6]

Microarray technology [7] has advanced the study of *K. pneumoniae* by profiling its complex surface glycans, such as capsular polysaccharides (CPS) and lipopolysaccharides (LPS). These glycans interact with host immune receptors, influencing immune recognition and pathogen dynamics. [8] Lectins, a class of sugar pattern recognition receptors, play a crucial role in detecting bacterial glycans, though *K. pneumoniae* can exploit these interactions to evade immune responses. [9,10]

The emergence of multidrug-resistant (MDR-*Kp*) and hypervirulent (hv*Kp*) strains of *K. pneumoniae* has become a global health concern. These strains exhibit diverse virulence profiles linked to specific capsular types used as epidemiological markers. [8,11] Recent advances in glycomics and bacterial phenotyping have highlighted the need to move beyond genomic analyses to better understand the role of structural glycan diversity. [12] However, the contribution of these interactions to the differential immune response elicited by hv*Kp* and MDR-*Kp* strains remains limited. [13,14]

This study aims to investigate the *K. pneumoniae* surface glycans and their differential recognition by specific glycan-binding proteins. To this end, bacterial microarrays comprising diversity of strains with variable CPS and LPS structures were developed and applied to analyze strain specific glycosignatures, with possible implications for immune evasion and pathogenicity. [14,15] Understanding these interactions is essential for developing effective therapeutic strategies against this opportunistic pathogen. [14]

2. Materials and Methods

2.1. *K. pneumoniae* strains and lectins

We selected twelve *K. pneumoniae* isolates, representing main MDR-*Kp* and hv*Kp* sublineages of clinical interest, exhibiting specific and relevant capsular (K) and O-antigen (O) types. These strains showed differential capsule expression (hypermucoid, regular-

mucoid, non-mucoid), and some with HMV phenotype, meaning that differential accessibility to varied glycan structures (Table 1).

Non-capsulated mutants were generated through serial passages of hypermucoid *K. pneumoniae* strains in LB broth (37°C, 24h cycles). Non-capsulated variants emerged as smaller, rough, translucent colonies on CLED agar within 4-7 days. Three non-capsulated isolates from each population were randomly selected and re-striked twice, to distinguish capsule inactivation by phase variation (transient) or genetic mutations (stable). Colonies that maintained the non-capsulated phenotype were confirmed by capsule quantification based on uronic acid measurement, as previously described by Domenico *et al.* [16] and Blumenkrantz *et al.*, [17] and by whole-genome sequencing (WGS) analysis, identifying mutations in the *cps* cluster.

2.2. Bacteria Fixation and Fluorescent Labeling

K. pneumoniae strains, control glycoproteins and lectins utilized in this assay are shown in Table 1. We selected isolates that exhibited diverse and representative capsular (K) types and sequence types (ST), along with varying levels of capsular production (hypermucoid, regular-mucoid and non-mucoid). This included MDR-*Kp* and hv*Kp*, as detailed in Table 1. Bacterial strains were grown overnight in LB broth at standard conditions (37 °C, 200rpm shake), and then washed twice in Tris-buffered saline (TBS) by centrifugation (at 8500 RCF for 4 minutes), to remove the growth media. The pellets were then resuspended in 1 mL of 4% paraformaldehyde and incubated for 30 minutes at room temperature for fixation. Cells were then washed twice with TBS to remove residual paraformaldehyde.

Fixed bacterial suspensions were centrifuged at 9000 × *g* for 4 minutes, and resuspended in TBS. The suspensions concentrations were adjusted to OD_{600} = 1, and then fluorescent labeled with CellTrace (stock solution 20 ng/mL), adding 1 µL per mL of suspension. After thorough mixing, the samples were incubated for 1 hour in the dark at room temperature. Finally, labeled bacteria were washed once with TBS post-labeling.

2.3. Microarray Preparation

CellTrace-labeled bacterial suspensions in TBS (OD_{600} = 1) were centrifuged at 15,000 × *g* for 2 minutes or 9000 × *g* for 4 minutes. Two-thirds of the supernatant volume was removed and replaced with bacteria printing buffer (70.5% glycerol and 0.09% v/v Triton X-100, previously filtered with a 0.2 µm syringe filter). Two dilutions of bacteria (OD_{600} = 0.1 and 1) were prepared in an arrayer washing buffer (47% glycerol and 0.06% v/v Triton X-100, filtered) and stored at -20°C until use. Control glycoproteins were serially diluted

from 1 to 0.03 mg/mL in an arrayer washing buffer, containing 1 µL/mL of Cy3 dye solution (GE Healthcare), used to control the spots after the printing.

Samples of 10 µL each were transferred to a 384-microwell plate, following a recognizable layout. The plate was sealed, centrifuged at 200 × *g* for 1 minute, and immediately used for manual printing using a MicroCaster™ 8-Pin System (Whatman®, Schleider&Schuell). Bacterial and control glycoprotein dilutions were printed in replicates on nitrocellulose-coated, 2-pad glass slides (ONCYTE® NOVA, Grace Biolabs), with each pad containing a 12 x 18 spot matrix. Slides were dried overnight in the dark and stored at room temperature in a dry and dark place, until usage.

The glycoprotein asialofetuin, and the polysaccharides glucoronoxylomannan (GXM), PGG glucan and α-mannan, were also included as probes to serve as positive control for each binding assay.

2.4. Microarray Binding Assays

Printed slides were assembled using a proplate slide module, and pads initially humidified with ultrapure water. Blocking procedure was performed with 300 µL of 1% BSA in TBS-Ca^{2+}-Mg^{2+} for 60 minutes at room temperature. After washing with TBS-Ca^{2+}-Mg^{2+}, an amount of 300 µL of biotin-tagged lectin solution (5-20 µg/mL, Table 2) was added to each pad, and incubated for 90 minutes at room temperature.

Following lectin incubation and washing, 300 µL of AF647-labeled streptavidin (1 µg/mL) were added to each pad and incubated for 45 minutes at room temperature. After a final washing step, slides were rinsed with Milli-Q water and dried overnight in the dark. Fluorescence signals for CellTrace and Alexa Fluor 647 were detected using excitation wavelenghts of 532 nm and 647 nm, respectively, utilizing a microarray scanner model GenePix 4300A (Molecular Devices), together with the software GenePix Pro (v.7, Molecular Devices).

A diverse panel of lectins with characterized glycan-binding specificities was chosen to probe the bacterial microarrays (Table 2). These lectins had different origins: plants (RCA120, GNL/GNA); fungal (AAL); bacterial (LecA, LecB); and mammals (Dectin-1, Dectin-2, DC-SIGN, SP-D).

3. Results and Discussion

3.1. Lectin binding patterns overview

The microarray binding assays revealed diverse lectin recognition patterns across *K. pneumoniae* strains, with non-capsulated strains, exposing more LPS structures, being recognized by a higher number and diversity of lectins (7/7 lectins) and hypermucoid strains showing reduced or no binding (4/7 lectins). Among the nine lectins tested, six exhibited

significant binding, particularly RCA120, AAL, LecA, LecB, Dectin-2 and DC-SIGN, whereas others showed residual weak binding (GLN, Dectin 1) or no binding (SP-D). For all except AAL and GNL/GNA, binding was dose-dependent, as higher bacterial densities (OD600 = 1) increased or revealed binding signals for some strains (Figure 1). Binding patterns were in most cases strain-dependent, varying according to pathotype (MDR-*Kp* vs hv*Kp*), K- and O-type, and capsular amount (Figure 1). The recognition patterns observed in the tested experimental conditions will be disclosed hereafter, according to the different types of tested lectins.

3.2. Plant β-galactose and α-mannose specific lectins RCA120 and GNL

The binding assay for RCA120 showed that this plant lectin recognized strain A26 (hv*Kp,* hypermucoid, HMV, ST23-K1/O1) and its non-capsulated variant (A26M), A12 (MDR-*Kp*, hypermucoid, HMV, ST147-KL64/O2a) H2379M (ST380-KL2/O1). In case of strains A12 and A26, RCA120 may bind to the β-D-galactose units [19] present in the KL64/K1 capsule, eventually favoured by an overproduction of capsular polysaccharides enriched in β-galactosylated structures. [36] This is also suggested by the fact that RCA120 didn't bind to other regular or non-mucoid ST147-KL64 strains (A12M, A6, A6M). We hypothesized that RCA120 binds to the O1 LPS of A26M and H2379M, both non-capsulated mutant, where β-D-galactose (β-D-Galp) forms part of the backbone.

Plant lectin GNL (also known as GNA), produced by *Galanthus nivalis*, showed binding to the mutant A6M strain only (MDR-*Kp*, non-mucoid, ST147-KL64/O2a). GNL is known to bind α-1,3-linked mannose, [20] a structure that is not present neither in the KL64 CPS nor in the O2a LPS. Accordingly, we reason that the glycoepytopes recognized by GNL belong to other cellular glycoconjugate or polysaccharide structures, and that those are masked by the CPS production in the wild-type, regular-mucoid A6.

3.3. Fungal α-fucose-specific lectin AAL

The fungal α-fucose-specific lectin AAL showed binding only to A12M (c*Kp,* non-mucoid, ST147-KL64/O2a), without significant variation between bacterial concentrations. This result, and the absence of binding to other non-mucoid strains with variable genotype, including K and O in A6M, suggests the presence in A12M of strain-specific fucosylated structures that contain a high quantity of α-1,6/α-1,3-linked fucose, [22] possibly masked by the abundant capsule production of the wild-type A12.

3.4. Bacterial α-galactose and α-fucose specific lectins LecA and LecB

Pseudomonas aeruginosa bacterial lectin LecA exhibited the highest binding of the array (Figure 1), strongly recognizing all K1/K2-O1 strains independently on capsular

amount (A26, A26M, H2379, H2379M). A weak binding was additionally detected at higher bacterial concentration for strains H2351M, a non-mucoid version of hv*Kp* with different K/O-type (KL20/O2a). As LecA is known to exhibit specificity towards terminal α-galactose (as in glycolipid Gb3), [24] this lectin may recognize the terminal α-galactose residues that are present in both galactan I and galactan II of the O1 Serotype LPS. [37]

Lectin LecB, also produced by *P. aeruginosa*, strongly binds A12M and A6M, both ST147-KL64/O2a, non-capsulated mutants, and weakly A26 and A26M, both ST23-K1/O1. LecB is specific for α-fucose, [26] which can be enzymatically incorporated via α-1,2, α-1,3, or α-1,6 linkages [38] in surface adhesin glycoprotein (e.g. fimbrial proteins), which are more exposed in non-capsulated A12M, A6M and A26M.

3.5. Mammalian immune system lectin receptors

Mouse Dectin-1 yielded weak signals with two non-capsulated strains A12M (MDR-*Kp*, non-mucoid, ST147-KL64/O2a) and H2351M (hv*Kp*, non-mucoid, ST268-KL20/O2a) exclusively at a higher bacterial concentration (OD_{600} = 1). Dectin-1, a C-type lectin-like receptor critical for fungal pathogen recognition, binds specifically to β-1,3-glucooligomers with a minimum chain length of 10-11 glucose units. [28,29] These sugar are not inherent structural components of CPS and LPS, therefore we can speculate the binding activity involves other cellular polysaccharides.

Human Dectin-2, a C-type lectin, is known to bind α-mannose residues. [30] In this experiment, Dectin-2 recognized most (5/6) of the non-capsulated mutants (A12M, H2351M, A6M, A26M, H2379M), together with two wild-type hypermucoid (H2351, ST268-KL20/O2a, and H2379, ST380-KL2/O1), and one regular-mucoid (A6, ST147-KL64/O2a), showing recognition of common structures among diverse genetic backgrounds and independently on the type and amount of K-type and on the O-type.

DC-SIGN, a human C-type lectin expressed by dendritic cells (DCs), is a highly versatile pathogen-recognition receptor that binds a wider range of glycoepitopes, which include fuco-, [31] manno- [30,32,33] and gluco-oligosaccharides. [29] Notably, at higher bacterial concentrations, DC-SIGN clearly recognized all the non-capsulated mutants (A12M, H2351M, A6M, A26M, A5M) and regular-mucoid strains (A5 and A6), showing no biding activity with hypermucoid/HMV strains. This result confirms that high CPS production, resulting in hypermucoidy phenotype, increases *K. pneumoniae* virulence and invasiveness by acting as a molecular cloak, hiding key sugar structures targeted by the host immune system. [10,37,39]

No binding was observed for surfactant protein D (SP-D), a lung collectin, though it has been previously shown to recognize non-capsulated *K. pneumoniae* strains. [13] This lectin binds to mannose-containing O-antigens in *K. pneumoniae* LPS, [35] and preferentially associated with the O3 and O5 serotypes. [40,41] Our results might be justified by the fact that all the strains were either O1 or O2, by the experimental conditions (higher concentrations of bacteria or lectin could have improved sensitivity) or by inadequate concentrations or functional states of SP-D.

3.6. Contextualization of the results with other studies

Other studies using bacterial microarrays have also shown that different *K. pneumoniae* strains, including HMV variants, exhibit distinct binding patterns to galectins and other lectins. Some siglecs and galectins of the human immune system strongly recognize specific but distinct sugar epitopes on *K. pneumoniae*, [14] while others show minimal interaction, highlighting variability in glycan structures. Interestingly, previous studies demonstrated that the O-antigen structure from the LPS seems to be the main ligand target of these interactions. [13,14] Our data support that non-capsulated strains have a higher probability to be recognized by different types of lectins, probably because other glycans, including LPS, become available. Though, lectins with wider specificity, such as DC-SIGN, appear to recognize both CPS and LPS, yet targeting distinct epitopes in each glycoconjugate structure. [13]

3.7. Study rationale and limitations

This study evaluated the glycan-recognition patterns of MDR-*Kp* and hv*Kp* strains of variable CPS and LPS, by using a whole-cell approach and highly diverse lectins. Our results revealed strain-specific patterns associated with variations in *K. pneumoniae* CPS, LPS or other surface glycans. Moreover, we showed that the recognition, or lack of recognition, of specific lectins depends on their surface accessibility, which in some cases results masked by capsule production. However, we recognized several limitations that characterized this assay. Firstly, the bacterial sample set was small and not fully representative of the main *K. pneumoniae* pathotypes and lineages. As such, the effectiveness of a microarray binding assay is limited by the probe library, as missing glycan structures targeted by lectins can yield inconclusive results, despite not being the focus of this study. [42] Secondly, the unknown limits of interaction sensitivity also represents an experimental limitations; further adjustments on bacteria and lectin concentration would show more significant interaction patterns. Lastly, as the spatial arrangement of glycans is critical for effective lectin recognition, the presentation of glycostructures on the microarray may differ from their *in vivo* density and accessibility on bacterial surfaces. [9] Moreover, the possibility that

structures identified in the microarray may not play an actual significant role in the interactions between lectins and bacterial cells exists. [9]

4. Conclusions

This study demonstrated that the interaction between lectins and different *K. pneumoniae* sublineages is highly heterogeneous and influenced by multiple factors, including the specific lectin tested, the composition of capsular polysaccharide (CPS) and lipopolysaccharide (LPS), and the capsule expression.

The research highlights the need for broader analyses to better understand these interactions and their implications for the immune response. This approach could unveil further strain-specific binding patterns, identify lectins with diagnostic or therapeutic potential, and clarify how CPS variations influence immune evasion. Such insights are critical for developing targeted antimicrobial strategies, including glycan-based vaccines and carbohydrate-binding molecules to disrupt infection processes.

Acknowledgements

We are thankful to Olaya Rendueles-Garcia for sharing optimized protocols for capsule quantification and hypermucoviscosity assay, and Sylvain Brisse for providing some of the hypervirulent strains used in this study.

Suppplementary material

Tables and graphs showing detailed fluorescence values obtained during the binding assay for each *Kp*-lectin interaction are available in the supplementary material section of this thesis.

Bibliography

1. Rocha J, Henriques I, Gomila M, Manaia CM. Common and distinctive genomic features of *Klebsiella pneumoniae* thriving in the natural environment or in clinical settings. *Sci Rep* 2022; **12**: 10441.

2. Russo TA, Marr CM. Hypervirulent *Klebsiella pneumoniae*. *Clin Microbiol Rev* 2019; **32**: e00001-19.

3. Lam MMC, Wick RR, Judd LM, Holt KE, Wyres KL. Kaptive 2.0: updated capsule and lipopolysaccharide locus typing for the *Klebsiella pneumoniae* species complex. *Microbial Genomics* 2022; **8**. Available at:

https://www.microbiologyresearch.org/content/journal/mgen/10.1099/mgen.0.000800. Accessed February 19, 2025.

4. Hsu C-R, Lin T-L, Chen Y-C, Chou H-C, Wang J-T. The role of *Klebsiella pneumoniae* rmpA in capsular polysaccharide synthesis and virulence revisited. *Microbiology* 2011; **157**: 3446–57.

5. Wang W, Tian D, Hu D, Chen W, Zhou Y, Jiang X. Different regulatory mechanisms of the capsule in hypervirulent *Klebsiella* pneumonia: “direct” wcaJ variation vs. “indirect” rmpA regulation. *Front Cell Infect Microbiol* 2023; **13**: 1108818.

6. Chen J, Zhang H, Liao X. Hypervirulent *Klebsiella pneumoniae*. *IDR* 2023; **Volume 16**: 5243–9.

7. Ekins RP. Multi-analyte immunoassay. *Journal of Pharmaceutical and Biomedical Analysis* 1989; **7**: 155–68.

8. Follador R, Heinz E, Wyres KL, *et al.* The diversity of *Klebsiella pneumoniae* surface polysaccharides. *Microbial Genomics* 2016; **2**. Available at: https://www.microbiologyresearch.org/content/journal/mgen/10.1099/mgen.0.000073. Accessed January 29, 2025.

9. Campanero-Rhodes MA, Palma AS, Menéndez M, Solís D. Microarray Strategies for Exploring Bacterial Surface Glycans and Their Interactions With Glycan-Binding Proteins. *Front Microbiol* 2020; **10**: 2909.

10. Bai R, Guo J. Interactions and Implications of *Klebsiella pneumoniae* with Human Immune Responses and Metabolic Pathways: A Comprehensive Review. *IDR* 2024; **Volume 17**: 449–62.

11. Rodrigues C, Sousa C, Lopes JA, Novais Â, Peixe L. A Front Line on *Klebsiella pneumoniae* Capsular Polysaccharide Knowledge: Fourier Transform Infrared Spectroscopy as an Accurate and Fast Typing Tool Dorrestein PC, ed. *mSystems* 2020; **5**: e00386-19.

12. McKitrick TR, Ackerman ME, Anthony RM, *et al.* The Crossroads of Glycoscience, Infection, and Immunology. *Front Microbiol* 2021; **12**: 731008.

13. Sahly H, Keisari Y, Crouch E, Sharon N, Ofek I. Recognition of Bacterial Surface Polysaccharides by Lectins of the Innate Immune System and Its Contribution to Defense against Infection: the Case of Pulmonary Pathogens. *Infect Immun* 2008; **76**: 1322–32.

14. Campanero-Rhodes MA, Martí S, Hernández-Ortiz N, *et al.* Insights into the recognition of hypermucoviscous *Klebsiella pneumoniae* clinical isolates by innate immune lectins of the Siglec and galectin families. *Front Immunol* 2024; **15**: 1436039.

15. Bengoechea JA, Sa Pessoa J. *Klebsiella pneumoniae* infection biology: living to counteract host defences. *FEMS Microbiology Reviews* 2019; **43**: 123–44.

16. Domenico P, Schwartz S, Cunha BA. Reduction of capsular polysaccharide production in *Klebsiella pneumoniae* by sodium salicylate. *Infect Immun* 1989; **57**: 3778–82.

17. Blumenkrantz N, Asboe-Hansen G. New method for quantitative determination of uronic acids. *Analytical Biochemistry* 1973; **54**: 484–9.

18. Palma AS, Liu Y, Childs RA, *et al.* The human epithelial carcinoma antigen recognized by monoclonal antibody AE3 is expressed on a sulfoglycolipid in addition to neoplastic mucins. *Biochemical and Biophysical Research Communications* 2011; **408**: 548–52.

19. Wang Y, Yu G, Han Z, *et al.* Specificities of *Ricinus communis* agglutinin 120 interaction with sulfated galactose. *FEBS Letters* 2011; **585**: 3927–34.

20. Bojar D, Meche L, Meng G, *et al.* A Useful Guide to Lectin Binding: Machine-Learning Directed Annotation of 57 Unique Lectin Specificities. *ACS Chem Biol* 2022; **17**: 2993–3012.

21. Hester G, Wright CS. The Mannose-specific Bulb Lectin fromGalanthus nivalis(Snowdrop) Binds Mono- and Dimannosides at Distinct Sites. Structure Analysis of Refined Complexes at 2.3 Å and 3.0 Å Resolution. *Journal of Molecular Biology* 1996; **262**: 516–31.

22. Romano PR, Mackay A, Vong M, *et al.* Development of recombinant Aleuria aurantia lectins with altered binding specificities to fucosylated glycans. *Biochemical and Biophysical Research Communications* 2011; **414**: 84–9.

23. Kochibe N, Furukawa K. Purification and properties of a novel fucose-specific hemagglutinin of Aleuria aurantia. *Biochemistry* 1980; **19**: 2841–6.

24. Sych T, Omidvar R, Ostmann R, *et al.* The bacterial lectin LecA from P. aeruginosa alters membrane organization by dispersing ordered domains. *Commun Phys* 2023; **6**: 153.

25. Blanchard B, Nurisso A, Hollville E, *et al.* Structural Basis of the Preferential Binding for Globo-Series Glycosphingolipids Displayed by Pseudomonas aeruginosa Lectin I. *Journal of Molecular Biology* 2008; **383**: 837–53.

26. Thuenauer R, Landi A, Trefzer A, *et al.* The Pseudomonas aeruginosa Lectin LecB Causes Integrin Internalization and Inhibits Epithelial Wound Healing Fleiszig SMJ, Salama NR, eds. *mBio* 2020; **11**: e03260-19.

27. Loris R, Tielker D, Jaeger K-E, Wyns L. Structural Basis of Carbohydrate Recognition by the Lectin LecB from Pseudomonas aeruginosa. *Journal of Molecular Biology* 2003; **331**: 861–70.

28. Palma AS, Feizi T, Zhang Y, *et al.* Ligands for the β-glucan receptor, Dectin-1, assigned using "designer" microarrays of oligosaccharide probes (neoglycolipids) generated from glucan polysaccharides. VOLUME 281 (2006) PAGES 5771-5779. *Journal of Biological Chemistry* 2006; **281**: 24999.

29. Palma AS, Liu Y, Zhang H, *et al.* Unravelling Glucan Recognition Systems by Glycome Microarrays Using the Designer Approach and Mass Spectrometry. *Molecular & Cellular Proteomics* 2015; **14**: 974–88.

30. Vendele I, Willment JA, Silva LM, *et al.* Mannan detecting C-type lectin receptor probes recognise immune epitopes with diverse chemical, spatial and phylogenetic heterogeneity in fungal cell walls Hohl TM, ed. *PLoS Pathog* 2020; **16**: e1007927.

31. Silva LM, Correia VG, Moreira ASP, *et al.* Helicobacter pylori lipopolysaccharide structural domains and their recognition by immune proteins revealed with carbohydrate microarrays. *Carbohydrate Polymers* 2021; **253**: 117350.

32. Gao C, Stavenhagen K, Eckmair B, *et al.* Differential recognition of oligomannose isomers by glycan-binding proteins involved in innate and adaptive immunity. *Sci Adv* 2021; **7**: eabf6834.

33. Geissner A, Reinhardt A, Rademacher C, *et al.* Microbe-focused glycan array screening platform. *Proc Natl Acad Sci USA* 2019; **116**: 1958–67.

34. Allen MJ, Laederach A, Reilly PJ, Mason RJ. Polysaccharide Recognition by Surfactant Protein D: Novel Interactions of a C-Type Lectin with Nonterminal Glucosyl Residues. *Biochemistry* 2001; **40**: 7789–98.

35. Sahly H, Ofek I, Podschun R, *et al.* Surfactant Protein D Binds Selectively to *Klebsiella pneumoniae* Lipopolysaccharides Containing Mannose-Rich O-Antigens. *The Journal of Immunology* 2002; **169**: 3267–74.

36. Choby JE, Howard-Anderson J, Weiss DS. Hypervirulent *Klebsiella pneumoniae* – clinical and molecular perspectives. *J Intern Med* 2020; **287**: 283–300.

37. Wantuch PL, Knoot CJ, Robinson LS, *et al.* Capsular polysaccharide inhibits vaccine-induced O-antigen antibody binding and function across both classical and hypervirulent K2:O1 strains of *Klebsiella pneumoniae* Hakansson AP, ed. *PLoS Pathog* 2023; **19**: e1011367.

38. Pekdemir B, Karav S. Exploring the diverse biological significance and roles of fucosylated oligosaccharides. *Front Mol Biosci* 2024; **11**: 1403727.

39. Huang X, Li X, An H, *et al.* Capsule type defines the capability of *Klebsiella pneumoniae* in evading Kupffer cell capture in the liver Mecsas J, ed. *PLoS Pathog* 2022; **18**: e1010693.

40. Guachalla LM, Stojkovic K, Hartl K, *et al.* Discovery of monoclonal antibodies cross-reactive to novel subserotypes of K. pneumoniae O3. *Sci Rep* 2017; **7**: 6635.

41. Merino S, Altarriba M, Izquierdo L, Nogueras MM, Regué M, Tomás JM. Cloning and Sequencing of the *Klebsiella pneumoniae* O5 *wb* Gene Cluster and Its Role in Pathogenesis O'Brien AD, ed. *Infect Immun* 2000; **68**: 2435–40.

42. Varki A, Cummings RD, Esko JD, *et al.* eds. *Essentials of glycobiology*. Fourth edition. Cold Spring Harbor, New York: Cold Spring Harbor Laboratory Press; 2022.

Table 1. *K. pneumoniae* isolates, set of analysis.

ISOLATE	TYPE	Phenotype	Mucoidity	ST	K-type	O-type
A12	MDR-*Kp*	HMV	HM	ST147	KL64	O2a
A26	hv*Kp*	HMV	HM	ST23	K1	O1
H2351	hv*Kp*	HMV	HM	ST268	KL20	O2a
H2379	hv*Kp*	HMV	HM	ST380	K2	O1
A5	MDR-*Kp*	-	RM	ST45	KL24	O2a
A6	MDR-*Kp*	-	RM	ST147	KL64	O2a
A12M	MDR-*Kp*	C_{sp}- **(M)**	NM	ST147	KL64	O2a
A6M	MDR-*Kp*	C_{sp}- **(M)**	NM	ST147	KL64	O2a
A5M (A4*)	MDR-*Kp*	-	NM	ST45	KL24	O2a
H2351M	hv*Kp*	C_{sp}- **(M)**	NM	ST268	KL20	O2a
H2379M	hv*Kp*	C_{sp}- **(M)**	NM	ST380	K2	O1
A26M	hv*Kp*	C_{sp}- **(M)**	NM	ST23	K1	O1

Legend: C_{sp}- (M) = Non-capsulated mutants. ST = Sequence Type, obtained by MLST; K-Type = Capsular type (CPS); O-Type = O-antigen type (LPS)

Table 2. Lectins used for the binding experiment.

Lectin	Exp. code	Source[a]	Reported carbohydrate-binding specificity / Recognition[b]	Binding conc.	Detection reagents & concentrations[c]	Blocking solution[d]
***Ricinus communis* agglutinin 120**	**RCA120**	Vector B-1085-1 (Biotinylated)	Terminal polylactosamine structures [18] and terminal β-D-galactose (Galβ) [18,19]	5 µg/mL	NA	Blocker X
***Galanthus nivalis* lectin**	**GNL/GNA**	Vector B-1245-2 (Biotinylated)	Terminal α-1,3-linked mannose [20,21]	5 µg/mL	NA	Blocker X
***Aleuria aurantia* lectin**	**AAL**	Vector B-1395-1 (Biotinylated)	Terminal α-1,6/α-1,3-linked fucose [22,23]	5 µg/mL	NA	Blocker X
***Pseudomonas aeruginosa* lectin A (PA-IL)**	**LecA**	Elicityl LEC102-Bt (Biotinylated)	Terminal α-galactosylated glycans [24,25]	10µg/mL	NA	Blocker X
***Pseudomonas aeruginosa* lectin B (PA-IIL)**	**LecB**	Elicityl LEC101-Bt (Biotinylated)	Fucose and mannose [26,27]	10 µg/mL	NA	Blocker X
Mouse Dectin-1-His	**Dectin-1**	Sino Biological (hexa-histidine-tagged) 50233-M07H	β-1,3-glucooligomers with a minimum chain length of DP-10 or DP-11 [28,29]	10 µg/ml	Ab1: mouse monoclonal anti-poly-Histidine (Sigma SAB4200620); 30 µg/mL; Ab2: BI anti-mouse IgG (whole molecule) (Sigma B7264); 30 µg/mL	Blocker Z
Human His-Dectin-2	**Dectin-2**	R&D Systems (hexa-histidine-tagged) 1525-DC-050	α-mannose residues, such as high mannose-type *N*-glycans ($Man_8GlcNAc_2$) [30]	20 µg/mL	Ab1: mouse monoclonal anti-poly-Histidine (Sigma SAB4200620); 30 µg/mL; Ab2: BI anti-mouse IgG (whole molecule) (Sigma B7264); 30 µg/mL	Blocker Z
Human DC-SIGN (Dendritic cell-specific ICAM-3-grabbing non-integrin)	**DC-SIGN**	Sino Biological (human Fc tagged) 10200-H01H	Recognition of fuco-, [31] manno- [30,32,33] and gluco-oligosaccharides [29]	10 µg/ml	BI anti-human IgG (Vector BA-3000); 10 µg/mL	Blocker X
C-type lectin surfactant protein D	**SP-D**	Sino Biological (hexa-histidine-tagged) 11041-H08H	Recognition of gluco-oligosaccharides [34] and Mannose-rich glycans (O-antigen) [35]	10 µg/ml	Ab1: mouse monoclonal anti-poly-Histidine (Sigma SAB4200620); 20 µg/mL; Ab2: BI anti-mouse IgG (whole molecule) (Sigma B7264); 20 µg/mL	Blocker Z

Sources, conditions of analysis and reported carbohydrate-binding specificity.
Legend: [a]Commercial source is indicated. [b]The main carbohydrate-binding specificity assigned is indicated with a reference. [c]Ab1, primary antibody; Ab2, secondary antibody; BI, biotinylated. [d]Blocker X: 1% BSA A7030 + Tween20 0.05% in TBS with 2mM $CaCl_2$, 2mM $MgCl_2$. Blocker Z: 1% BSA A7030 in 2 mM $CaCl_2$, 2mM $MgCl_2$. BSA, bovine serum albumin (Sigma A7030).

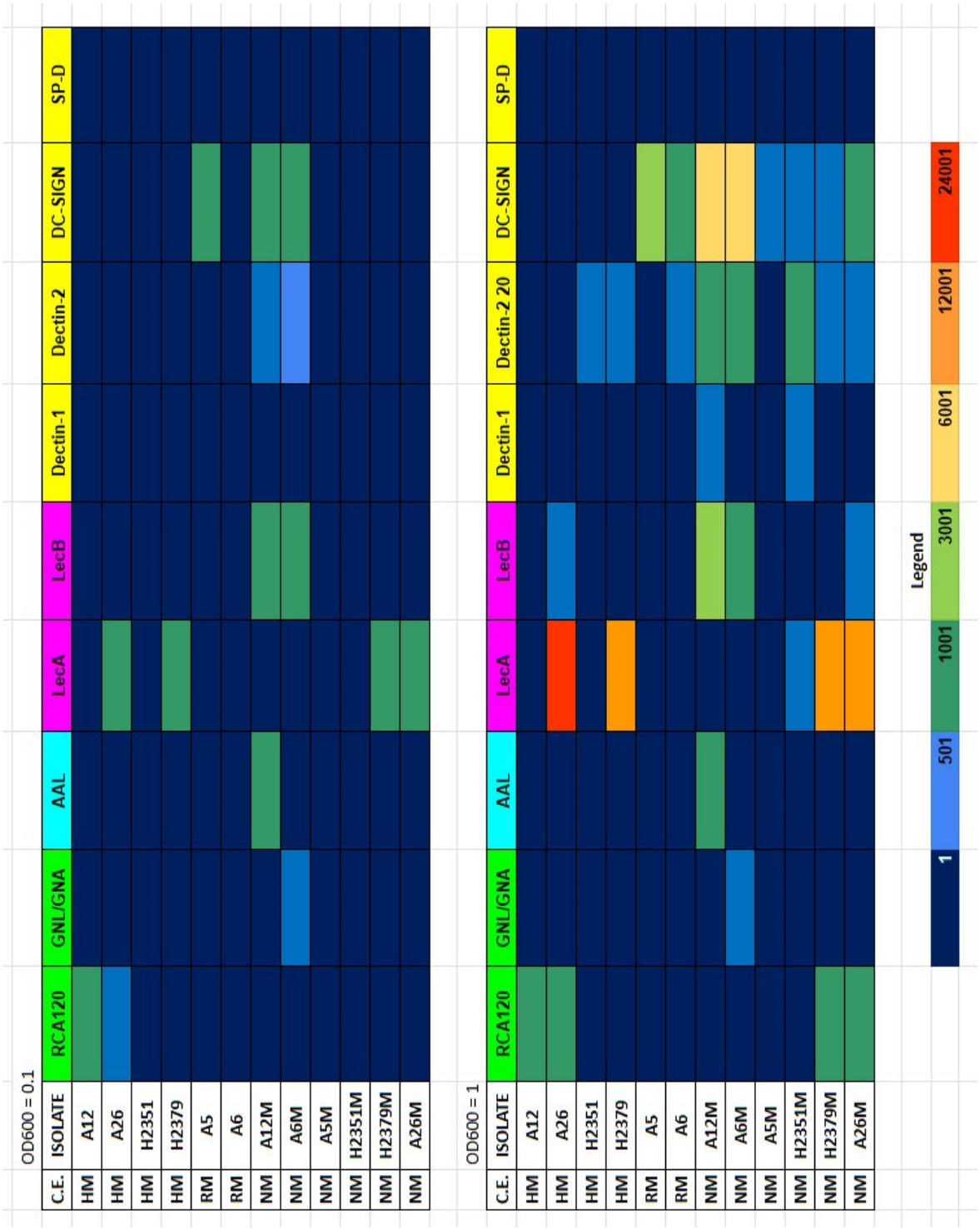


Figure 1: Matrix showing lectins binding activity (fluorescence) to a heterogeneous set of *K. pneumoniae* isolates.

Bacterial cells printed using suspensions with OD_{600} = 0.1 (up) and OD_{600} = 1 (down). Legend: C.E. = capsule expression: HM = hypermucoid; RM = regular-mucoid; NM = non-mucoid. Fluorescence expressed in relative fluorescence units (rfu). Lectins colour code: lime green = plant lectins; cyan = fungal lectin; purple = bacterial lectins: bright yellow = animal and human lectins. Fluorescence colour code: dark blue <500; light blue 500 - 1,000; dark green 1,000–3,000; light green 3,000–6,000; yellow 6,000–12,000; orange 12,000–24,000; red >24,000.

Conclusions

This thesis advances fundamental knowledge on **phenotypic and structural** *Klebsiella pneumoniae* features shaping **adaption and virulence**. By characterizing rheological properties and patterns of glycan-lectin recognition, this study shed light on strain-specific glycan-mediated mechanisms putatively associated with pathogen recognition and disease progression. More specifically, this thesis shows that the **diversity** and **abundance** of **capsule** directly modulates bacterial behavior by impacting host interaction and adaptation of clinically relevant multidrug-resistant (MDR-*Kp*) and hypervirulent (hv*Kp*) strains. This thesis contributed also to validate experimental protocols (CPS characterization and high-throughput microarrays) and assess diversity estimates that will support the rationale for future research combining these data with detailed glycan structural analysis (e.g. GC-MS, NMR), *in vivo* functional assays and evaluation of clinical and host parameters.

The identification of **rheological** and **textural properties,** and **differential glycan recognition patterns** integrated with information on **pathogen genetic background**, **epidemiological** and **phenotypic data,** is a new approach in the field to understand molecular features responsible for environment-pathogen-host interactions**.**

This **innovative approach** demonstrated potential to bring new light on fundamental aspects of pathogenic *K. pneumoniae* strains, as well as to guide future structural and functional *in vivo* studies that will allow clarifying the involvement of surface antigens variation in pathogenicity and disease establishment. Furthermore, it can be extended to other clinically relevant ESKAPE pathogens and improve global research strategies in the field.

I. Diversity and prevalence of MDR-*Kp* and hv*Kp* in a northern Portuguese hospital

The characterization of a collection of *K. pneumoniae* isolates responsible for invasive infections in a hospital from northern Portugal highlighted a proportion of MDR-*Kp* much higher than that reported at national level (49% vs 28%), alerting for a worrying scenario. We detected the expansion of global high-risk sublineages carrying specific ESBL (CTX-M-15) or carbapenemases (KPC-3 or OXA-48 in a lesser extent) and capsular types (KL19, KL64, KL102), whose expansion occurs most likely due to host factors and/or pathogen opportunities. While hv*Kp* strains were rare (1.1%), their presence underscored the urgent need for improved surveillance and enhanced detection methods. These strains exhibited enhanced

capsule production (KL2, KL20) and hypermucoviscosity phenotypes that were subsequently explored.

II. Integrating molecular and rheological features

Rheological and textural profiling of representative MDR-*Kp* and hv*Kp* demonstrated that CPS abundance and composition dictate *K. pneumoniae* physical behavior, with distinct implications for virulence. While hypermucoid (HM) strains exhibited low shear viscosity, facilitating rapid dissemination in flow conditions like the bloodstream, non-mucoid strains showed heightened adhesiveness, enhancing tissue colonization. Hypermucoviscosity phenotype (HMV) correlated non-linearly with CPS levels, driven by genomic variability (e.g. *wcaJ*/*wzc* mutations) proving that HM (copious CPS) and HMV (CPS elasticity) are dissociable traits. This biophysical distinction refines hv*Kp* characterization and suggests therapies targeting flow dynamics (e.g., viscosity-enhancing agents) or adhesion (e.g., biofilm disruptors).

III. *K. pneumoniae* glycan-lectin binding signatures

Patterns of glycan-lectin recognition were dose-dependent and varied significantly with strain background and the diversity of surface glycan structures (CPS/K-types, LPS/O-types, and other unrecognized sugars). Lectin binding patters were linked to specific glycan structures (e.g. K1/K2; O1-type) or attributed to unidentified glycans, revealing the contribution of glycans other than surface antigens for pathogen recognition. We also show that hypercapsule production masks the accessibility of certain surface glycans, which prevents recognition by certain human lectins such as DC-SIGN. These data suggest that capsule production, rather than capsule composition, is a key factor in pathogen recognition. Using a representative set of MDR-*Kp* and hv*Kp* strains validated this proof-of-concept study, which should be expanded with a larger and more diverse sample and a broader range of lectins.

IV. CPS-driven diagnostic and therapeutic opportunities

CPS abundance and composition modulates strain behaviour and immune evasion strategies of MDR-*Kp* and hv*Kp* strains, offering a framework for strain-specific risk prediction. Potential diagnostic markers would include CPS profiling for risk stratification, while therapeutic strategies could target CPS biosynthesis (e.g., capsule export inhibitors) or rheological properties (e.g., biofilm viscosity modulation). Validation using *in vivo* and *in vitro* models is essential.

The work integrated knowledge on molecular epidemiology, biophysical and molecular recognition properties of capsular polysaccharides and other surface glycans. It established the foundation for glycan-centric strategies to mitigate the burden of *K. pneumoniae* infections, and proposes a paradigm shift in understanding bacterial adaptation. It focused on surface glycans, not merely as static virulence factors, but as dynamic mediators of ecological fitness and evolutionary success in *K. pneumoniae*.

Further insights into glycan-mediated host-pathogen interactions could guide vaccine development and precision medicine approaches for infection control. Future research should incorporate genomic and glycan-based surveillance for high-risk clones, investigating genetic factors linking CPS production to biomechanical traits. Further studies should explore how host characteristics (e.g., pH, fluid shear) modulate CPS expression and virulence, as well as their impact within *in vivo* models.

References

1. Friedlaender, C. Ueber die Schizomyceten bei der acuten fibrösen Pneumonie. *Archiv f. pathol. Anat.* **87**, 319–324 (1882).
2. Ding, L. *et al. Klebsiella pneumoniae* carbapenemase variants: the new threat to global public health. *Clin Microbiol Rev* **36**, e00008-23 (2023).
3. Wyres, K. L., Lam, M. M. C. & Holt, K. E. Population genomics of *Klebsiella pneumoniae*. *Nat Rev Microbiol* **18**, 344–359 (2020).
4. Founou, R. C., Founou, L. L. & Essack, S. Y. Clinical and economic impact of antibiotic resistance in developing countries: A systematic review and meta-analysis. *PLoS ONE* **12**, e0189621 (2017).
5. Naghavi, M. *et al.* Global burden of bacterial antimicrobial resistance 1990–2021: a systematic analysis with forecasts to 2050. *The Lancet* **404**, 1199–1226 (2024).
6. Verani, J. R. *et al.* Child deaths caused by *Klebsiella pneumoniae* in sub-Saharan Africa and south Asia: a secondary analysis of Child Health and Mortality Prevention Surveillance (CHAMPS) data. *The Lancet Microbe* **5**, e131–e141 (2024).
7. Sands, K. *et al.* Characterization of antimicrobial-resistant Gram-negative bacteria that cause neonatal sepsis in seven low- and middle-income countries. *Nat Microbiol* **6**, 512–523 (2021).
8. European Centre for Disease Prevention and Control & WHO Regional Office for Europe. Surveillance of antimicrobial resistance in Europe, 2023 data: executive summary. Stockholm: European Centre for Disease Prevention and Control; 2024.
9. World Health Organization. *WHO Bacterial Priority Pathogens List 2024: Bacterial Pathogens of Public Health Importance, to Guide Research, Development, and Strategies to Prevent and Control Antimicrobial Resistance*. (World Health Organization, Geneva, 2024).
10. Podschun, R. & Ullmann, U. *Klebsiella* spp. as Nosocomial Pathogens: Epidemiology, Taxonomy, Typing Methods, and Pathogenicity Factors. *Clin Microbiol Rev* **11**, 589–603 (1998).
11. Bengoechea, J. A. & Sa Pessoa, J. *Klebsiella pneumoniae* infection biology: living to counteract host defences. *FEMS Microbiology Reviews* **43**, 123–144 (2019).
12. Zhou, C., Sun, L., Li, H., Huang, L. & Liu, X. Risk Factors and Mortality of Elderly Patients with Hospital-Acquired Pneumonia of Carbapenem-Resistant *Klebsiella pneumoniae* Infection. *IDR* **Volume 16**, 6767–6779 (2023).
13. Vock, I. & Tschudin-Sutter, S. Persisting intrahospital transmission of multidrug-resistant *Klebsiella pneumoniae* and challenges for infection control. *Infect. Control Hosp. Epidemiol.* **40**, 904–909 (2019).

14. Xu, L., Sun, X. & Ma, X. Systematic review and meta-analysis of mortality of patients infected with carbapenem-resistant *Klebsiella pneumoniae*. *Ann Clin Microbiol Antimicrob* **16**, 18 (2017).
15. Karampatakis, T., Tsergouli, K. & Roilides, E. Infection Control Measures Against Multidrug-Resistant Gram-Negative Bacteria in Children and Neonates. *Future Microbiol.* **18**, 751–765 (2023).
16. Paczosa, M. K. & Mecsas, J. *Klebsiella pneumoniae*: Going on the Offense with a Strong Defense. *Microbiol Mol Biol Rev* **80**, 629–661 (2016).
17. Martin, R. M. & Bachman, M. A. Colonization, Infection, and the Accessory Genome of *Klebsiella pneumoniae*. *Front. Cell. Infect. Microbiol.* **8**, 4 (2018).
18. Siu, L. K., Yeh, K.-M., Lin, J.-C., Fung, C.-P. & Chang, F.-Y. *Klebsiella pneumoniae* liver abscess: a new invasive syndrome. *The Lancet Infectious Diseases* **12**, 881–887 (2012).
19. Zhang, J.-Q. *et al.* Fatal systemic emphysematous infection caused by *Klebsiella pneumoniae* : A case report. *WJCC* **10**, 2610–2615 (2022).
20. Tsay, R.-W., Siu, L. K., Fung, C.-P. & Chang, F.-Y. Characteristics of Bacteremia Between Community-Acquired and Nosocomial *Klebsiella pneumoniae* Infection: Risk Factor for Mortality and the Impact of Capsular Serotypes as a Herald for Community-Acquired Infection. *Arch Intern Med* **162**, 1021 (2002).
21. Kocsis, B. Hypervirulent *Klebsiella pneumoniae*: An update on epidemiology, detection and antibiotic resistance. *AMicr* **70**, 278–287 (2023).
22. European Centre for Disease Prevention and Control. *Emergence of Hypervirulent Klebsiella pneumoniae ST23 Carrying Carbapenemase Genes in EU/EEA Countries, First Update*. (Publications Office, LU, 2024).
23. Centers for Disease Control and Prevention (U.S.). *Antibiotic Resistance Threats in the United States, 2019*. https://stacks.cdc.gov/view/cdc/82532 (2019) doi:10.15620/cdc:82532.
24. Boucher, H. W. *et al.* Bad Bugs, No Drugs: No ESKAPE! An Update from the Infectious Diseases Society of America. *CLIN INFECT DIS* **48**, 1–12 (2009).
25. Navon-Venezia, S., Kondratyeva, K. & Carattoli, A. *Klebsiella pneumoniae*: a major worldwide source and shuttle for antibiotic resistance. *FEMS Microbiology Reviews* **41**, 252–275 (2017).
26. Brisse, S. & Verhoef, J. Phylogenetic diversity of *Klebsiella pneumoniae* and *Klebsiella* oxytoca clinical isolates revealed by randomly amplified polymorphic DNA, gyrA and parC genes sequencing and automated ribotyping. *International Journal of Systematic and Evolutionary Microbiology* **51**, 915–924 (2001).

27. Holt, K. E. *et al.* Genomic analysis of diversity, population structure, virulence, and antimicrobial resistance in *Klebsiella pneumoniae*, an urgent threat to public health. *Proc. Natl. Acad. Sci. U.S.A.* **112**, (2015).
28. Bialek-Davenet, S. *et al.* Genomic Definition of Hypervirulent and Multidrug-Resistant *Klebsiella pneumoniae* Clonal Groups. *Emerg. Infect. Dis.* **20**, 1812–1820 (2014).
29. Rodrigues, C., Passet, V., Rakotondrasoa, A. & Brisse, S. Identification of *Klebsiella pneumoniae*, *Klebsiella* quasipneumoniae, *Klebsiella* variicola and Related Phylogroups by MALDI-TOF Mass Spectrometry. *Front. Microbiol.* **9**, 3000 (2018).
30. Brenner, D. J. Some Taxonomic Recommendations and a Proposal of Neotype Strains for Nineteen Species of Enterobacteriaceae ICSB Subcommittee on Taxonomy of Enterobacteriaceae. *International Journal of Systematic Bacteriology* **29**, 38–41 (1979).
31. Brisse, S., Passet, V. & Grimont, P. A. D. Description of *Klebsiella* quasipneumoniae sp. nov., isolated from human infections, with two subspecies, *Klebsiella* quasipneumoniae subsp. quasipneumoniae subsp. nov. and *Klebsiella* quasipneumoniae subsp. similipneumoniae subsp. nov., and demonstration that *Klebsiella* singaporensis is a junior heterotypic synonym of *Klebsiella* variicola. *International Journal of Systematic and Evolutionary Microbiology* **64**, 3146–3152 (2014).
32. Rosenblueth, M., Martínez, L., Silva, J. & Martínez-Romero, E. *Klebsiella* variicola, A Novel Species with Clinical and Plant-Associated Isolates. *Systematic and Applied Microbiology* **27**, 27–35 (2004).
33. Rodrigues, C. *et al.* Description of *Klebsiella* africanensis sp. nov., *Klebsiella* variicola subsp. tropicalensis subsp. nov. and *Klebsiella* variicola subsp. variicola subsp. nov. *Research in Microbiology* **170**, 165–170 (2019).
34. Long, S. W. *et al.* Whole-Genome Sequencing of a Human Clinical Isolate of the Novel Species *Klebsiella quasivariicola* sp. nov. *Genome Announc* **5**, e01057-17 (2017).
35. Fevre, C., Passet, V., Weill, F.-X., Grimont, P. A. D. & Brisse, S. Variants of the *Klebsiella pneumoniae* OKP Chromosomal Beta-Lactamase Are Divided into Two Main Groups, OKP-A and OKP-B. *Antimicrob Agents Chemother* **49**, 5149–5152 (2005).
36. Wesevich, A. *et al.* Newly Named *Klebsiella* aerogenes (formerly Enterobacter aerogenes) Is Associated with Poor Clinical Outcomes Relative to Other *Enterobacter* Species in Patients with Bloodstream Infection. *J Clin Microbiol* **58**, e00582-20 (2020).
37. Ma, Y. *et al.* Proposal for reunification of the genus Raoultella with the genus *Klebsiella* and reclassification of Raoultella electrica as *Klebsiella* electrica comb. nov. *Research in Microbiology* **172**, 103851 (2021).

38. Mettler, S. K., Charoenngam, N. & Colgrove, R. C. Clinical differences between Raoultella spp. and *Klebsiella* oxytoca. *Front. Cell. Infect. Microbiol.* **14**, 1260212 (2024).
39. Long, S. W. *et al.* Whole-Genome Sequencing of Human Clinical *Klebsiella pneumoniae* Isolates Reveals Misidentification and Misunderstandings of *Klebsiella pneumoniae*, *Klebsiella* variicola, and *Klebsiella* quasipneumoniae. *mSphere* **2**, e00290-17 (2017).
40. Wyres, K. L. & Holt, K. E. *Klebsiella pneumoniae* as a key trafficker of drug resistance genes from environmental to clinically important bacteria. *Current Opinion in Microbiology* **45**, 131–139 (2018).
41. Vezina, B. *et al.* A metabolic atlas of the *Klebsiella pneumoniae* species complex reveals lineage-specific metabolism that supports persistent co-existence of diverse lineages. Preprint at https://doi.org/10.1101/2024.07.24.605038 (2024).
42. Blin, C., Passet, V., Touchon, M., Rocha, E. P. C. & Brisse, S. Metabolic diversity of the emerging pathogenic lineages of *Klebsiella pneumoniae*. *Environmental Microbiology* **19**, 1881–1898 (2017).
43. Bagley, S. T. Habitat Association of *Klebsiella* Species. *Infect. Control* **6**, 52–58 (1985).
44. Gorrie, C. L. *et al.* Gastrointestinal Carriage Is a Major Reservoir of *Klebsiella pneumoniae* Infection in Intensive Care Patients. *Clinical Infectious Diseases* **65**, 208–215 (2017).
45. Constantinides, B. *et al.* Genomic surveillance of Escherichia coli and *Klebsiella* spp. in hospital sink drains and patients. *Microbial Genomics* **6**, (2020).
46. Cano, Á. *et al.* Association between Timing of Colonization and Risk of Developing *Klebsiella pneumoniae* Carbapenemase-Producing *K. pneumoniae* Infection in Hospitalized Patients. *Microbiol Spectr* **10**, e01970-21 (2022).
47. Gorrie, C. L. *et al.* Genomic dissection of *Klebsiella pneumoniae* infections in hospital patients reveals insights into an opportunistic pathogen. *Nat Commun* **13**, 3017 (2022).
48. Sun, Y. *et al.* Pathogen Profile of *Klebsiella variicola*, the Causative Agent of Banana Sheath Rot. *Plant Disease* **107**, 2325–2334 (2023).
49. Duran-Bedolla, J., Garza-Ramos, U., Rodríguez-Medina, N., Aguilar Vera, A. & Barrios-Camacho, H. Exploring the environmental traits and applications of *Klebsiella* variicola. *Braz J Microbiol* **52**, 2233–2245 (2021).
50. Giannattasio-Ferraz, S. *et al.* Multidrug-Resistant *Klebsiella* variicola Isolated in the Urine of Healthy Bovine Heifers, a Potential Risk as an Emerging Human Pathogen. *Appl Environ Microbiol* **88**, e00044-22 (2022).
51. Altayb, H. N. *et al.* Molecular insights into novel environmental strains of *Klebsiella* quasipneumoniae harboring different antimicrobial-resistance genes. *Front. Public Health* **10**, 1068888 (2023).

52. Henson, S. P. *et al.* Molecular epidemiology of *Klebsiella pneumoniae* invasive infections over a decade at Kilifi County Hospital in Kenya. *International Journal of Medical Microbiology* **307**, 422–429 (2017).
53. Loiodice, M., Ribeiro, M., Peixe, L. & Novais, Â. Emergence of NDM-1 and KPC-3 carbapenemases in *Kluyvera cryocrescens*: Investigating genetic heterogeneity and acquisition routes of blaNDM-1 in Enterobacterales species in Portugal. *Journal of Global Antimicrobial Resistance* **34**, 195–198 (2023).
54. Woodford, N., Turton, J. F. & Livermore, D. M. Multiresistant Gram-negative bacteria: the role of high-risk clones in the dissemination of antibiotic resistance. *FEMS Microbiol Rev* **35**, 736–755 (2011).
55. Baquero, F. & Coque, T. M. Multilevel population genetics in antibiotic resistance. *FEMS Microbiol Rev* **35**, 705–706 (2011).
56. Maiden, M. C. J. *et al.* MLST revisited: the gene-by-gene approach to bacterial genomics. *Nat Rev Microbiol* **11**, 728–736 (2013).
57. Diancourt, L., Passet, V., Verhoef, J., Grimont, P. A. D. & Brisse, S. Multilocus Sequence Typing of *Klebsiella pneumoniae* Nosocomial Isolates. *J Clin Microbiol* **43**, 4178–4182 (2005).
58. Magiorakos, A.-P. *et al.* Multidrug-resistant, extensively drug-resistant and pandrug-resistant bacteria: an international expert proposal for interim standard definitions for acquired resistance. *Clinical Microbiology and Infection* **18**, 268–281 (2012).
59. EUCAST, E. C. on A. S. T. Expected Resistant Phenotypes, Version 1.2 January 2023.
60. Chen, F.-J., Lauderdale, T.-L., Ho, M. & Lo, H.-J. The Roles of Mutations in *gyrA, parC*, and *ompK35* in Fluoroquinolone Resistance in *Klebsiella pneumoniae*. *Microbial Drug Resistance* **9**, 265–271 (2003).
61. Ejaz, H. Analysis of diverse β-lactamases presenting high-level resistance in association with OmpK35 and OmpK36 porins in ESBL-producing *Klebsiella pneumoniae*. *Saudi Journal of Biological Sciences* **29**, 3440–3447 (2022).
62. Ozma. Antibiotic therapy for pan-drug-resistant infections. *infez med* **30**, (2022).
63. Karampatakis, T., Tsergouli, K. & Behzadi, P. Carbapenem-Resistant *Klebsiella pneumoniae*: Virulence Factors, Molecular Epidemiology and Latest Updates in Treatment Options. *Antibiotics* **12**, 234 (2023).
64. Gomes, M. Z. R. *et al.* Outbreak report of polymyxin-carbapenem-resistant *Klebsiella pneumoniae* causing untreatable infections evidenced by synergy tests and bacterial genomes. *Sci Rep* **13**, 6238 (2023).
65. Ljungquist, O. *et al.* Pandrug-resistant *Klebsiella pneumoniae* isolated from Ukrainian war victims are hypervirulent. *Journal of Infection* **89**, 106312 (2024).

66. Guducuoglu, H. *et al.* Hospital Outbreak of a Colistin-Resistant, NDM-1- and OXA-48-Producing *Klebsiella pneumoniae* : High Mortality from Pandrug Resistance. *Microbial Drug Resistance* **24**, 966–972 (2018).
67. Petrosillo, N., Taglietti, F. & Granata, G. Treatment Options for Colistin Resistant *Klebsiella pneumoniae*: Present and Future. *JCM* **8**, 934 (2019).
68. European Centre for Disease Prevention and Control., E. Antimicrobial resistance in the EU/EEA (EARS-Net) - Annual Epidemiological Report 2023. Stockholm: ECDC; 2024.
69. Munoz-Price, L. S. *et al.* Clinical epidemiology of the global expansion of *Klebsiella pneumoniae* carbapenemases. *The Lancet Infectious Diseases* **13**, 785–796 (2013).
70. David, S. *et al.* Epidemic of carbapenem-resistant *Klebsiella pneumoniae* in Europe is driven by nosocomial spread. *Nat Microbiol* **4**, 1919–1929 (2019).
71. Faria, N. A. *et al.* Genomic insights into the expansion of carbapenem-resistant *Klebsiella pneumoniae* within Portuguese hospitals. *Journal of Hospital Infection* **148**, 62–76 (2024).
72. Elias, R. *et al.* Emergence of KPC-3- and OXA-181-producing ST13 and ST17 *Klebsiella pneumoniae* in Portugal: genomic insights on national and international dissemination. *Journal of Antimicrobial Chemotherapy* **78**, 1300–1308 (2023).
73. European Centre for Disease Prevention and Control. *Carbapenem-Resistant Enterobacterales: Third Update*. (Publications Office, LU, 2025).
74. Yigit, H. *et al.* Novel Carbapenem-Hydrolyzing β-Lactamase, KPC-1, from a Carbapenem-Resistant Strain of *Klebsiella pneumoniae*. *Antimicrob Agents Chemother* **45**, 1151–1161 (2001).
75. Bush, K. & Bradford, P. A. Epidemiology of β-Lactamase-Producing Pathogens. *Clin Microbiol Rev* **33**, e00047-19 (2020).
76. Peirano, G. & Pitout, J. D. D. Rapidly spreading *Enterobacterales* with OXA-48-like carbapenemases. *J Clin Microbiol* **63**, e01515-24 (2025).
77. Papagiannitsis, C. C. *et al.* Emergence of sequence type 11 *Klebsiella pneumoniae* coproducing NDM-1 and VIM-1 metallo-β-lactamases in a Greek hospital. *Diagnostic Microbiology and Infectious Disease* **87**, 295–297 (2017).
78. Han, R. *et al.* Dissemination of Carbapenemases (KPC, NDM, OXA-48, IMP, and VIM) Among Carbapenem-Resistant Enterobacteriaceae Isolated From Adult and Children Patients in China. *Front. Cell. Infect. Microbiol.* **10**, 314 (2020).
79. Wu, W. *et al.* NDM Metallo-β-Lactamases and Their Bacterial Producers in Health Care Settings. *Clin Microbiol Rev* **32**, e00115-18 (2019).
80. Pitout, J. D. D., Nordmann, P. & Poirel, L. Carbapenemase-Producing *Klebsiella pneumoniae*, a Key Pathogen Set for Global Nosocomial Dominance. *Antimicrob Agents Chemother* **59**, 5873–5884 (2015).

81. Jana, B. *et al.* The secondary resistome of multidrug-resistant *Klebsiella pneumoniae*. *Sci Rep* **7**, 42483 (2017).
82. Nang, S. C., Li, J. & Velkov, T. The rise and spread of *mcr* plasmid-mediated polymyxin resistance. *Critical Reviews in Microbiology* **45**, 131–161 (2019).
83. Liu, M. *et al.* Global epidemiology and genetic diversity of mcr-positive *Klebsiella pneumoniae*: A systematic review and genomic analysis. *Environmental Research* **259**, 119516 (2024).
84. Liu, Y.-Y. *et al.* Emergence of plasmid-mediated colistin resistance mechanism MCR-1 in animals and human beings in China: a microbiological and molecular biological study. *The Lancet Infectious Diseases* **16**, 161–168 (2016).
85. Tansarli, G. S. *et al.* Colistin resistance in carbapenemase-producing *Klebsiella pneumoniae* bloodstream isolates: Evolution over 15 years and temporal association with colistin use by time series analysis. *International Journal of Antimicrobial Agents* **52**, 397–403 (2018).
86. Gandra, S. *et al.* Trends in antibiotic resistance among major bacterial pathogens isolated from blood cultures tested at a large private laboratory network in India, 2008–2014. *International Journal of Infectious Diseases* **50**, 75–82 (2016).
87. Dixit, A., Kumar, N., Kumar, S. & Trigun, V. Antimicrobial resistance: Progress in the decade since emergence of New Delhi metallo-β-lactamase in India. *Indian J Community Med* **44**, 4 (2019).
88. Khoshbayan, A. *et al.* Global prevalence of mutation in the mgrB gene among clinical isolates of colistin-resistant *Klebsiella pneumoniae*: a systematic review and meta-analysis. *Front. Microbiol.* **15**, 1386478 (2024).
89. Bray, A. S. *et al.* MgrB-Dependent Colistin Resistance in *Klebsiella pneumoniae* Is Associated with an Increase in Host-to-Host Transmission. *mBio* **13**, e03595-21 (2022).
90. Liu, X. *et al.* Emergence of colistin-resistant hypervirulent *Klebsiella pneumoniae* (CoR-Hv*Kp*) in China. *Emerging Microbes & Infections* **11**, 648–661 (2022).
91. European Centre for Disease Prevention and Control. *ECDC Strategic Framework for the Integration of Molecular and Genomic Typing into European Surveillance and Multi-Country Outbreak Investigations: 2019–2021*. (Publications Office, LU, 2019).
92. Tryfinopoulou, K. *et al.* Emergence and persistent spread of carbapenemase-producing *Klebsiella pneumoniae* high-risk clones in Greek hospitals, 2013 to 2022. *Eurosurveillance* **28**, (2023).
93. Turton, J. F., Perry, C., McGowan, K., Turton, J. A. & Hope, R. *Klebsiella pneumoniae* sequence type 147: a high-risk clone increasingly associated with plasmids carrying both resistance and virulence elements. *Journal of Medical Microbiology* **73**, (2024).

94. Rodrigues, C., Desai, S., Passet, V., Gajjar, D. & Brisse, S. Genomic evolution of the globally disseminated multidrug-resistant *Klebsiella pneumoniae* clonal group 147. *Microbial Genomics* **8**, (2022).

95. Fostervold, A. *et al.* A nationwide genomic study of clinical *Klebsiella pneumoniae* in Norway 2001–15: introduction and spread of ESBLs facilitated by clonal groups CG15 and CG307. *Journal of Antimicrobial Chemotherapy* **77**, 665–674 (2022).

96. Vásquez-Ponce, F. *et al.* Global epidemiological trend of *Klebsiella pneumoniae* ST340: emergence of subclade KL15 co-producing K pneumoniae carbapenemase-2 and New Delhi metallo-β-lactamase-7 in the Americas. *The Lancet Microbe* **6**, 100990 (2025).

97. Furlan, J. P. R. *et al.* Genomic features of an extensively drug-resistant and NDM-1–positive *Klebsiella pneumoniae* ST340 isolated from river water. *Environ Sci Pollut Res* **30**, 114678–114684 (2023).

98. Ranieri, S. C. *et al.* First report of a blaNDM-producing extensively drug resistant *Klebsiella pneumoniae* ST437 in Italy. *Front. Cell. Infect. Microbiol.* **14**, 1426817 (2024).

99. Novais, Â., Freitas, A. R., Rodrigues, C. & Peixe, L. Fourier transform infrared spectroscopy: unlocking fundamentals and prospects for bacterial strain typing. *Eur J Clin Microbiol Infect Dis* **38**, 427–448 (2019).

100. Novais, Â. *et al.* Development and validation of a quick, automated, and reproducible ATR FT-IR spectroscopy machine-learning model for *Klebsiella pneumoniae* typing. *J Clin Microbiol* **62**, e01211-23 (2024).

101. Mathers, A. J., Peirano, G. & Pitout, J. D. D. The Role of Epidemic Resistance Plasmids and International High-Risk Clones in the Spread of Multidrug-Resistant Enterobacteriaceae. *Clin Microbiol Rev* **28**, 565–591 (2015).

102. Rodrigues, C., Lanza, V. F., Peixe, L., Coque, T. M. & Novais, Â. Phylogenomics of Globally Spread Clonal Groups 14 and 15 of *Klebsiella pneumoniae*. *Microbiol Spectr* **11**, e03395-22 (2023).

103. Villa, L. *et al.* Diversity, virulence, and antimicrobial resistance of the KPC-producing *Klebsiella pneumoniae* ST307 clone. *Microbial Genomics* **3**, (2017).

104. Russo, T. A. & Marr, C. M. Hypervirulent *Klebsiella pneumoniae*. *Clin Microbiol Rev* **32**, e00001-19 (2019).

105. Liu, Y.-C. *Klebsiella pneumoniae* Liver Abscess Associated With Septic Endophthalmitis. *Arch Intern Med* **146**, 1913 (1986).

106. Lam, M. M. C. *et al.* Population genomics of hypervirulent *Klebsiella pneumoniae* clonal-group 23 reveals early emergence and rapid global dissemination. *Nat Commun* **9**, 2703 (2018).

107. Choby, J. E., Howard-Anderson, J. & Weiss, D. S. Hypervirulent *Klebsiella pneumoniae* – clinical and molecular perspectives. *J Intern Med* **287**, 283–300 (2020).

108. Shon, A. S., Bajwa, R. P. S. & Russo, T. A. Hypervirulent (hypermucoviscous) *Klebsiella pneumoniae*: A new and dangerous breed. *Virulence* **4**, 107–118 (2013).

109. Chang, D., Sharma, L., Dela Cruz, C. S. & Zhang, D. Clinical Epidemiology, Risk Factors, and Control Strategies of *Klebsiella pneumoniae* Infection. *Front. Microbiol.* **12**, 750662 (2021).

110. Russo, T. A. *et al.* Identification of Biomarkers for Differentiation of Hypervirulent *Klebsiella pneumoniae* from Classical *K. pneumoniae*. *J Clin Microbiol* **56**, e00776-18 (2018).

111. Bachman, M. A. *et al. Klebsiella pneumoniae* Yersiniabactin Promotes Respiratory Tract Infection through Evasion of Lipocalin 2. *Infect Immun* **79**, 3309–3316 (2011).

112. Russo, T. A., Olson, R., MacDonald, U., Beanan, J. & Davidson, B. A. Aerobactin, but Not Yersiniabactin, Salmochelin, or Enterobactin, Enables the Growth/Survival of Hypervirulent (Hypermucoviscous) *Klebsiella pneumoniae Ex Vivo* and *In Vivo*. *Infect Immun* **83**, 3325–3333 (2015).

113. Russo, T. A. *et al.* Differentiation of hypervirulent and classical *Klebsiella pneumoniae* with acquired drug resistance. *mBio* **15**, e02867-23 (2024).

114. Lam, M. M. C. *et al.* A genomic surveillance framework and genotyping tool for *Klebsiella pneumoniae* and its related species complex. *Nat Commun* **12**, 4188 (2021).

115. Al Ismail, D., Campos-Madueno, E. I., Donà, V. & Endimiani, A. Hypervirulent *Klebsiella pneumoniae* (hvKp): Overview, Epidemiology, and Laboratory Detection. *PAI* **10**, 80–119 (2025).

116. Liang, Q. *et al.* Co-occurrence of ST412 *Klebsiella pneumoniae* isolates with hypermucoviscous and non-mucoviscous phenotypes in a short-term hospitalized patient. *mSystems* **9**, e00262-24 (2024).

117. Catalán-Nájera, J. C., Garza-Ramos, U. & Barrios-Camacho, H. Hypervirulence and hypermucoviscosity: Two different but complementary *Klebsiella* spp. phenotypes? *Virulence* **8**, 1111–1123 (2017).

118. Mike, L. A. *et al.* A systematic analysis of hypermucoviscosity and capsule reveals distinct and overlapping genes that impact *Klebsiella pneumoniae* fitness. *PLoS Pathog* **17**, e1009376 (2021).

119. Marr, C. M. & Russo, T. A. Hypervirulent *Klebsiella pneumoniae* : a new public health threat. *Expert Review of Anti-infective Therapy* **17**, 71–73 (2019).

120. Walker, K. A., Treat, L. P., Sepúlveda, V. E. & Miller, V. L. The Small Protein RmpD Drives Hypermucoviscosity in *Klebsiella pneumoniae*. *mBio* **11**, e01750-20 (2020).

121. Zhang, Y. *et al.* High Prevalence of Hypervirulent *Klebsiella pneumoniae* Infection in China: Geographic Distribution, Clinical Characteristics, and Antimicrobial Resistance. *Antimicrob Agents Chemother* **60**, 6115–6120 (2016).

122. Matsuda, N. *et al.* Prevalence, clonal diversity, and antimicrobial resistance of hypervirulent *Klebsiella pneumoniae* and *Klebsiella* variicola clinical isolates in northern Japan. *Journal of Global Antimicrobial Resistance* **35**, 11–18 (2023).

123. Tang, M., Kong, X., Hao, J. & Liu, J. Epidemiological Characteristics and Formation Mechanisms of Multidrug-Resistant Hypervirulent *Klebsiella pneumoniae*. *Front. Microbiol.* **11**, 581543 (2020).

124. Chen, Y. & Chen, Y. Clinical challenges with hypervirulent *Klebsiella pneumoniae* (hvKP) in China. *Journal of Translational Internal Medicine* **9**, 71–75 (2021).

125. Shankar, C. *et al.* Hybrid Plasmids Encoding Antimicrobial Resistance and Virulence Traits Among Hypervirulent *Klebsiella pneumoniae* ST2096 in India. *Front. Cell. Infect. Microbiol.* **12**, 875116 (2022).

126. Xie, M. *et al.* Clinical evolution of ST11 carbapenem resistant and hypervirulent *Klebsiella pneumoniae*. *Commun Biol* **4**, 650 (2021).

127. Dey, T. *et al.* Unusual Hypermucoviscous Clinical Isolate of *Klebsiella pneumoniae* with No Known Determinants of Hypermucoviscosity. *Microbiol Spectr* **10**, e00393-22 (2022).

128. Yang, P. *et al.* Clinical Outcomes and Microbiological Characteristics of Sequence Type 11 *Klebsiella pneumoniae* Infection. *Front. Med.* **9**, 889020 (2022).

129. Guembe, M. *et al.* Virulence profile of carbapenem-resistant *Klebsiella pneumoniae* strains by an *in vivo* model of *Galleria mellonella*. *Microbiol Spectr* **13**, e02215-24 (2025).

130. Holt, K. E., Lassalle, F., Wyres, K. L., Wick, R. & Mostowy, R. J. Diversity and evolution of surface polysaccharide synthesis loci in Enterobacteriales. *The ISME Journal* **14**, 1713–1730 (2020).

131. Xu, L., Li, J., Wu, W., Wu, X. & Ren, J. *Klebsiella pneumoniae* capsular polysaccharide: Mechanism in regulation of synthesis, virulence, and pathogenicity. *Virulence* **15**, 2439509 (2024).

132. Hsu, C.-R. *et al.* Identification of a capsular variant and characterization of capsular acetylation in *Klebsiella pneumoniae* PLA-associated type K57. *Sci Rep* **6**, 31946 (2016).

133. Lam, M. M. C., Wick, R. R., Judd, L. M., Holt, K. E. & Wyres, K. L. Kaptive 2.0: updated capsule and lipopolysaccharide locus typing for the *Klebsiella pneumoniae* species complex. *Microbial Genomics* **8**, (2022).

134. Orskov, I. & Fife-Asbury, M. A. New *Klebsiella* Capsular Antigen, K82, and the Deletion of Five of Those Previously Assigned. *International Journal of Systematic Bacteriology* **27**, 386–387 (1977).

135. Patro, L. P. P. & Rathinavelan, T. Targeting the Sugary Armor of *Klebsiella* Species. *Front. Cell. Infect. Microbiol.* **9**, 367 (2019).

136. Khadka, S., Ring, B. E., Pariseau, D. A. & Mike, L. A. Characterization of *Klebsiella pneumoniae* Extracellular Polysaccharides. *Current Protocols* **3**, e937 (2023).
137. Wang, W. *et al.* Different regulatory mechanisms of the capsule in hypervirulent *Klebsiella* pneumonia: "direct" wcaJ variation vs. "indirect" rmpA regulation. *Front. Cell. Infect. Microbiol.* **13**, 1108818 (2023).
138. Brisse, S. *et al. wzi* Gene Sequencing, a Rapid Method for Determination of Capsular Type for *Klebsiella* Strains. *J Clin Microbiol* **51**, 4073–4078 (2013).
139. Hsu, C.-R., Lin, T.-L., Chen, Y.-C., Chou, H.-C. & Wang, J.-T. The role of *Klebsiella pneumoniae* rmpA in capsular polysaccharide synthesis and virulence revisited. *Microbiology* **157**, 3446–3457 (2011).
140. Singh, S. *et al.* LPS O Antigen Plays a Key Role in *Klebsiella pneumoniae* Capsule Retention. *Microbiol Spectr* **10**, e01517-21 (2022).
141. Follador, R. *et al.* The diversity of *Klebsiella pneumoniae* surface polysaccharides. *Microbial Genomics* **2**, (2016).
142. Bulati, M. *et al. Klebsiella pneumoniae* Lipopolysaccharides Serotype O2afg Induce Poor Inflammatory Immune Responses Ex Vivo. *Microorganisms* **9**, 1317 (2021).
143. Ko, K. S. The contribution of capsule polysaccharide genes to virulence of *Klebsiella pneumoniae*. *Virulence* **8**, 485–486 (2017).
144. Wantuch, P. L. & Rosen, D. A. *Klebsiella pneumoniae*: adaptive immune landscapes and vaccine horizons. *Trends in Immunology* **44**, 826–844 (2023).
145. Nucci, A., Rocha, E. P. C. & Rendueles, O. Adaptation to novel spatially-structured environments is driven by the capsule and alters virulence-associated traits. *Nat Commun* **13**, 4751 (2022).
146. Buffet, A., Rocha, E. P. C. & Rendueles, O. Nutrient conditions are primary drivers of bacterial capsule maintenance in *Klebsiella*. *Proc. R. Soc. B.* **288**, 20202876 (2021).
147. Buffet, A., Rocha, E. P. C. & Rendueles, O. Selection for the bacterial capsule in the absence of biotic and abiotic aggressions depends on growth conditions. Preprint at https://doi.org/10.1101/2020.04.27.059774 (2020).
148. Lenchenko, E., Blumenkrants, D., Sachivkina, N., Shadrova, N. & Ibragimova, A. Morphological and adhesive properties of *Klebsiella pneumoniae* biofilms. *Vet World* **13**, 197–200 (2020).
149. Dzul, S. P. *et al.* Contribution of the *Klebsiella pneumoniae* Capsule to Bacterial Aggregate and Biofilm Microstructures. *Appl Environ Microbiol* **77**, 1777–1782 (2011).
150. Portela, R., Almeida, P. L., Sobral, R. G. & Leal, C. R. Motility and cell shape roles in the rheology of growing bacteria cultures. *Eur. Phys. J. E* **42**, 26 (2019).

151. Bai, R. & Guo, J. Interactions and Implications of *Klebsiella pneumoniae* with Human Immune Responses and Metabolic Pathways: A Comprehensive Review. *IDR* **Volume 17**, 449–462 (2024).
152. Campanero-Rhodes, M. A. *et al.* Insights into the recognition of hypermucoviscous *Klebsiella pneumoniae* clinical isolates by innate immune lectins of the Siglec and galectin families. *Front. Immunol.* **15**, 1436039 (2024).
153. Wyres, K. L. *et al.* Identification of *Klebsiella* capsule synthesis loci from whole genome data. *Microbial Genomics* **2**, (2016).
154. Zierke, L., Mourad, R., Kohler, T. P., Müsken, M. & Hammerschmidt, S. Influence of the polysaccharide capsule on virulence and fitness of *Klebsiella pneumoniae*. *Front. Microbiol.* **16**, 1450984 (2025).
155. Liu, X. *et al.* Capsular polysaccharide enables *Klebsiella pneumoniae* to evade phagocytosis by blocking host-bacteria interactions. *mBio* e03838-24 (2025) doi:10.1128/mbio.03838-24.
156. Huang, X. *et al.* Capsule type defines the capability of *Klebsiella pneumoniae* in evading Kupffer cell capture in the liver. *PLoS Pathog* **18**, e1010693 (2022).
157. Favre-Bonte, S., Joly, B. & Forestier, C. Consequences of Reduction of *Klebsiella pneumoniae* Capsule Expression on Interactions of This Bacterium with Epithelial Cells. *Infect Immun* **67**, 554–561 (1999).
158. Kaszowska, M. *et al.* The Mutation in wbaP cps Gene Cluster Selected by Phage-Borne Depolymerase Abolishes Capsule Production and Diminishes the Virulence of *Klebsiella pneumoniae*. *IJMS* **22**, 11562 (2021).
159. Calderon-Gonzalez, R. *et al.* Modelling the Gastrointestinal Carriage of *Klebsiella pneumoniae* Infections. *mBio* **14**, e03121-22 (2023).
160. Struve, C. & Krogfelt, K. A. Role of capsule in *Klebsiella pneumoniae* virulence: lack of correlation between in vitro and in vivo studies. *FEMS Microbiology Letters* **218**, 149–154 (2003).
161. Rendueles, O. Deciphering the role of the capsule of *Klebsiella pneumoniae* during pathogenesis: A cautionary tale. *Molecular Microbiology* **113**, 883–888 (2020).
162. Clegg, S. & Murphy, C. N. Epidemiology and Virulence of *Klebsiella pneumoniae*. *Microbiol Spectr* **4**, 4.1.06 (2016).
163. Haudiquet, M. *et al.* Capsules and their traits shape phage susceptibility and plasmid conjugation efficiency. Preprint at https://doi.org/10.1101/2023.04.12.536574 (2023).
164. Rojas, D., Ramos, A., Gálvez-Silva, M., Marcoleta, A. E. & Chávez, F. P. Flow Cytometry and Automated Microscopy Integration for Phagocytic Analysis of Hypervirulent *Klebsiella pneumoniae* in Dictyostelium discoideum. in *Foodborne Bacterial Pathogens* (ed. Bridier, A.) vol. 2852 181–196 (Springer US, New York, NY, 2025).

165. Campanero-Rhodes, M. A. & Solís, D. Bacterial Microarrays for Examining Bacterial Glycosignatures and Recognition by Host Lectins. in *Glycan Microarrays* (eds. Kilcoyne, M. & Gerlach, J. Q.) vol. 2460 147–160 (Springer US, New York, NY, 2022).

Supplementary material

Journal of Global Antimicrobial Resistance 34 (2023) 195–198

Contents lists available at ScienceDirect

Journal of Global Antimicrobial Resistance

journal homepage: www.elsevier.com/locate/jgar

Genome Note

Emergence of NDM-1 and KPC-3 carbapenemases in *Kluyvera cryocrescens*: Investigating genetic heterogeneity and acquisition routes of bla_{NDM-1} in *Enterobacterales* species in Portugal

Michele Loiodice[a,b], Manuela Ribeiro[c], Luísa Peixe[a,b], Ângela Novais[a,b,*]

[a] UCIBIO – Applied Molecular Biosciences Unit, Faculty of Pharmacy, University of Porto, Porto, Portugal
[b] Associate Laboratory i4HB - Institute for Health and Bioeconomy, Faculty of Pharmacy, University of Porto, Porto, Portugal
[c] Service of Clinical Pathology, Hospital University Centre São João, Porto, Portugal

ARTICLE INFO

Article history:
Received 26 April 2023
Revised 7 July 2023
Accepted 12 July 2023
Available online 17 July 2023

Editor: Stefania Stefani

Keywords:
Multidrug resistance (MDR)
Carbapenemase
Carbapenemase-producing *Enterobacterales* (CPE)
IncN
Tn*3000*
Tn*4401*
Whole genome sequencing (WGS)

ABSTRACT

Objectives: A higher diversity of species, clones and genes have been increasingly implicated in carbapenemases spread, though the mobile genetic elements responsible for their acquisition and dispersion at local and global levels are less explored, particularly in species other than *Klebsiella pneumoniae* or *Escherichia coli*. We aim to explain the emergence of NDM-1 and KPC-3 carbapenemases in a *Kluyvera cryocrescens* isolate, and to shed light on the heterogeneity of genetic platforms and acquisition routes of bla_{NDM-1} in diverse *Enterobacterales* species in Portugal.

Methods: A KPC-3 and NDM-1-producing *K. cryocrescens* colonizing a hospitalized patient in 2019 was characterized by whole-genome sequencing and antibiotic resistance profiling following standard methods. Conjugative transfer of carbapenemases genes was assessed by filter mating. Plasmids were reconstructed with *in silico* and *in vitro* approaches. bla_{NDM-1} genetic context was compared with that of diverse NDM-1-producing *Enterobacterales* species, previously described in Portugal.

Results: *K. cryocrescens* K629 showed a multidrug resistance profile. Resistance gene bla_{KPC-3} was harboured by a Tn*4401d* transposon within a worldwide-spread IncN-ST15 plasmid (pKLU-KPC3), whereas bla_{NDM-1} was located in a Tn*3000* within a non-typeable mosaic plasmid (pKLU-NDM1). The heterogeneous bla_{NDM-1} genetic platforms and variable plasmid backbones identified in various *Enterobacterales* species suggested multiple introductions of bla_{NDM-1} in Portugal, mediated by variable insertion sequences.

Conclusions: We report the convergence of KPC-3 and NDM-1 in *K. cryocrescens* and the variable dissemination modes of these carbapenemases in different *Enterobacterales* species, underlining the need to track down genetic platforms responsible for carbapenemases diffusion.

© 2023 The Author(s). Published by Elsevier Ltd on behalf of International Society for Antimicrobial Chemotherapy.
This is an open access article under the CC BY-NC-ND license (http://creativecommons.org/licenses/by-nc-nd/4.0/)

1. Introduction

The spread of carbapenemase-producing *Enterobacterales* (CPE) in hospitalized patients represents a major challenge, exacerbated by a growing diversity of species, clones, and carbapenemase genes. Infrequent *Enterobacterales* species are emerging as carbapenemase-producers [1], but there is limited knowledge on MGEs associated with carbapenemase acquisition in species other than *Klebsiella pneumoniae* or *Escherichia coli*. The emergence of carbapanemases in infrequent species raises concerns regarding their accurate identification and the limited knowledge on pathogenicity and intrinsic antibiotic resistance, representing a challenge for unnoticed dissemination and subsequent infection control. *Kluyvera cryocrescens* is a sporadic opportunistic pathogen, rarely associated with multidrug resistance (MDR) or CPE [2].

Portugal is a country with a high and increasing incidence of CPE (0.3% to 11.6% in 2011–2021 for *K. pneumoniae*, atlas.ecdc.europa.eu). KPC-3 and OXA-48 are the most widespread carbapenemases, while NDM-1 has been sporadically reported in different *Enterobacterales* [3]. We report the characterization of a

* Corresponding author. Mailing Address: UCIBIO, Laboratory of Microbiology, Faculty of Pharmacy, University of Porto, Rua Jorge Viterbo Ferreira n° 228, 4050–313 Porto; Portugal.
E-mail address: aamorim@ff.up.pt (Â. Novais).

https://doi.org/10.1016/j.jgar.2023.07.008
2213-7165/© 2023 The Author(s). Published by Elsevier Ltd on behalf of International Society for Antimicrobial Chemotherapy. This is an open access article under the CC BY-NC-ND license (http://creativecommons.org/licenses/by-nc-nd/4.0/)

A)

Plasmid name	Organism	Size (bp)	Region	Year	Source	NCBI acc. n.	Coverage	Identity	NDM variant
pKLU-NDM1	*K. cryocrescens*	324406	Portugal	2019	rectal swab, human	-	-	-	NDM-1
pNUITM-VR1_1	*R. ornithinolytica*	378524	Japan	2021	N/A	AP025010.1	75%	99.96%	NDM-1
pKP-13-14-NDM-9	*K. pneumoniae*	358655	China	2013	wound on male, human	MN175386.1	66%	99.17%	NDM-9
pKP-14-2-131-NDM-1	*K. pneumoniae*	358158	China	2014	urine tube tip, veterinary	MZ836808.1	66%	99.17%	NDM-1
pC39-334kb	*K. pneumoniae*	334893	China	2019	infant sputum, human	CP061701.1	65%	99.11%	NDM-1
pKP18-2110-2-1	*K. pneumoniae*	362034	China	2018	blood, human	CP084987.1	64%	98.73%	NDM-1
pKP19-3023-374k	*K. pneumoniae*	374513	China	2019	sputum, human	CP063748.1	64%	98.71%	NDM-1
pKP19-3088-375k	*K. pneumoniae*	375474	China	2019	blood culture, human	CP063149.1	64%	98.71%	NDM-1
pKO-16-21-NDM-1	*K. oxytoca*	376570	China	2016	sputum	MZ836807.1	63%	99.18%	NDM-1
p104922-NDM	*R. ornithinolytica*	361412	China	2019	human	MT062912.1	62%	99.17%	NDM-1

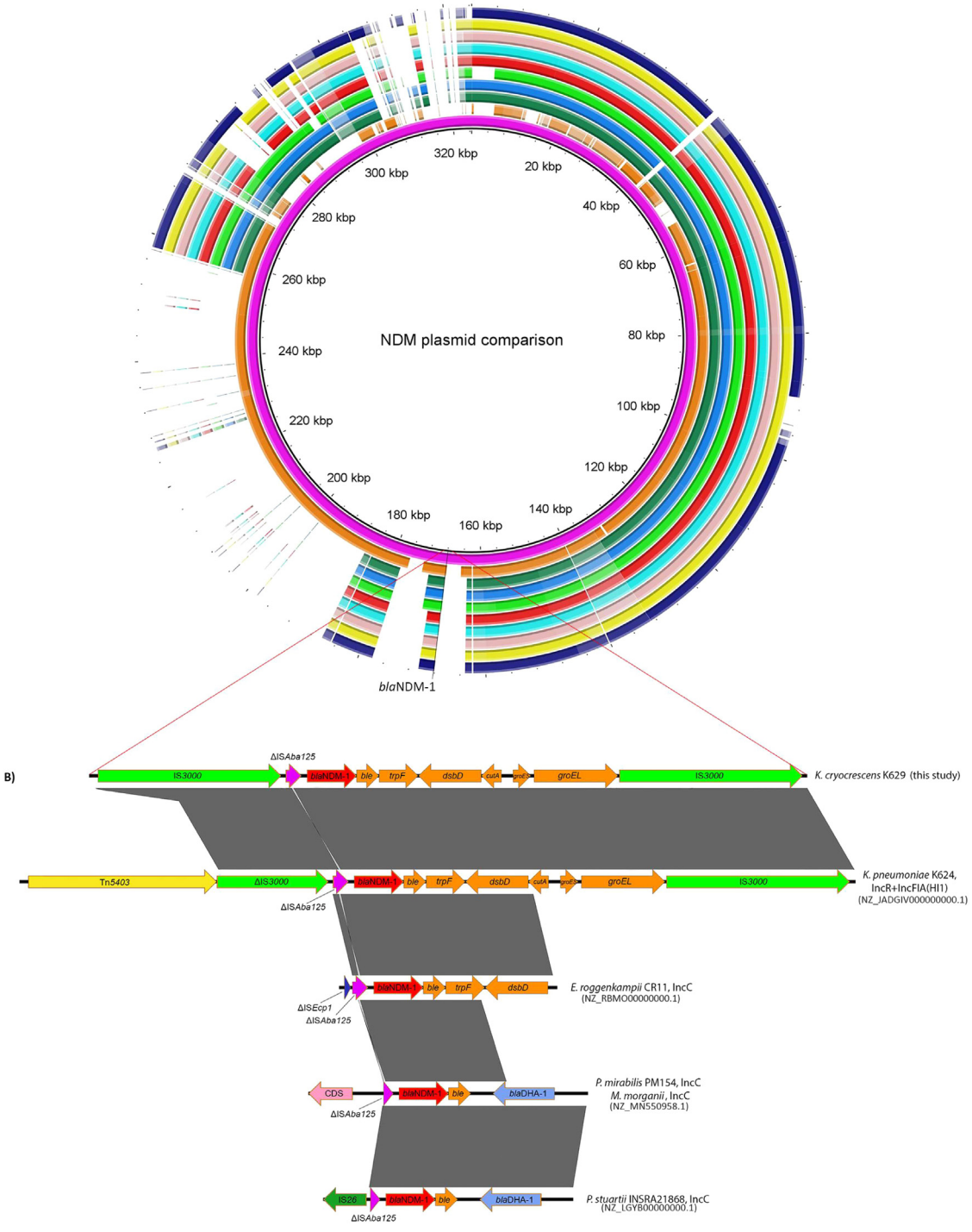


Fig. 1. Comparison of closely related NDM-encoding plasmids and bla_{NDM-1} genetic environments. (A) BRIG representation of pKLU-NDM1 and closely related NDM-encoding plasmids from GenBank database. (B) Diversity of bla_{NDM-1} genetic contexts identified in different *Enterobacterales* species from Portugal, represented using Easyfig. The numbers in parenthesis indicate the NCBI accession numbers for each sequence.

genome from a *K. cryocrescens* identified as a colonizer of a hospitalized patient, and exploredthe emergence of both NDM-1 and KPC-3 by analysing the genetic platforms and acquisition routes of bla_{NDM-1} among *Enterobacterales* in Portugal.

2. Material and methods

K. cryocrescens K629, isolated in October 2019 from a rectal colonization screening in hospitalized patients in Portugal, was identified by MALDI-TOF and whole genome sequencing (WGS). AbR profiles were assessed to third/fourth generation cephalosporins (ceftazidime, cefotaxime, cefepime), monobactams (aztreonam), cephamycins (cefoxitin), carbapenems (ertapenem, imipenem), β-lactam-β-lactamase inhibitors (ceftazidime/avibactam, amoxicillin/clavulanic acid), aminoglycosides (amikacin, gentamicin, tobramycin), tetracyclines (tetracycline, tigecycline), quinolones (nalidixic acid, ciprofloxacin), and trimethoprim-sulfamethoxazole, including broth microdilution test to colistin, agar dilution and E-test to fosfomycin and ciprofloxacin, respectively (EUCAST, eucast.org and CLSI-M100–30th, 2020).

From WGS data, short reads were *de novo* assembled with SPAdes (v.3.13.0, github.com/ablab/spades) and annotated by RAST (v.2.0, rast.nmpdr.org), resistance genes identified with Kleborate (v.2.2.0, github.com/katholt/Kleborate) and ResFinder (v.4.1, cge.food.dtu.dk/services/ResFinder). Mlplasmids (gitlab.com/sirarredondo/mlplasmids) and Mob-typer (github.com/jrober84/mob-typer) predicted plasmid/chromosome-derived sequences and type. Assemblies were confirmed by PCR/sequencing. Similarity between plasmids and bla_{NDM-1} genetic environments was analysed and represented by BRIG (v.0.95, brig.sourceforge.net) and EasyFig (v.2.2.5, mjsull.github.io/Easyfig) respectively. WGS and plasmid complete sequences were deposited on NCBI (ncbi.nlm.nih.gov) under accession number SAMN33188110.

The conjugation of the carbapenemase plasmids was tested by filter-mating, using *E. coli* HB101 as recipient (selective agents: imipenem 1 mg/mL, azide 13 mg/mL).

3. Results and discussion

To our knowledge, this is the firstly described *K. cryocrescens* co-producing NDM-1 and KPC-3. Strain K629 showed resistance to all the tested β-lactams, kanamycin, and trimethoprim-sulfamethoxazole. The MIC for ciprofloxacin was 0.125 mg/L, equivalent to *K. pneumoniae* ECOFF value, suggesting an acquired mechanism of resistance. In fact, we detected plasmid-mediated quinolone resistance *qnrS1*, together with aminoglycoside-modifying *aph(3')-Ia*, trimethoprim resistance *dfrA12*, streptomycin/spectinomycin cassette *aadA2*, carbapenemases bla_{KPC-3} and bla_{NDM-1}, and the chromosomally-encoded bla_{KLUC-2}.

The strain carried three plasmids. pKLU-KPC3 (54Kb IncN-pMLST ST15), the only one transferable by conjugation, harboured bla_{KPC-3} within a Tn*4401d* transposon. pKLU-KPC3 is identical (100% coverage, 99.9% identity) to pWI1-KPC3 (GenBank accession number LT838197), carried by an *E. coli* isolated in France from a patient initially hospitalized in Portugal suggesting a common origin [3]. Interestingly, highly similar ST15-IncN plasmids (>76% coverage, >99.9% identity) were identified in various continents and niches throughout a decade, with variable acquisition of bla_{KPC-2} within Tn*4401b*/*c* (Supplementary Table S1).

The newly described pKLU-NDM1 (324Kb non-typeable, with repU and MOBH-MOBP relaxases), harboured bla_{NDM-1} and showed high similarity (62–75% coverage, >98.7% identity) to other NDM-encoding plasmids from Asia in *Klebsiella*/*Raoutella* spp., suggesting a narrow-spectrum host range (Fig. 1A). pNUITM-VR1_1 was the closest (GenBank accession number AP025010, 75% coverage, 99.96% identity), sharing a 95Kb continuous sequence (Fig. 1A). bla_{NDM-1} was part of a composite Tn*3000* (Tn3-like, 11.8 Kb) (Fig. 1B), responsible for bla_{NDM-1} global dispersal in IncF/IncH plasmid types [4].

A similar structure, with the left IS*3000* copy truncated by Tn*5403*, was reported in a IncR+IncFIA$_{HI1}$ plasmid type described in an outbreak caused by NDM-1-producing ST11-KL105 *K. pneumoniae* [3] (Fig. 1B, further supporting the role of Tn*3000* in reshuffling bla_{NDM-1} into distinct plasmid backbones. Moreover, diverse genetic contexts upstream/downstream bla_{NDM-1} were identified in IncC plasmids from several *Enterobacterales* in Portugal, from different sources (Fig. 1B), suggesting multiple introduction/recombination events involving bla_{NDM-1} within variable plasmids (IncU, IncC, IncR+IncFIA$_{HI1}$) and species in this country (2015–2019), without a subsequent expansion. Finding variable 5'-truncations of IS*Aba125* by IS*3000*, IS*26* or IS*Ecp1*, further supports the involvement of transposable elements in bla_{NDM-1} mobilization towards diverse plasmids [5].

Plasmid pKLU-IncX5 (44 Kb, IncX5 type) was devoid of antibiotic resistance genes and was identical to others described in China and the USA (GenBank accession numbers MF344556 and CP037738, respectively).

4. Conclusions

Our data highlights the involvement of common genetic backbones for the spread of bla_{KPC} (Tn*4401d*, IncN-ST15) in multiple countries, and, conversely, the heterogeneity of the genetic platforms capturing and re-shuffling bla_{NDM-1} into different backgrounds among *Enterobacterales* species. The emergence of strains resistant to all β-lactams with successful genetic platforms, carrying multiple carbapenemases, highlights the importance of controlling carbapenemases genes evolution and dissemination.

Funding: This work is financed by national funds from FCT - Fundação para a Ciência e a Tecnologia, I.P., in the scope of the project UIDP/04378/2020 and UIDB/04378/2020 of the Research Unit on Applied Molecular Biosciences - UCIBIO and the project LA/P/0140/2020 of the Associate Laboratory Institute for Health and Bioeconomy - i4HB, Faculty of Pharmacy, University of Porto, 4050-313 Porto, Portugal. This research received also support by HEALTH-UNORTE I&D&I project (NORTE-01–0145-FEDER-000039) co-financed by European Regional Development Fund (ERDF), through the NORTE 2020 (Programa Operacional Regional do Norte 2014/2020). M. Loiodice is supported by FCT (Fundação para a Ciência e a Tecnologia, I.P.) grant number 2020.07480.BD. Â. Novais is supported by national funds through FCT (Fundação para a Ciência e a Tecnologia, I.P.), through Scientific Employment Stimulus Program (2021.02252.CEECIND/CP1662/CT0009).

Competing Interests: All the authors involved in the writing of this document have nothing to declare.

Ethical approval: Not Required

Acknowledgements: We would like to kindly acknowledge Dr. Joana Mourão for providing guidance on the MOB-recon software usage.

Supplementary materials

Supplementary material associated with this article can be found, in the online version, at doi:10.1016/j.jgar.2023.07.008.

References

[1] Guerra AM, Lira A, Lameirão A, Selaru A, Abreu G, Lopes P, et al. Multiplicity of carbapenemase-producers three years after a KPC-3-producing *K.*

pneumoniae ST147-K64 hospital outbreak. Antibiotics 2020;9:806. doi:10.3390/antibiotics9110806.

[2] Gaibani P, Ambretti S, Scaltriti E, Cordovana M, Berlingeri A, Pongolini S, et al. A novel IncA plasmid carrying bla_{VIM-1} in a *Kluyvera cryocrescens* strain. J Antimicrob Chemother 2018;73:3206–8. doi:10.1093/jac/dky304.

[3] Novais Â, Ferraz RV, Viana M, da Costa PM. Peixe L NDM-1 Introduction in Portugal through a ST11 KL105 *Klebsiella pneumoniae* Widespread in Europe. Antibiotics 2022;11:92. doi:10.3390/antibiotics11010092.

[4] Campos JC, da Silva MJ, dos Santos PR, Barros EM, Pereira Mde O, Seco BM, et al. Characterization of Tn3000, a transposon responsible for blaNDM-1 dissemination among enterobacteriaceae in Brazil, Nepal, Morocco, and India. Antimicrob Agents Chemother 2015;59:7387–95. doi:10.1128/AAC.01458-15.

[5] Acman M, Wang R, van Dorp L, Shaw LP, Wang Q, Luhmann N, et al. Role of mobile genetic elements in the global dissemination of the carbapenem resistance gene bla_{NDM}. Nat Commun 2022;13:1131. doi:10.1038/s41467-022-28819-2.

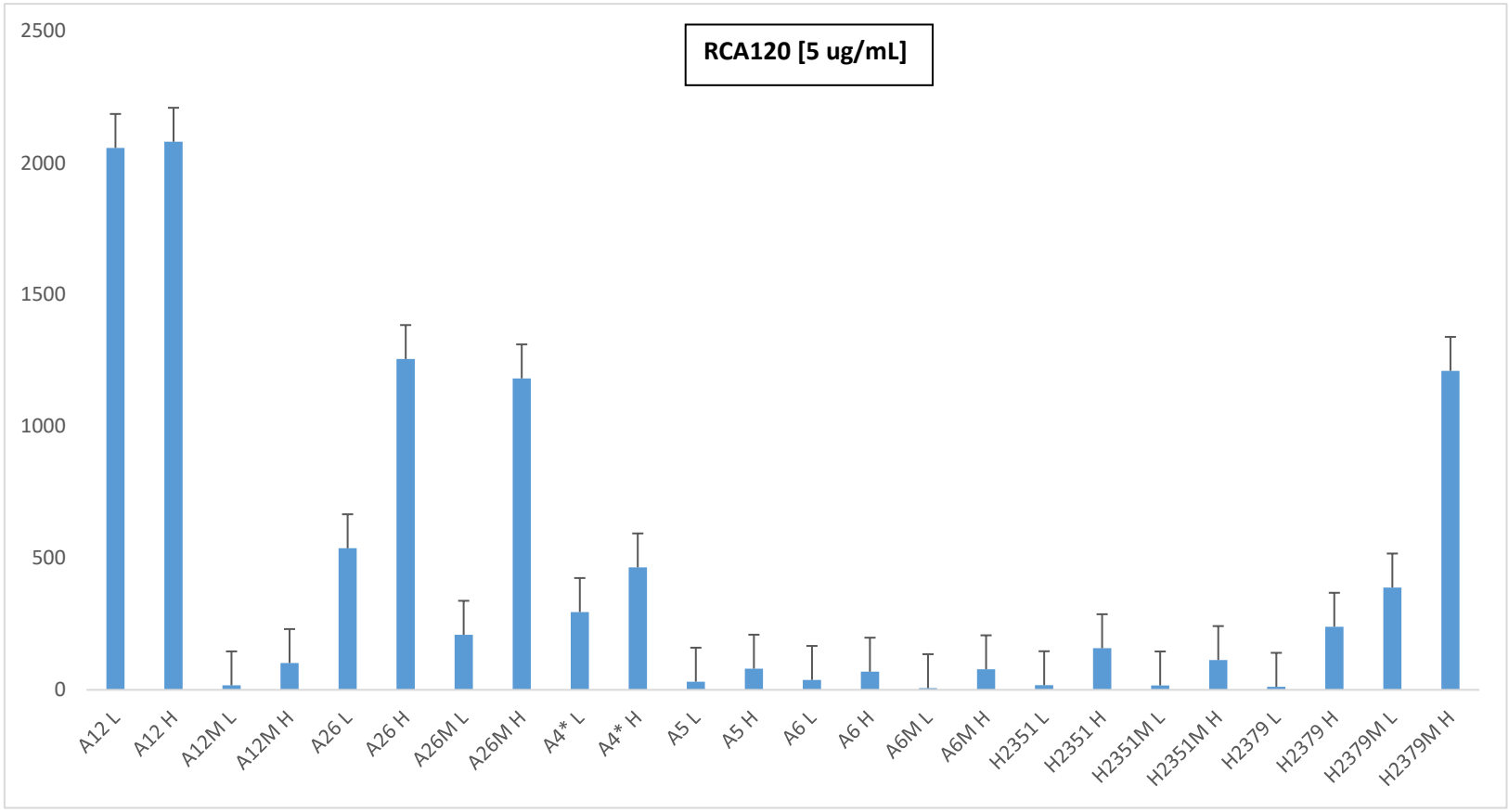
Strain-specific glycosignatures in representative multidrug resistant and hypervirulent *Klebsiella pneumoniae* sublineages

Tables S1: Fluorescence activity of lectin-bacteria microarrays.

	RCA120 [5 ug/mL]		
	Probe	**AVG F635 Mean - B635**	**STDEV**
positive control	Asialofetuin L	30356,50	581,95
positive control	Asialofetuin H	57174,50	610,23
positive control	Glucuronoxylomannan L	41,00	48,22
positive control	Glucuronoxylomannan H	101,67	63,14
MDR-*Kp*, HMV	A12 L	2056,50	94,05
MDR-*Kp*, HMV	A12 H	2080,00	203,65
MDR-*Kp*, CPS$^-$	A12M L	17,00	3,61
MDR-*Kp*, CPS$^-$	A12M H	101,67	60,12
hv*Kp*, HMV	A26 L	537,33	98,19
hv*Kp*, HMV	A26 H	1255,50	53,03
hv*Kp*, CPS$^-$	A26M L	209,00	5,66
hv*Kp*, CPS$^-$	A26M H	1182,00	77,78
MDR-*Kp*, CPS$^-$	A4* L	295,33	181,68
MDR-*Kp*, CPS$^-$	A4* H	464,67	108,96
MDR-*Kp*	A5 L	31,00	15,13
MDR-*Kp*	A5 H	80,33	21,57
MDR-*Kp*	A6 L	37,67	9,07
MDR-*Kp*	A6 H	69,00	57,09
MDR-*Kp*, CPS$^-$	A6M L	6,33	2,08
MDR-*Kp*, CPS$^-$	A6M H	78,00	32,45
hv*Kp*, HMV	H2351 L	17,50	6,36
hv*Kp*, HMV	H2351 H	158,00	11,27
hv*Kp*, CPS$^-$	H2351M L	16,67	10,21
hv*Kp*, CPS$^-$	H2351M H	113,00	22,87

	Probe	AVG F635 Mean - B635	STDEV
hv*Kp*, HMV	H2379 L	11,50	9,19
hv*Kp*, HMV	H2379 H	239,33	22,94
hv*Kp*, CPS$^-$	H2379M L	388,33	69,50
hv*Kp*, CPS$^-$	H2379M H	1210,50	20,51
positive control	PGG glucan L	18,67	15,95
positive control	PGG glucan H	30,67	12,86
positive control	αmannan L	46,33	22,19
positive control	αmannan H	157,67	22,55

Values in relative fluorescence units (RFU). AVG = average; F635 Mean = median pixel values for the foreground of the red (Cy5) channel; B635 = background of the red channel; STDEV = standard deviation.

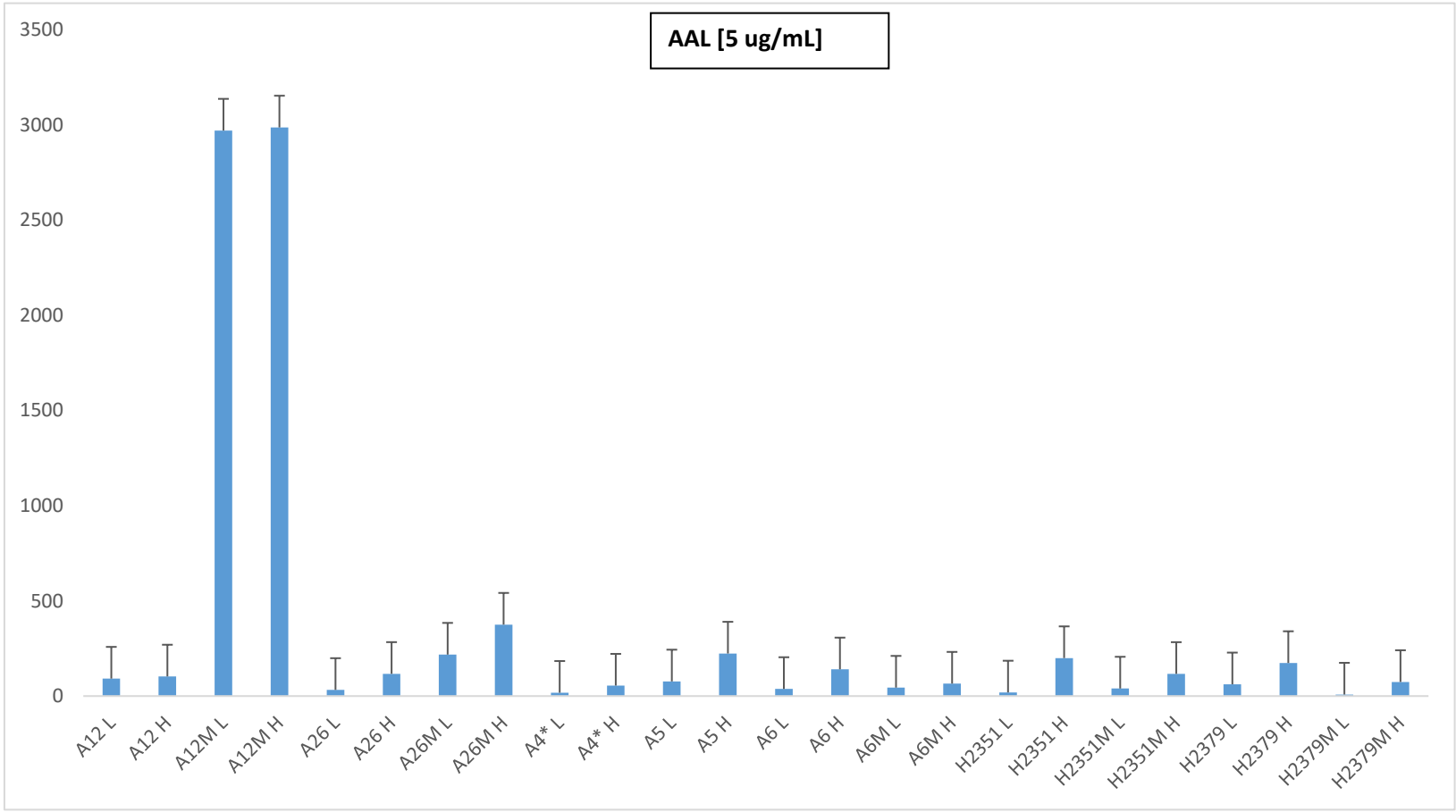


AAL [5 ug/mL]

	Probe	AVG F635 Mean - B635	STDEV
positive control	Asialofetuin L	103	84,22
positive control	Asialofetuin H	9545	634
positive control	Glucuronoxylomannan L	1095	99
positive control	Glucuronoxylomannan H	60838	1119
MDR-*Kp*, HMV	A12 L	92	13
MDR-*Kp*, HMV	A12 H	103	10
MDR-*Kp*, CPS$^-$	A12M L	2969	222
MDR-*Kp*, CPS$^-$	A12M H	2986	76
hv*Kp*, HMV	A26 L	32	6
hv*Kp*, HMV	A26 H	117	17
hv*Kp*, CPS$^-$	A26M L	218	13
hv*Kp*, CPS$^-$	A26M H	375	24
MDR-*Kp*, CPS$^-$	A4* L	17	14
MDR-*Kp*, CPS$^-$	A4* H	55	7
MDR-*Kp*	A5 L	77	12
MDR-*Kp*	A5 H	223	29
MDR-*Kp*	A6 L	37	5
MDR-*Kp*	A6 H	140	36
MDR-*Kp*, CPS$^-$	A6M L	44	24
MDR-*Kp*, CPS$^-$	A6M H	65	3
hv*Kp*, HMV	H2351 L	19	1
hv*Kp*, HMV	H2351 H	199	8
hv*Kp*, CPS$^-$	H2351M L	40	20
hv*Kp*, CPS$^-$	H2351M H	117	25
hv*Kp*, HMV	H2379 L	62	85
hv*Kp*, HMV	H2379 H	174	52

Type	Probe	AVG F635 Mean - B635	STDEV
hv*Kp*, CPS$^-$	H2379M L	8	3
hv*Kp*, CPS$^-$	H2379M H	74	55
positive control	PGG glucan L	2	9
positive control	PGG glucan H	36	2
positive control	αmannan L	31	14
positive control	αmannan H	459	79

Values in relative fluorescence units (RFU). AVG = average; F635 Mean = median pixel values for the foreground of the red (Cy5) channel; B635 = background of the red channel; STDEV = standard deviation.

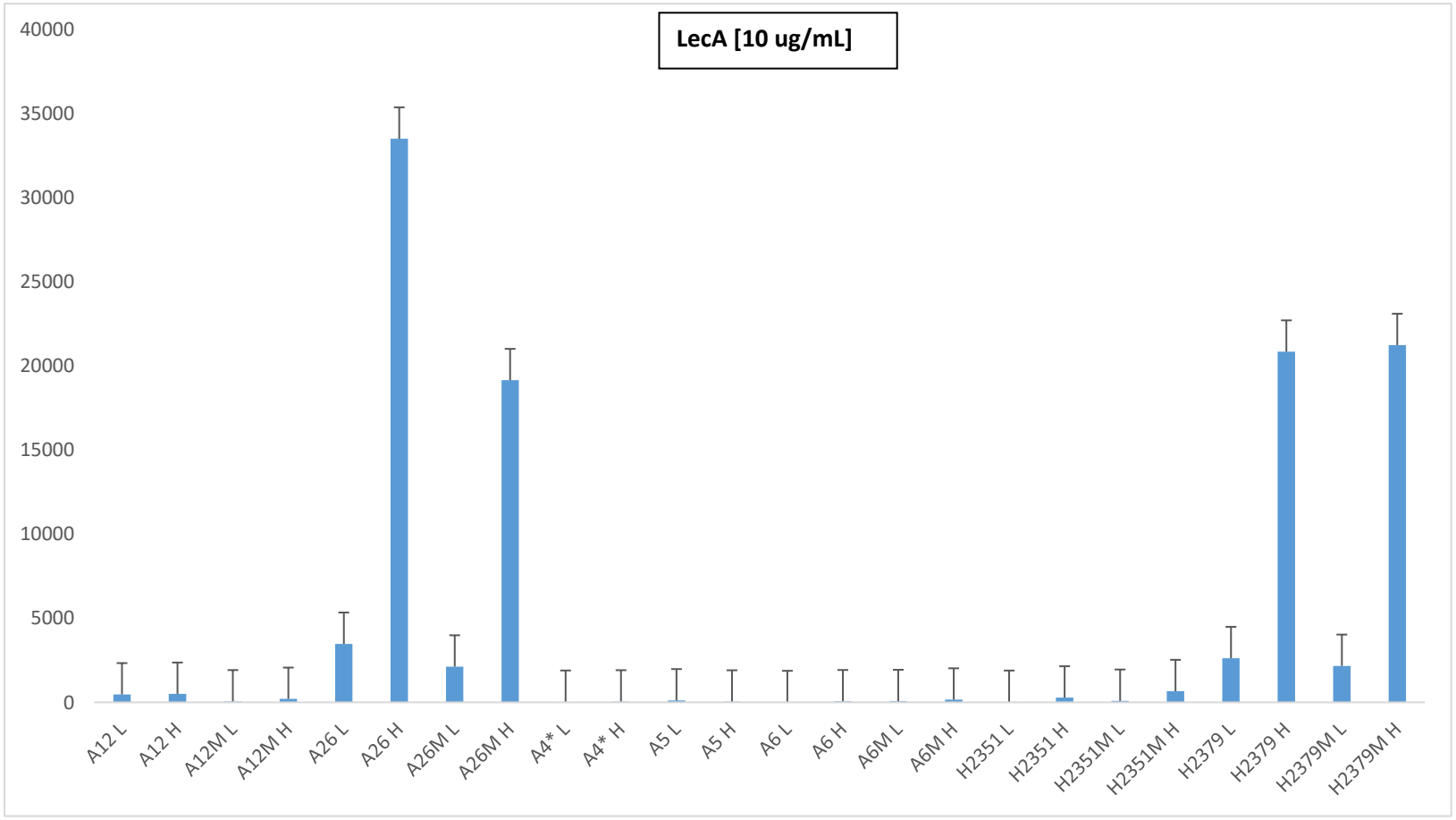


LecA [10 ug/mL]

	Probe	AVG F635 Mean - B635	STDEV
positive control	Asialofetuin L	12536,00	1260,87
positive control	Asialofetuin H	39547,00	2655,64
positive control	Glucuronoxylomannan L	389,67	143,21
positive control	Glucuronoxylomannan H	1651,00	143,43
MDR-*Kp*, HMV	A12 L	469,50	17,68
MDR-*Kp*, HMV	A12 H	502,67	59,80
MDR-*Kp*, CPS^-	A12M L	54,00	10,15
MDR-*Kp*, CPS^-	A12M H	202,67	29,19
hv*Kp*, HMV	A26 L	3479,00	811,76
hv*Kp*, HMV	A26 H	33524,50	5113,09
hv*Kp*, CPS^-	A26M L	2124,50	157,68
hv*Kp*, CPS^-	A26M H	19161,00	377,60
MDR-*Kp*, CPS^-	A4* L	29,33	19,30
MDR-*Kp*, CPS^-	A4* H	47,00	37,51
MDR-*Kp*	A5 L	113,33	56,89
MDR-*Kp*	A5 H	42,00	26,96
MDR-*Kp*	A6 L	10,00	2,83
MDR-*Kp*	A6 H	59,67	3,21
MDR-*Kp*, CPS^-	A6M L	71,67	50,52
MDR-*Kp*, CPS^-	A6M H	159,33	50,86
hv*Kp*, HMV	H2351 L	26,67	22,48
hv*Kp*, HMV	H2351 H	281,00	29,05
hv*Kp*, CPS^-	H2351M L	88,00	27,84
hv*Kp*, CPS^-	H2351M H	664,50	270,82
hv*Kp*, HMV	H2379 L	2627,50	420,73

	Probe	AVG F635 Mean - B635	STDEV
hv*Kp*, HMV	H2379 H	20855,50	119,50
hv*Kp*, CPS$^-$	H2379M L	2166,00	219,20
hv*Kp*, CPS$^-$	H2379M H	21251,00	3521,39
positive control	PGG glucan L	0,50	0,71
positive control	PGG glucan H	55,00	71,04
positive control	αmannan L	498,00	504,87
positive control	αmannan H	549,50	253,85

Values in relative fluorescence units (RFU). AVG = average; F635 Mean = median pixel values for the foreground of the red (Cy5) channel; B635 = background of the red channel; STDEV = standard deviation.

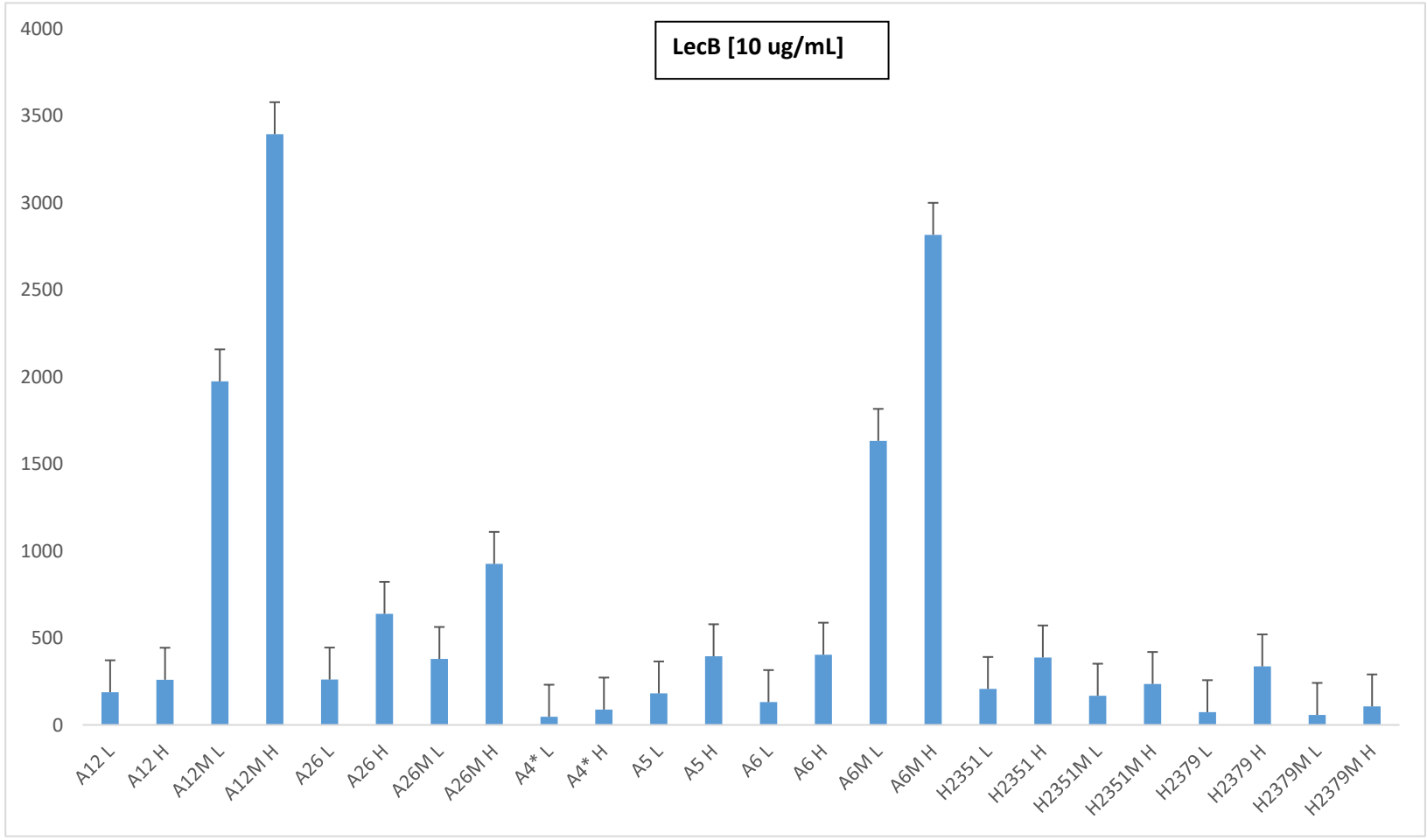


LecB [10 ug/mL]

	Probe	AVG F635 Mean - B635	STDEV
positive control	Asialofetuin L	3322	379,67
positive control	Asialofetuin H	25222	1551
positive control	Glucuronoxylomannan L	63325	1081
positive control	Glucuronoxylomannan H	60972	2831
MDR-*Kp*, HMV	A12 L	188	48
MDR-*Kp*, HMV	A12 H	260	106
MDR-*Kp*, CPS$^-$	A12M L	1974	131
MDR-*Kp*, CPS$^-$	A12M H	3394	627
hv*Kp*, HMV	A26 L	261	132
hv*Kp*, HMV	A26 H	638	29
hv*Kp*, CPS$^-$	A26M L	379	74
hv*Kp*, CPS$^-$	A26M H	925	39
MDR-*Kp*, CPS$^-$	A4* L	47	9
MDR-*Kp*, CPS$^-$	A4* H	88	31
MDR-*Kp*	A5 L	181	44
MDR-*Kp*	A5 H	395	36
MDR-*Kp*	A6 L	131	91
MDR-*Kp*	A6 H	404	193
MDR-*Kp*, CPS$^-$	A6M L	1632	468
MDR-*Kp*, CPS$^-$	A6M H	2816	586
hv*Kp*, HMV	H2351 L	207	178
hv*Kp*, HMV	H2351 H	388	55
hv*Kp*, CPS$^-$	H2351M L	168	58
hv*Kp*, CPS$^-$	H2351M H	235	46
hv*Kp*, HMV	H2379 L	73	42
hv*Kp*, HMV	H2379 H	336	21

	Probe	AVG F635 Mean - B635	STDEV
hv*Kp*, CPS$^-$	H2379M L	58	10
hv*Kp*, CPS$^-$	H2379M H	106	45
positive control	PGG glucan L	73	112
positive control	PGG glucan H	196	179
positive control	αmannan L	64558	105
positive control	αmannan H	59891	1911

Values in relative fluorescence units (RFU). AVG = average; F635 Mean = median pixel values for the foreground of the red (Cy5) channel; B635 = background of the red channel; STDEV = standard deviation.

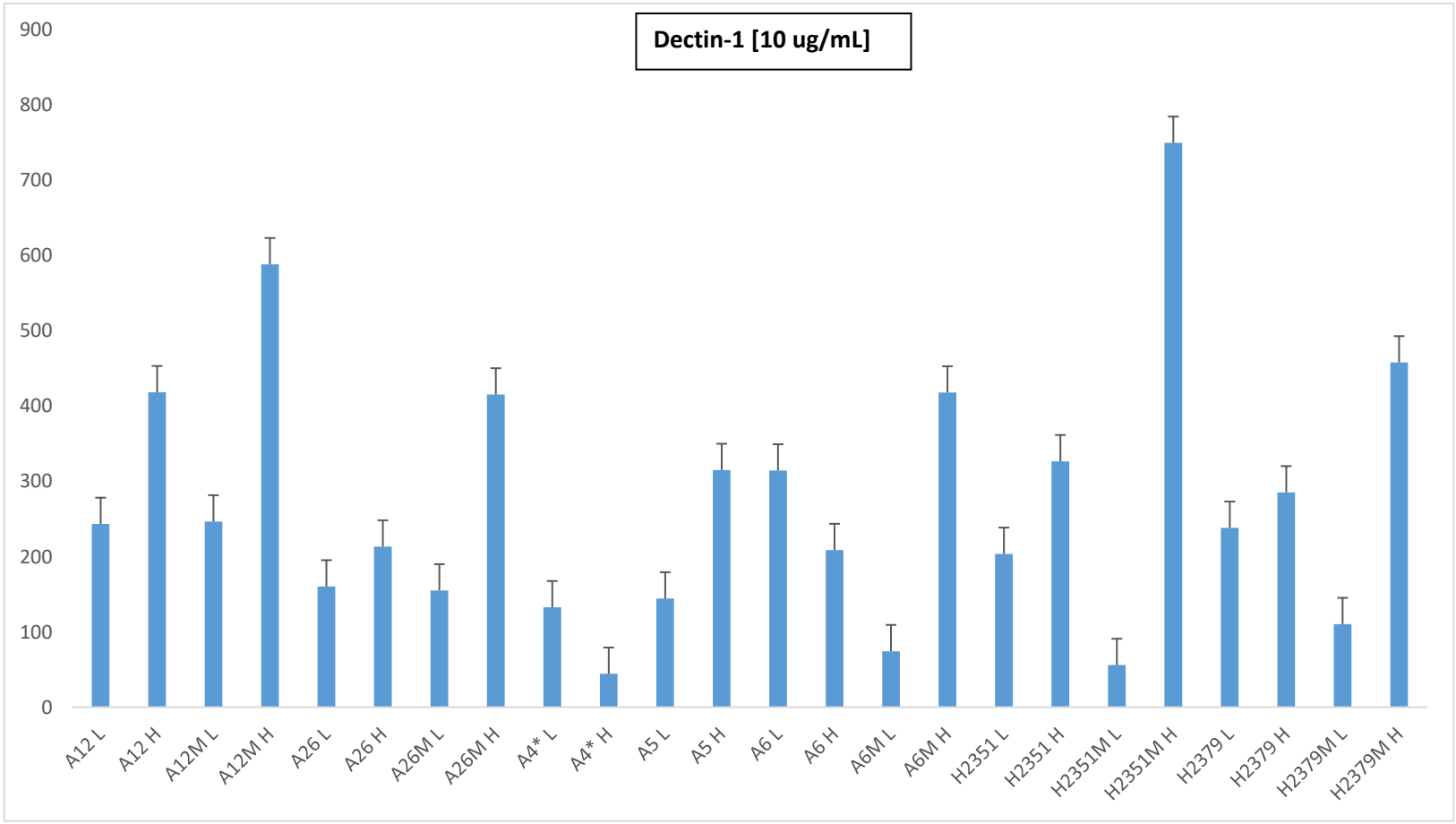


Dectin-1 [10 ug/mL]

	Probe	AVG F635 Mean - B635	STDEV
positive control	Asialofetuin L	87,33	151,27
positive control	Asialofetuin H	0,00	0,00
positive control	Glucuronoxylomannan L	57,00	19,29
positive control	Glucuronoxylomannan H	1401,33	53,93
MDR-*Kp*, HMV	A12 L	243,33	145,20
MDR-*Kp*, HMV	A12 H	418,33	60,35
MDR-*Kp*, CPS$^-$	A12M L	246,67	45,65
MDR-*Kp*, CPS$^-$	A12M H	588,33	199,19
hv*Kp*, HMV	A26 L	160,33	167,44
hv*Kp*, HMV	A26 H	213,33	86,37
hv*Kp*, CPS$^-$	A26M L	155,00	42,58
hv*Kp*, CPS$^-$	A26M H	415,33	97,35
MDR-*Kp*, CPS$^-$	A4* L	132,67	182,66
MDR-*Kp*, CPS$^-$	A4* H	44,33	30,09
MDR-*Kp*	A5 L	144,33	87,03
MDR-*Kp*	A5 H	315,00	25,51
MDR-*Kp*	A6 L	314,33	37,02
MDR-*Kp*	A6 H	208,67	40,00
MDR-*Kp*, CPS$^-$	A6M L	74,33	46,54
MDR-*Kp*, CPS$^-$	A6M H	418,00	173,31
hv*Kp*, HMV	H2351 L	203,67	124,33
hv*Kp*, HMV	H2351 H	326,67	65,53
hv*Kp*, CPS$^-$	H2351M L	56,00	21,07
hv*Kp*, CPS$^-$	H2351M H	749,67	146,43
hv*Kp*, HMV	H2379 L	238,33	26,01

	Probe	AVG F635 Mean - B635	STDEV
hv*Kp*, HMV	H2379 H	285,33	47,59
hv*Kp*, CPS$^-$	H2379M L	110,33	90,78
hv*Kp*, CPS$^-$	H2379M H	458,00	234,67
positive control	PGG glucan L	55984,67	3100,70
positive control	PGG glucan H	50274,00	2165,04
positive control	αmannan L	0,00	0,00
positive control	αmannan H	147,67	20,98

Values in relative fluorescence units (RFU). AVG = average; F635 Mean = median pixel values for the foreground of the red (Cy5) channel; B635 = background of the red channel; STDEV = standard deviation.

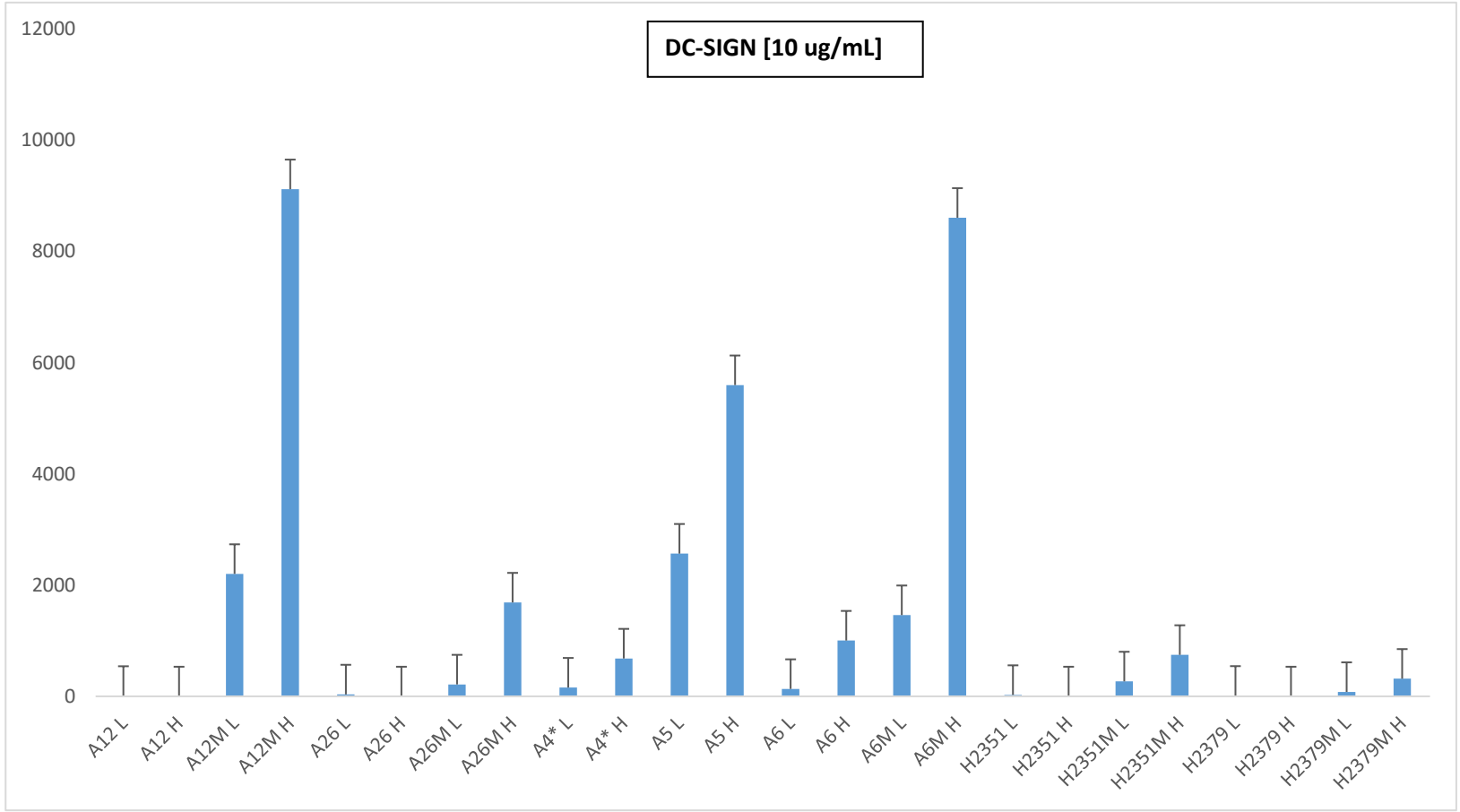


DC-SIGN [10 ug/mL]

	Probe	AVG F635 Mean - B635	STDEV
positive control	Asialofetuin L	0,00	0,00
positive control	Asialofetuin H	0,00	0,00
positive control	Glucuronoxylomannan L	299,67	65,07
positive control	Glucuronoxylomannan H	0,00	0,00
MDR-*Kp*, HMV	A12 L	8,67	15,01
MDR-*Kp*, HMV	A12 H	0,00	0,00
MDR-*Kp*, CPS$^-$	A12M L	2201,33	284,99
MDR-*Kp*, CPS$^-$	A12M H	9116,67	713,93
hv*Kp*, HMV	A26 L	35,00	30,32
hv*Kp*, HMV	A26 H	0,00	0,00
hv*Kp*, CPS$^-$	A26M L	214,00	65,39
hv*Kp*, CPS$^-$	A26M H	1687,33	391,49
MDR-*Kp*, CPS$^-$	A4* L	158,00	14,14
MDR-*Kp*, CPS$^-$	A4* H	680,67	145,03
MDR-*Kp*	A5 L	2566,00	314,38
MDR-*Kp*	A5 H	5595,67	176,54
MDR-*Kp*	A6 L	133,33	25,70
MDR-*Kp*	A6 H	1003,33	133,95
MDR-*Kp*, CPS$^-$	A6M L	1460,33	234,15
MDR-*Kp*, CPS$^-$	A6M H	8603,67	663,14
hv*Kp*, HMV	H2351 L	25,33	12,42
hv*Kp*, HMV	H2351 H	0,00	0,00
hv*Kp*, CPS$^-$	H2351M L	269,00	7,81
hv*Kp*, CPS$^-$	H2351M H	745,33	255,20
hv*Kp*, HMV	H2379 L	10,67	10,07

	Probe	AVG F635 Mean - B635	STDEV
hv*Kp*, HMV	H2379 H	0,00	0,00
hv*Kp*, CPS$^-$	H2379M L	78,67	28,99
hv*Kp*, CPS$^-$	H2379M H	317,33	43,88
positive control	PGG glucan L	204,67	41,19
positive control	PGG glucan H	1513,67	96,77
positive control	αmannan L	7581,33	273,40
positive control	αmannan H	14513,67	1298,12

Values in relative fluorescence units (RFU). AVG = average; F635 Mean = median pixel values for the foreground of the red (Cy5) channel; B635 = background of the red channel; STDEV = standard deviation.

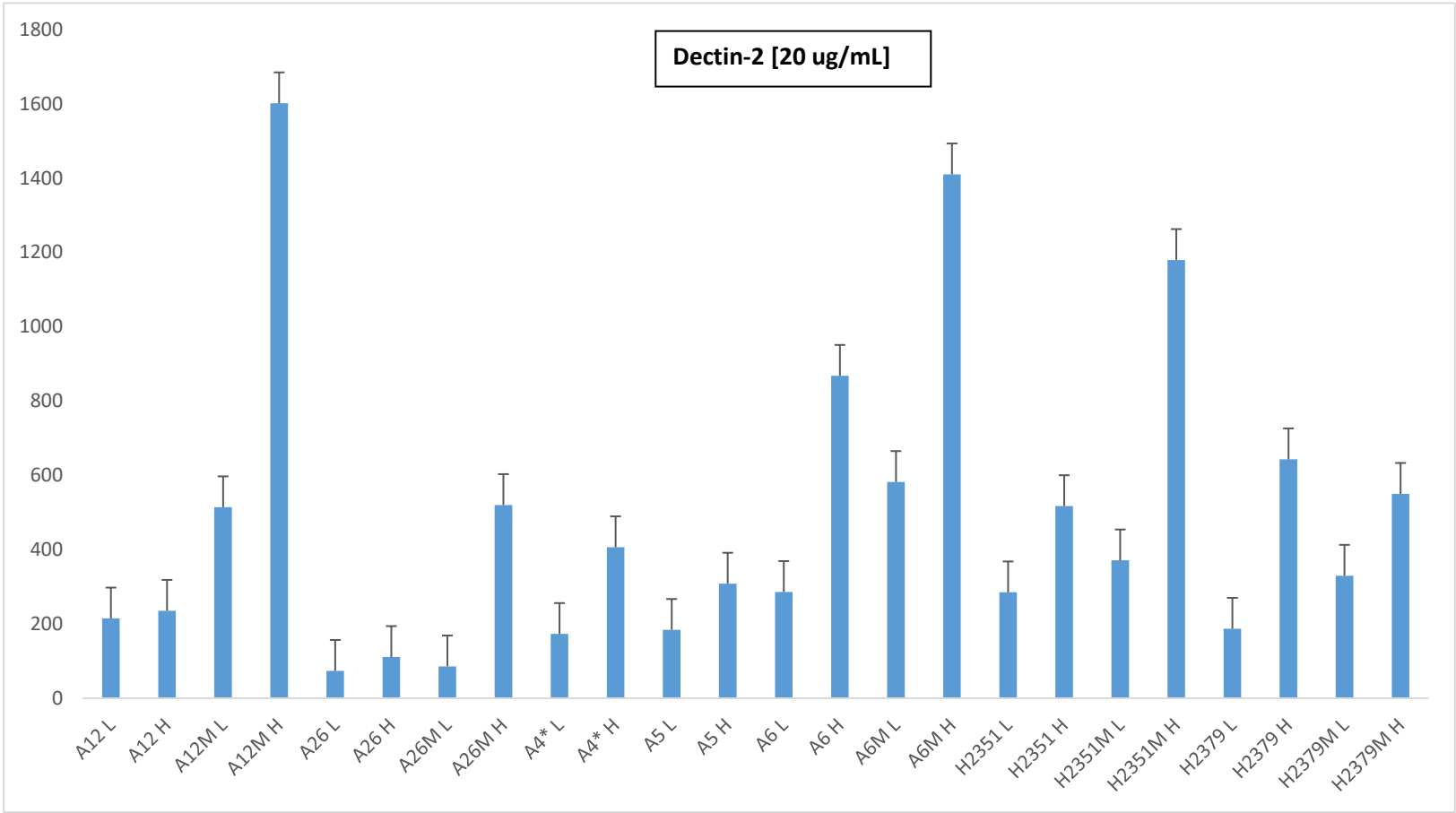


Dectin-2 [20 ug/mL]

	Probe	AVG F635 Mean - B635	STDEV
positive control	Asialofetuin L	116,33	82,57
positive control	Asialofetuin H	568,33	210,54
positive control	Glucuronoxylomannan L	526,67	153,76
positive control	Glucuronoxylomannan H	2775,67	116,43
MDR-*Kp*, HMV	A12 L	214,67	157,30
MDR-*Kp*, HMV	A12 H	235,33	170,34
MDR-*Kp*, CPS$^-$	A12M L	514,00	140,46
MDR-*Kp*, CPS$^-$	A12M H	1601,00	212,06
hv*Kp*, HMV	A26 L	73,67	55,18
hv*Kp*, HMV	A26 H	111,00	67,55
hv*Kp*, CPS$^-$	A26M L	85,67	60,87
hv*Kp*, CPS$^-$	A26M H	520,00	195,07
MDR-*Kp*, CPS$^-$	A4* L	173,00	44,80
MDR-*Kp*, CPS$^-$	A4* H	406,33	18,01
MDR-*Kp*	A5 L	184,00	79,27
MDR-*Kp*	A5 H	308,33	91,05
MDR-*Kp*	A6 L	286,00	24,02
MDR-*Kp*	A6 H	867,67	94,37
MDR-*Kp*, CPS$^-$	A6M L	582,00	49,27
MDR-*Kp*, CPS$^-$	A6M H	1409,67	214,83
hv*Kp*, HMV	H2351 L	285,00	80,91
hv*Kp*, HMV	H2351 H	517,00	41,87
hv*Kp*, CPS$^-$	H2351M L	371,00	15,87
hv*Kp*, CPS$^-$	H2351M H	1179,33	269,73
hv*Kp*, HMV	H2379 L	187,00	32,91

	Probe	AVG F635 Mean - B635	STDEV
hv*Kp*, HMV	H2379 H	643,00	26,51
hv*Kp*, CPS$^-$	H2379M L	329,67	133,06
hv*Kp*, CPS$^-$	H2379M H	550,00	92,99
positive control	PGG glucan L	0,00	0,00
positive control	PGG glucan H	158,00	157,99
positive control	αmannan L	14478,67	982,54
positive control	αmannan H	55802,00	6870,96

Values in relative fluorescence units (RFU). AVG = average; F635 Mean = median pixel values for the foreground of the red (Cy5) channel; B635 = background of the red channel; STDEV = standard deviation.



GNA/GNL [5 ug/mL]

	Probe	AVG F635 Mean - B635	STDEV
positive control	Asialofetuin L	6290,67	287,38
positive control	Asialofetuin H	24677,33	1630,60
positive control	Glucuronoxylomannan L	3579,67	149,48
positive control	Glucuronoxylomannan H	19198,33	1187,02
MDR-*Kp*, HMV	A12 L	243,00	22,87
MDR-*Kp*, HMV	A12 H	218,67	37,11
MDR-*Kp*, CPS$^-$	A12M L	115,00	38,16
MDR-*Kp*, CPS$^-$	A12M H	356,00	92,83
hv*Kp*, HMV	A26 L	60,00	9,54
hv*Kp*, HMV	A26 H	205,67	38,55
hv*Kp*, CPS$^-$	A26M L	14,00	8,72
hv*Kp*, CPS$^-$	A26M H	258,33	83,27
MDR-*Kp*, CPS$^-$	A4* L	21,33	13,65
MDR-*Kp*, CPS$^-$	A4* H	122,67	45,17
MDR-*Kp*	A5 L	21,00	3,46
MDR-*Kp*	A5 H	142,00	67,01
MDR-*Kp*	A6 L	6,67	9,07
MDR-*Kp*	A6 H	124,33	3,06
MDR-*Kp*, CPS$^-$	A6M L	707,33	265,17
MDR-*Kp*, CPS$^-$	A6M H	770,00	108,35
hv*Kp*, HMV	H2351 L	65,00	35,59
hv*Kp*, HMV	H2351 H	302,00	33,05
hv*Kp*, CPS$^-$	H2351M L	98,33	19,01
hv*Kp*, CPS$^-$	H2351M H	412,33	126,34
hv*Kp*, HMV	H2379 L	7,50	9,19

	Probe	AVG F635 Mean - B635	STDEV
hv*Kp*, HMV	H2379 H	270,67	110,94
hv*Kp*, CPS$^-$	H2379M L	86,33	42,16
hv*Kp*, CPS$^-$	H2379M H	104,00	19,70
positive control	PGG glucan L	0,67	1,15
positive control	PGG glucan H	25,00	13,11
positive control	αmannan L	59535,67	1299,63
positive control	αmannan H	59133,33	916,43

Values in relative fluorescence units (RFU). AVG = average; F635 Mean = median pixel values for the foreground of the red (Cy5) channel; B635 = background of the red channel; STDEV = standard deviation.

